1-1-2013

Development And Optimization Of The First High Throughput In Vitro Fret Assay To Characterize The Saccharomyces Cerevisiae Gpi-T

Sandamali Amarasingha Ekanayaka
Wayne State University,

DEVELOPMENT AND OPTIMIZATION OF THE FIRST HIGH THROUGHPUT *IN VITRO* FRET ASSAY TO CHARACTERIZE THE *SACCHAROMYCES CEREVISIAE* GPI-T

by

SANDAMALI AMARASINGHA EKANAYAKA

DISSERTATION

Submitted to the Graduate School

of Wayne State University,

Detroit, Michigan

in partial fulfillment of the requirements

for the degree of

DOCTOR OF PHILOSOPHY

2013

MAJOR: CHEMISTRY (Biochemistry)

Approved by:

_____

Advisor Date

_____

_____

_____

DEDICATION

To my parents Dharmadasa Amarasingha Ekanayaka,

and Karunawathie Amarasingha Ekanayaka,

my husband Udesh Indika Dias Dahanayaka

and my lovely children Sayuni and Senith.

ACKNOWLEDGMENT

I would like to express my greatest gratitude to my graduate advisor Dr. Tamara Hendrickson, with my utmost respect. Joining to Hendrickson lab in 2008 was a turning point in my life. During the last five years, Dr. Hendrickson's continuous guidance, support and encouragement directs me towards where I am today as a Scientist. Under her outstanding mentorship, I learnt many new skills and techniques to be succeed as a biochemist. Moreover, as a mother of two young children, I am grateful for Dr. Hendrickson for understanding my situation very well and encourages me at all the time so that I was able to present this dissertation today.

I would like to extend my sincere gratitude to my committee members, Dr. Ashok Bhagwat, Dr. Colin Poole and Dr. Rafael Fridman for their time, consideration, valuable suggestions and reviewing my dissertation.

I am thankful to all past and present Hendrickson lab members, Dr. Rachel Morissette, Dr. Yug Varma, Dr. Keng-Ming Chang, Megan Ehrenwerth, Dilani Gamage, Gayathri Silva, Shirin Fatima, Liangjun Zhao, Sairaman Seetharaman, Nilesh Joshi, Udumbara Rathnayaka and Travis Ness for their support and friendship.

My thanks are extended to Pflum, Trimpin, Bhagwat and Mathews labs for letting me use their instruments. I acknowledge staff members of the Wayne State Chemistry Department and all my friends who helped me in numerous ways.

I would like to express my heartiest gratefulness to my parents for their never-ending love and support. They are my first teachers and role models in my life whose always praying for my success.

Finally, I would like to express my heartiest thanks to my loving husband Udesh and my two wonderful children Sayuni and Senith. His caring and motivation never left me behind and always directs me towards success. Lovely smiles from my children and their cuteness always refresh me and motivate myself. I really appreciate all the sacrifices you three have made during my graduate studies and thank you very much for being with me.

TABLE OF CONTENTS

LIST OF FIGURES

LIST OF TABLES

LIST OF ABBREVIATIONS

*Y	3-Nitrotyrosine
Abz	2-Aminobenzoic acid
Ac	Acetyl
AChE	Acetylcholinesterase
ACN	Acetonitrile
AMC	Amino-4-methylcoumarin
APase	Alkaline phosphatase
ATP	Adenosine Tri-Phosphate
Boc	Tert-butoxycarbonyl
CA26	Campath-1 antigen
CBP	Calmodulin binding protein
CD46	Cluster of differentiation 46 protein
CD52	Campath–1 antigen
cDNA	complementary Deoxyribonucleic acid
CHO	Chinese hamster ovary
COPI	Coat protein complex I
COPII	Coat protein complex II
CMC	Critical micellar concentration
CS	Circumsporozoite
DAF	Decay accelerating factor
DIPEA	N, N-Diisopropylethylamine
DMSO	Dimethylsulfoxide

DNAse	Deoxyribonuclease
Dol-P-Man	Dolicholphosphomanose
DTT	Dithiothreitol
EBV	Ebola virus
EDTA	Ethylenediaminetetraacetic acid
Endo H	Endoglycosidase H
EPME	Ethanolamine phosphate methyl ester
ER	Endoplasmic reticulum
ERES	ER-exit sites
ESI	Electrospray ionization
EtN	Ethanolamine
EtNP	Ethanolamine phosphate
F	Fluorophore
Fmoc	*N*-α-(9-Fluorenylmethoxycarbonyl)
FR	Folate receptor
FRET	Fluorescence resonance energy transfer
Gas1	Glycophospholipid-anchored surface protein
GlcN	Glucosamine
GlcNAc	*N*-acetylglucosamine
GlcNAc-PI	N-acetylglucosaminylphosphatidylinositol
GlcN-PI	Glucosaminylphosphatidylinositol
gp63	gp63 surface protein

GPI	Glycosylphosphatidylinositol
GPI-AP	Glycosylphosphatidylinositol anchored protein
GPI-GnT	Glycosylphosphatidylinositol -*N*-acetylglucosaminyltransferase
GPI-ET I-II	Glycosylphosphatidylinositol -ethanolamine phosphate transferase
GPI-MT I-IV	Glycosylphosphatidylinositol mannosyltransferases I-IV
GPI-T	Glycosylphosphatidylinositol transamidase
GST	Glutathione S-transferase
GTP	Guanosine-5'-triphosphate
HBTU	O-Benzotriazole-N, N, N' ,N'-tetramethyl-uronium-hexafluoro-phosphate
Hepes	4-(2-Hydroxyethyl)-1-piperazine ethanesulfonic acid
hGH	Human growth hormone
HPLC	High performance liquid chromatography
IgG	Immunoglobulin G
INV	Invertase
L. Mexicana	*Leishmania mexicana*
Man	Mannose
MALDI-TOF	Matrix assisted laser desorption / ionization time of flight
mRNA	Messenger RNA
MW	Molecular weight
NH_2NH_2	Hydrazine
NH_2OH	Hydroxylamine
NMP	N-methyl-2-pyrrolidinone

NMR	Nuclear magnetic spectroscopy
NTP	Nucleoside triphosphate
OD	Optical density
P. berghei	*Plasmodium berghei*
pCMPSA	p-chloromercuriphenylsulfate
PEG	Polyethelene glycol
PI	Phosphatidylinositol
PI-PLC	Phosphatidylinositol-specific phospholipase C
PLAP	Placental alkaline phosphatase
PMSF	Phenylmethylsulfonyl fluoride
Poly-Met	Poly methionine
PrP^{c}	Prion protein (normal)
PrP^{sc}	Prion protein (disease associated)
Q	Quencher
RG	Reduced glutathione
RM	Rough microsomes
RNA	Ribonucleic acid
S. cerevisiae	*Saccharomyces cerevisiae*
SD	Standard deviation
SDS-PAGE	Sodium dodecyl sulfate polyacrylamide gel electrophoresis
T. brucei	*Trypanosoma brucei*
TAP	Tandem affinity purification

TEV	Tobacco etch virus
TFA	Trifluoroacetic acid
Thy-1	Thy-1 cell surface antigen
TM	Transmembrane
Tris	tris(hydroxymethyl)aminomethane
TS	Temperature-sensitive
UP30	Urokinase type plasminogen activated receptor
VSG	Variant surface glycoprotein
WT	Wild type
Y21	Yapsin 2
YPD	Yeast peptone dextrose

Chapter 1

Introduction

Glycosylphosphatidylinositol Anchoring: An Essential Post-Translational Modification Mediated by GPI-T

1.INTRODUCTION

Glycosylphosphatidylinositol transamidase (GPI-T) is a multi-subunit, membrane-bound enzyme localized in the endoplasmic reticulum (ER) *(1)*. In eukaryotes, this enzyme mediates GPI (glycosylphosphatidylinositol) transamidation, an essential post-translational protein modification *(2-4)*. GPI-T utilizes a proprotein substrate with a C-terminal GPI-T signal sequence and a nucleophilic substrate (the GPI anchor) to mediate the GPI transamidation reaction (Figure 1.1).

During this process, GPI-T first recognizes and cleaves the C-terminal signal sequence of the proprotein substrate. Next GPI-T mediates the attachment of the GPI anchor to the new C-terminus of the protein substrate to produce the GPI anchored protein (GPI-AP) *(1)*. During this process, a new amide linkage is formed between the protein and the GPI anchor. GPI-APs are then transported from the ER to extracellular membranes/cell wall via intracellular secretory pathways.

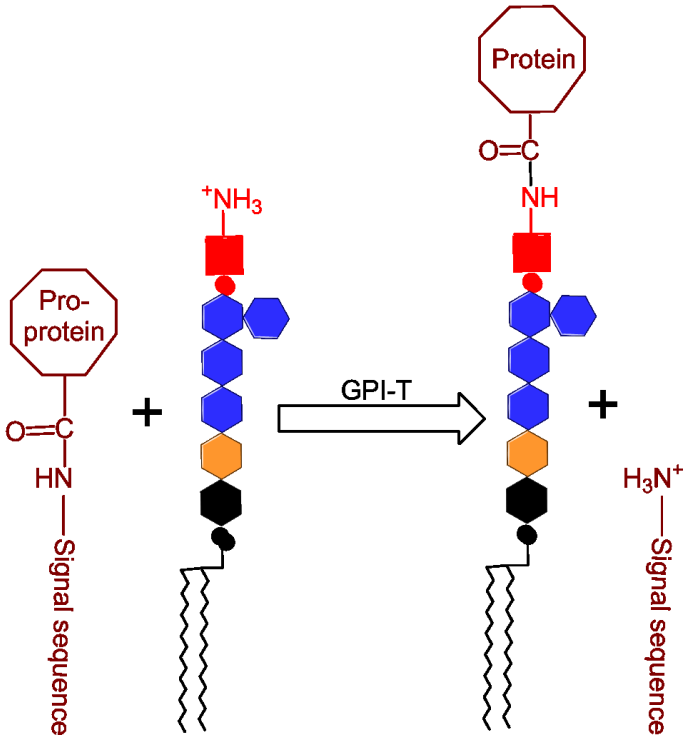

Figure 1.1 The GPI transamidation reaction. GPI-T mediates the attachment of a GPI anchor to a protein based on recognition and cleavage of the C-terminal GPI-T signal sequence to produce GPI-APs.

Roughly, 0.5% of proteins encoded in eukaryotes (10–20% of all membrane proteins) are predicted to be GPI anchored *(5,6)*. GPI-APs perform a wide variety of functions essential for the well-being of eukaryotic organisms (e.g. enzymes, receptors, etc). In yeast, GPI anchored cell wall proteins are necessary for cell viability and cellular morphology *(4,7)*. In parasitic protozoa, the high density of GPI-anchored glycoproteins acts as a protective coat against host specific immune responses *(8)*. In addition to GPI-APs contributions towards the well-being of eukaryotic organisms, GPI-T itself and several GPI-APs are associated with various disorders and diseases. For instance, overexpression of certain GPI-T subunits induces tumorigenesis *(9-11)* and deficiencies in GPI transamidation lead to paroxysmal nocturnal hemoglobinuria, an acquired hemolytic disease *(12,13)*.

GPI transamidation is an essential reaction for eukaryotic organisms *(2-4)*. However, because of being a structurally complicated, multi-subunit, transmembrane protein complex, little is known about GPI-T at a molecular level. So far five subunits have been identified which make the putative GPI-T complex *(1)*. In yeast, these subunits are Gpi8, Gpi16, Gaa1, Gpi17 and Gab1. The corresponding human homologues are PIG-K, PIG-T, GPAA1, PIG-S and PIG-U respectively. Gpi8/PIG-K is the catalytically active subunit; functions for the other subunits are not well established. Therefore, it is important to conduct further research to obtain a clear picture of the structure, stoichiometry, and the functions of the GPI-T subunits and hence the overall GPI-T complex.

1.1 The Substrates for GPI-T

1.1.1 GPI Anchor - the Nucleophilic Substrate for GPI-T

GPI anchors are group of complex glycolipids found in eukaryotic organisms. These anchors are essential for well being of eukaryotic organisms *(2,4,7,13-15)*. In eukaryotic cell, one major role of GPI anchors is as a substrate for GPI-T that is used to produce GPI-APs. These GPI-APs are ultimately tethered to extracellular membranes as peripheral proteins via their attached GPI anchor. In addition, GPI anchors are involved in a plethora of other biological roles. Such roles of GPI anchor include structural and conformational changes of GPI anchored proteins *(16,17)*, signal transduction *(18,19)*, cellular communication *(20)*, sorting of GPI-APs to different domains of cell membrane *(21,22)*, etc.

1.1.1a The Discovery of GPI anchor

The pathway to the discovery of the GPI anchor was initiated in 1976, when a new phospholipase was purified from *Bacillus cereus* by Ikezawa and coworkers *(23)*. This phospholipase, named phosphatidylinositol phospholipase C (PI-PLC), converts alkaline phosphatase (APase) from a membrane-anchored form to a completely soluble protein *(24)*. Following this discovery, several other isoforms of PI-PLC, all capable of releasing soluble APase from the membrane, were identified from different bacteria including *Staphylococcus aureus*, *Clostridium novyi* and *Bacillus thuringiensis (25-27)*. In addition to APase, treatment with PI-PLC converted other membrane-anchored proteins, including 5'-nucleotidase and erythrocyte acetylcholinesterase (AChE) into soluble forms *(28,29)* Interestingly, PI-PLC specific substrate proteins were not substrates for other phospholipases *(30)*. This observation indicated that the PI-PLC sensitive proteins were attached to the plasma membrane via an anchor containing phosphatidylinositol (PI).

The identification of other PI-PLC specific proteins, including variant surface glycoprotein (VSG) of *Trypanosoma brucei (31,32)*; rat brain and thymocyte Thy-1 *(33,34)*; *Torpedo* electric ray organ AChE *(35)*; and human erythrocyte AChE *(36)*; revealed many important aspects of the GPI anchor. For instance, analysis of the linkage and the membrane anchor of the rat brain and thymocyte Thy-1 revealed that this protein's C-terminal cysteine was connected to an ethanolamine (EtN) via an amide bond. Further, it also revealed that the membrane anchor of Thy-1 contained a glycan core and a phospholipid tail. This glycan core consists of glucosamine, galactosamine, mannose and *myo*-inositol residues and the

phospholipid tail consists of phosphate, glycerol and a stearic acid. Based on these findings and in combination with exoglycosidase digestions and structure analysis techniques such as nuclear magnetic spectroscopy (NMR), the first complete structure of the membrane anchor (GPI) of *Trypanosoma brucei* VSG *(37)* and the rat brain and thymocyte Thy-1*(38)* was elucidated in 1988 (Figure 1.2).

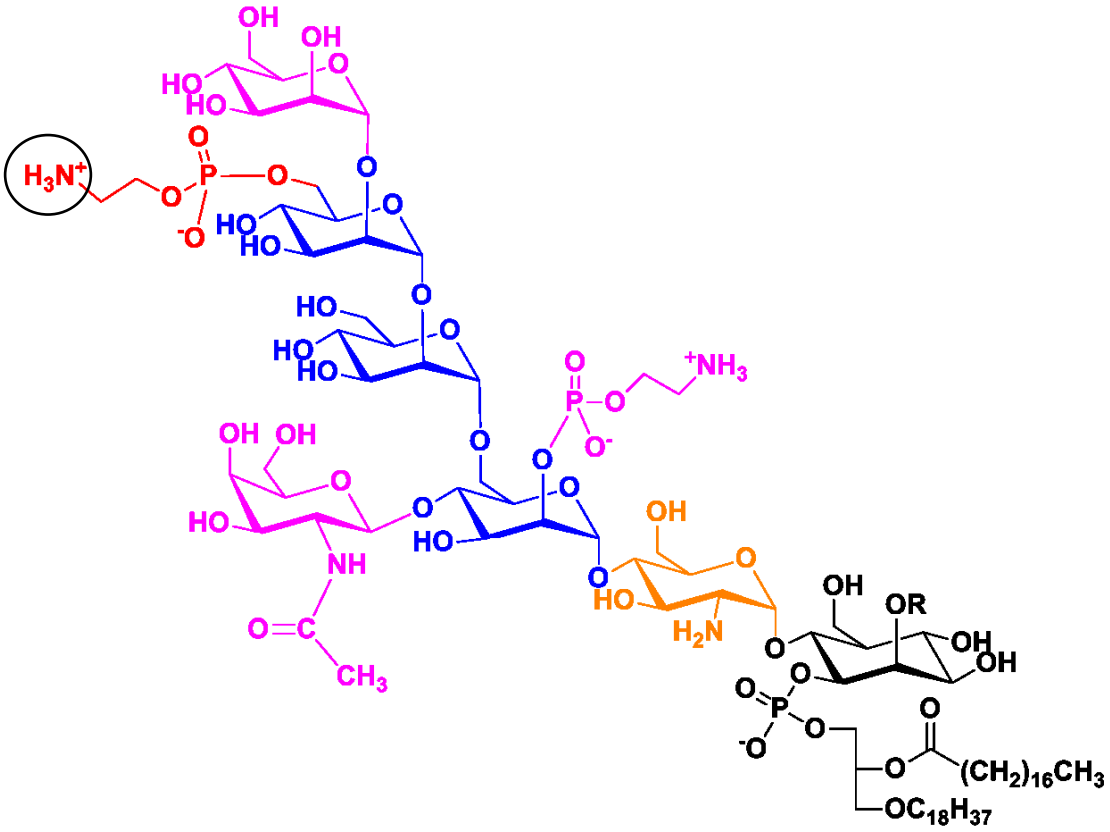

Figure 1.2 The structure of the rat brain and thymocyte Thy-1 GPI anchor. Phosphatidylinositol (black), glucosamine (orange), mannose 1, 2 and 3 (blue) and ethanolamine phosphate (red) represents the core GPI anchor of eukaryotic organisms. The structure of the lipid portion of the phosphatidylinositol can varied according to species and tissue of origin. Molecules highlighted in magenta are only part of Thy-1 GPI anchor and do not represents the eukaryotic GPI anchor core. The circled free amine group represents the nucleophile donor.

1.1.1b The Structural Diversity of GPI anchor

To date, complete structures of a diverse set of GPI anchors have been identified (Figure 1.3) *(39-44)*. All GPI anchors characterized so far have a common core structure: H_2N-$(CH_2)_2$-PO_4-6Man-(α1-2)-Man-(α1-6)-Man-(α1-4)-$GlcNH_2$-(α1-6)-*myo*-inositol-1-PO_4-lipid (Figure 1.2) *(45,46)*. Further modifications to this common core structure based on its protein, tissue, or species-specificity result in the structural diversity of GPI anchors *(30)*. Modifications occur frequently on the tetrasaccharide glycan core and the phospholipid tail of the GPI anchor, during its biosynthesis or after attachment to GPI anchoring proteins *(47)*. Attachment of additional carbohydrate side chains such as mannose, galactose and sialic acid, and extra phosphoethanolamine (EtNP) groups, are also known *(46,48-50)*. For most GPI anchors, the phospholipid tail contains a diacylglycerol *(31,51)*. However, in certain GPI anchors the phospholipid tail contains an alkylacylglycerol *(52-55)* or a ceramide moiety *(39,48,56,57)*. The length of the carbon chain and the level of saturation of these lipids vary based on the protein attached, and with tissue and species specificity *(48)*. Lipidation (acylation) at the 2'-hydroxyl position of the myo-inositol ring is also known *(58)*. This modification is significant, as it eliminates PI-PLC specificity.

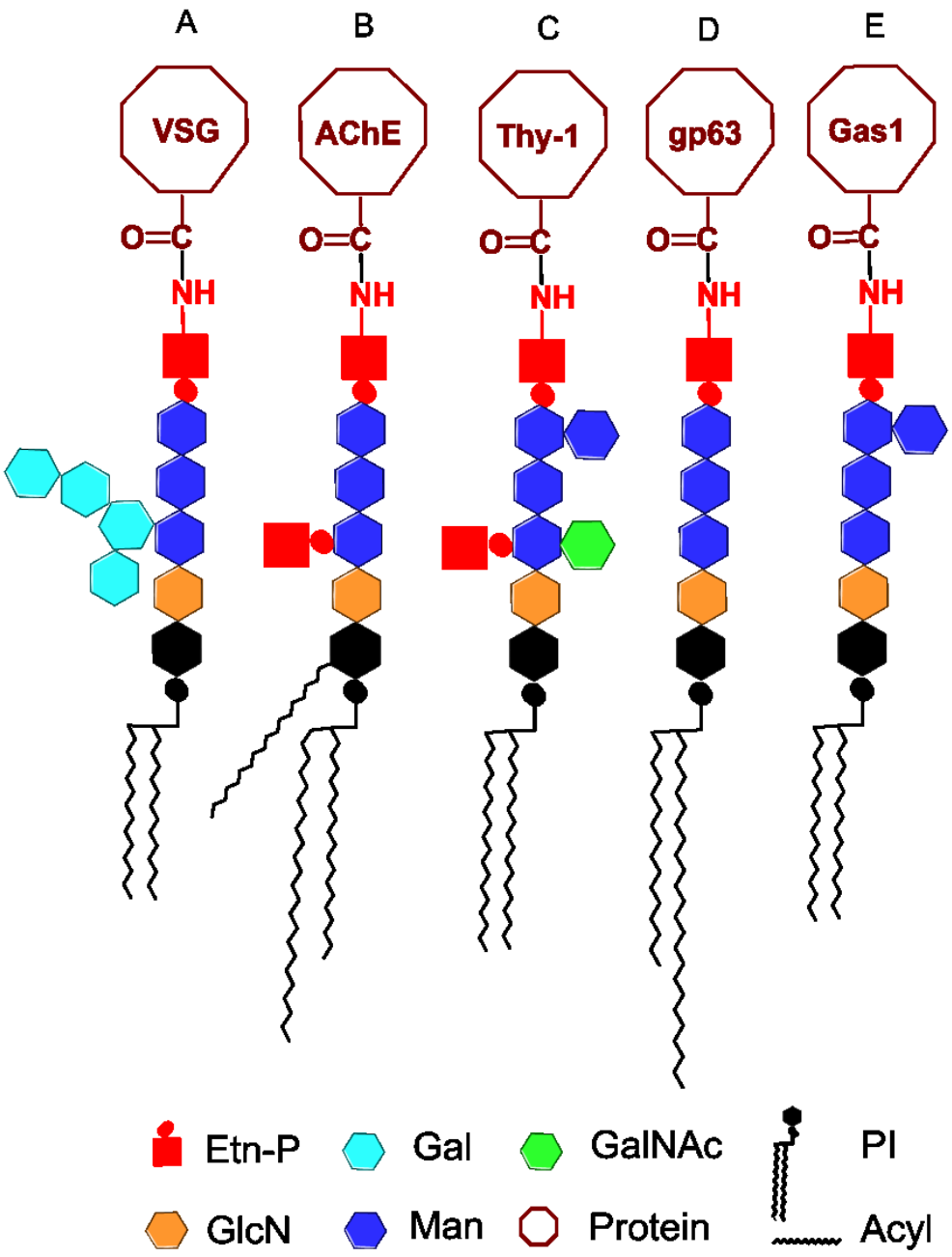

Figure 1.3 Structural diversity of GPI anchors. GPI-Aps of (A) *T.brucei* variant surface glycoprotein (VSG) (B) human erythrocyte acetylcholinesterase (AChE) (C) rat brain Thy-1 cell surface antigen (Thy-1) (D) *Leishmania major* gp63 surface protein (gp63) and (E) *S.cerevisiae* glycophospholipid-anchored surface protein (Gas1).

1.1.1c The Biosynthesis of GPI anchor

The assembly of the GPI anchor (Figure 1.4) is initiated at the cytoplasmic leaflet of the ER membrane.

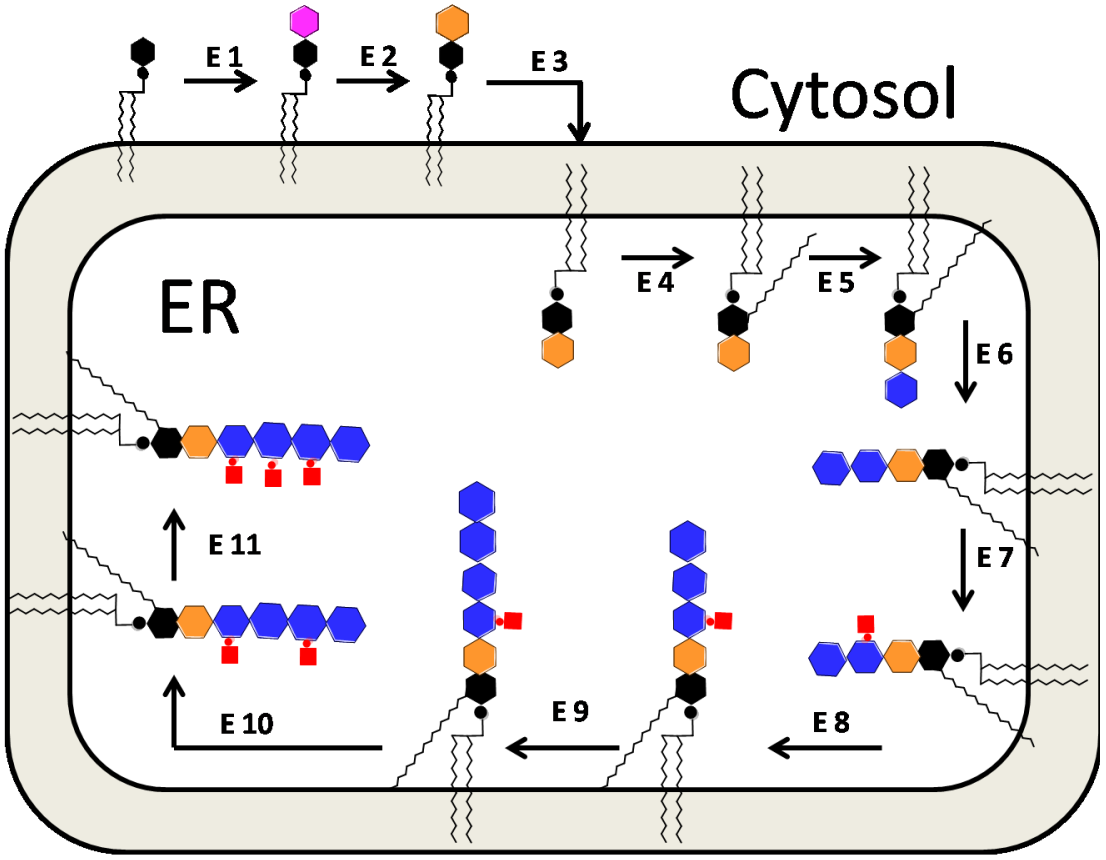

E 1 - GPI-GnT, **E 2** - GlcNAc-PI de-N-acetylase, **E 3** - Flippase, **E 4** - Inositol acyltransferase, **E 5** - GPI-MT 1, E 6 - GPI-MT II, **E 7** - GPI-ETI, **E 8** - PI -MTIII, **E 9** - GPI MTIV, **E 10** - GPI-ETII, **E 11** - GPI-ETIII

Figure 1.4 The GPI anchor biosynthetic pathway. This figure illustrates the general steps involved in GPI anchor biosynthesis in yeast and mammals. See text for further details.

First, an *N*-acetylglucosamine (GlcNAc) is added to phosphatidylinositol (PI). The PI is anchored to the cytoplasmic surface of the ER membrane via a

diacylglycerol *(59)*. This reaction is the first committed step in GPI anchor biosynthesis and generates N-acetylglucosaminylphosphatidylinositol (GlcNAc-PI). GlcNAc-PI production is mediated by GPI-*N*-acetylglucosaminyltransferase (GPI-GnT) *(60)*. The GlcNAc-PI is next deacetylated by GlcNAc-PI de-N-acetylase to generate glucosaminylphosphatidylinositol (GlcN-PI) *(61,62)*. In mammals and yeast, a flipping reaction, mediate by flippase, inverts GlcN-PI so that the GlcN is on the luminal side of the ER membrane *(63)*. The identity of this flippase has remained elusive. Interestingly, in *T. brucei,* flipping of GlcN-PI to ER lumen is not required. Instead, the last step in trypanosomal GPI anchor biosynthesis requires the corresponding intermediate to flip to the ER lumen to in order to undergo GPI transamidation *(64,65)*.

Next, the 2'-hydroxyl position of the inositol in GlcN-PI undergoes an acylation reaction (palmitoylation is most common) to produce GlcN-(acyl)-PI *(66-68)*. This reaction is mediated by an inositol acyltransferase and produces PI-PLC-resistant GPI anchors. Acylation enhances the efficiency of consequent mannosylation reactions *(66,69)*. The isoprenoid Dolicholphosphomanose (Dol-P-Man) provides the mannose residues required to construct the GPI glycan core *(70)*. A series of distinct mannosyltransferases (GPI-MT I-IV) *(71-79)* sequentially add each mannose to GlcN-(acyl)-PI. The first mannose (Man_1) is attached to GlcN-(acyl) PI via α1-4 linkage to produce Man_1-GlcN-(acyl)-PI; this reaction is mediated by α1-4 mannosyltransferase (GPI-MT I) *(71)*. In yeast and mammalian cells, the catalytically active site of GPI-MT I complex is on the luminal side of the ER. This enzyme indicates the importance of an early flipping of GlcN-(acyl) PI complex from the

cytosolic surface of the ER membrane to that of the lumenal surface *(43)*. The second mannose (Man_2) is attached to Man_1-GlcN-(acyl)-PI via α1-6 linkage to produce Man_2-Man_1-GlcN-(acyl)-PI. This reaction is mediated by α1-6 mannosyltransferase (GPI-MT II) *(74,75)*. The third mannose (Man_3) addition is mediated by α1-2 mannosyltransferase (GPI-MT III) that produces Man_3-Man_2-Man_1-GlcN-(acyl)-PI *(76,77)*.

Mutagenic studies revealed the existence of a Man_2-(EtNP)-Man_1-GlcN-(acyl)-PI, in which, an ethanolamine phosphate (EtNP) is attached to the Man_1 of the GPI glycan core. This modification, mediated by GPI-ethanolamine phosphate transferase (GPI-ET I), occurs prior to the attachment of the Man_3 to GPI glycan core *(50,80,81)*. This Man_1 modification is essential for GPI transamidation in yeast *(81)* but not in mammals or *T. brucei (80,82)*. A second EtNP is attached to the Man_3 of the glycan core to produce (EtNP)-Man_3-Man_2-(EtNP)-Man_1-GlcN-(acyl)-PI *(83,84)*. The free amine group (Figure 1.1, circled amine group) of this final EtNP attached to Man_3 is the nucleophile donor used in the GPI transamidation reaction. In yeast and certain mammalian cell lines, there is a stringent requirement for a fourth mannose group before addition of the EtNP to the Man_3 *(78,85)*. The enzyme α1-2 mannosyltransferase (GPI-MT IV) *(78,79)* mediates this reaction to produce Man_4-Man_3-Man_2-(EtNP)-Man_1-GlcN-(acyl)-PI. This reaction is followed by the addition of EtNP moiety to the Man_3 of the GPI anchor to produce the Man_4-(EtNP)-Man_3-Man_2-(EtNP)-Man_1-GlcN-(acyl)-PI. In addition to the EtNP groups attached to the Man_1 and Man_3 of the GPI anchor, a third EtNP is attached to the Man_2 *(86,87)*. In yeast,

this modification is important for ER to Golgi transport of GPI-APs, ceramide remodeling of the GPI phospholipid tail and to maintain cell wall integrity *(88)*.

The two structures, (EtNP)-Man_3-Man_2-(EtNP)-Man_1-GlcN-(acyl)-PI and Man_4-(EtNP)-Man_3-Man_2-(EtNP)-Man_1-GlcN-(acyl)-PI represent the minimalist GPI anchors of eukaryotic organisms. These structures can act as nucleophilic substrates for GPI transamidase to produce GPI-APs or can exist as free GPIs on extracellular membranes *(89)*. Further modifications can be introduced to the GPI anchor, even after its attachment to proteins. Such modifications, including inositol deacylation and lipid remodeling, will be discussed later in this chapter.

1.1.1d GPI Anchor Mimics to Substitute the GPI Anchor

GPI anchors are ubiquitous to eukaryotic systems. However, the extraction of GPI anchors from biological systems with high yield and purity is very challenging. As an alternative, currently there exist several synthetic pathways to construct GPI anchors and various derivatives *in vitro (90-101)*.These synthetic strategies provide an invaluable approach to successfully construct full-length GPI anchors and anchored peptides. However, large-scale production of GPI anchored products is challenging and still an ongoing problem. Further, the amphipathic nature of both natural and synthetic full-length GPI anchors restricts their use in soluble *in vitro* experiments.

Due to the challenges associated with the use of full-length GPI anchors, GPI-T researches seek GPI anchor mimics to substitute the GPI anchor. Inspired from the work of S. S. Tate and A. Meister *(102)*, in 1995, Udenfriend and co-

workers employed small nitrogen nucleophiles, such as hydrazine and hydroxylamine, to mimic the GPI anchor *(103,104)*. In *in vitro* assay systems, high concentrations of these mimics were successfully used as substrates in the GPI transamidation reaction. These small compounds were attached to the correct amino acid in the protein substrate in a manner that was analogous to that of the GPI anchor *(105)*.This discovery opened up a new avenue to characterize various aspects of GPI transamidation using more convenient soluble assay systems. The awareness that small molecules can substitute for the GPI anchor opened doors for the synthesis of simplified, but more realistic, soluble GPI anchor mimics to replace GPI anchors in *in vitro* studies *(97,106)*.

1.1.2 The Protein Substrate for GPI-T

The discovery of proteins post-translationaly modified with C-terminal GPI anchors was initiated in the late 1970s, when two research groups independently demonstrated the release of membrane bound alkaline phosphatase by bacterial PI-PLC treatment *(23,24)*. As detailed in section 1.1.1a, this experiment ultimately led to the identification of GPI anchor and the discovery of a diverse set of GPI-APs. Hundreds of proteins have been identified or predicted to be GPI anchored to date *(5,6)*. These proteins are first synthesized in the cytosol, as a preproprotein with a canonical N-terminal ER localizing signal sequence and a C-terminal GPI-T signal sequence *(107)*. The N-terminal signal sequence directs co-translational translocation of the precursor preproprotein to the ER lumen *(108,109)*. This localizing signal sequence is then cleaved by signal peptidases and the

preproprotein is converted to a proprotein. The cleaved N-terminal sequence is not a prerequisite for consequent GPI anchor attachment *(110)*. The C-terminal GPI-T signal sequence is important to target the proprotein substrate to the GPI-T and for GPI-T to recognize it's substrate proteins *(107,109)*. This signal sequence is not a consensus sequence. However, it can be divided into three key identity regions (Figure 1.5). These regions include the GPI-T cleavage and anchor attachment region (the so-called ω region, 3 amino acids), a hydrophilic spacer region (10-12 amino acids) and a terminal hydrophobic region (12-20 amino acids).

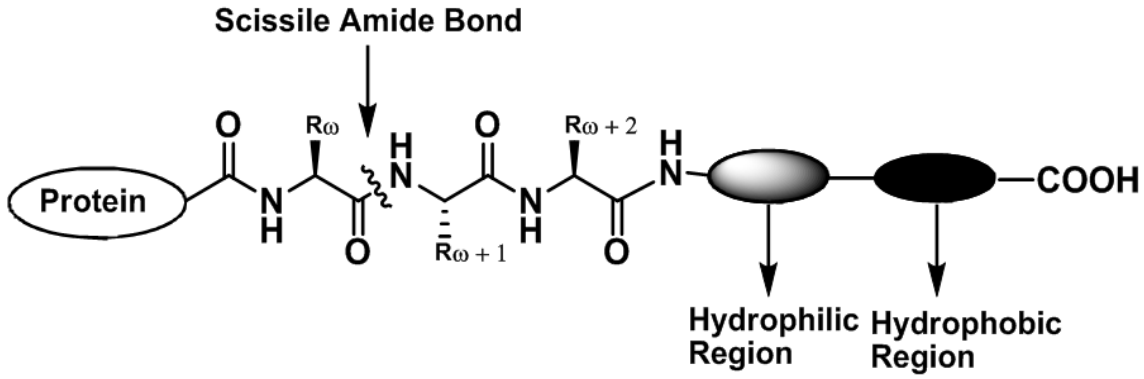

Figure 1.5 The protein substrate for GPI-T. The C-terminal GPI signal sequence begins at the ω site and is followed by stretches of hydrophilic and hydrophobic amino acids.

1.1.2a The ω Region

The ω region begins with a ω amino acid followed c-terminally by the ω+1 and ω+2 residues. GPI-T cleaves the amide bond between the ω and ω+1 positions, replacing the C-terminal peptide (from the ω+1 position to the C-terminus) with the GPI anchor. Site directed mutagenesis experiments to characterize the ω site were performed by various research groups *(111-118)*. Using nascent human placental

alkaline phosphatase (PLAP) and a minimalistic version of PLAP called miniPLAP, Udenfriend and co-workers evaluated the amino acid requirements at the ω site. The native ω site in wild-type PLAP is Asp484 (Asp179 in miniPLAP). When this position was mutated to glycine, alanine, cysteine, serine, or asparagine, the mutants were expressed well and the resultant protein was GPI anchored. However, mutation to glutamic acid, glutamine, proline, tryptophan, leucine, valine, phenylalanine, threonine, methionine, and tyrosine produced proproteins that were not converted to GPI-APs *(111-114)*.These results suggested that the ω site residue must be relatively small.

A similar set of experiments were carried out by Caras and co-workers *(115,116)*. They developed the fusion protein hGH-DAF, by appending the C-terminal GPI signal sequence of human decay accelerating factor (DAF) onto the C terminus of human growth hormone (hGH), a secretory protein. Site directed mutagenesis of the Ser319 ω site of DAF to alanine, aspartate, asparagine and glycine allowed for efficient GPI anchoring compared to mutations to either valine or glutamate. However, in contrast to the results of Udenfriend and co-workers, mutation to cysteine completely abolished GPI anchoring of hGH-DAF. In summary, these and other experiments led to the conclusion that the ω site amino acid should be a small and relatively hydrophobic amino acid for recognition by GPI-T.

A similar approach was used to characterize the amino acid specificity at the ω+1 and ω+2 residues *(117-120)*. In 1992, the amino acid specificity at ω+1 site was investigated using an *in vitro* cell free system built from rabbit reticulocyte lysates and rough microsomes (RM), using preprominiPLAP as the protein substrate

(120).This preprominiPLAP construct was designed by removing a significant amount (2/3) of internal sequence of humanPLAP. However, the N and C-terminal regions, which represent the pre and pro regions of hPLAP was retained as it is on preprominiPLAP. In the natural construct of preprominiPLAP, Asp179, Ala180 and Ala181 represent the ω, ω+1 and ω+2 sites, respectively. Mutations at Ala180 to Asp, Ser, Cys, Met, Thr, Glu, Arg, and Trp were well tolerated; however, mutation to proline eliminated GPI-T recognition and processing. Mutational studies at ω+1 and ω+2 were also carried out *in vivo* using wild type PLAP cDNA transfected to COS cells *(119)*. In conclusion, all of these studies revealed that the ω + 1 site tolerates all amino acids except proline, with a preference for small amino acids *(117,118)*. The amino acid specificity at ω+2 site is more stringent and restricted to very small amino acids including Ala, Gly, Ser and Cys *(117-120)*. In fact, alanine and glycine are optimal at ω+2 site although trace activity was observed with cysteine and serine *(120)*.

1.1.2b The Spacer Region

The ω region is followed by a stretch of hydrophilic amino acids also known as the spacer region. Mutational analysis of the GPI-T signal sequences of human DAF *(116,121)*, bovine liver 5'-nucleotidase *(122)*, *S. cerevisiae* Gas1*(57)*,*(118)*, and the unnatural signal sequence Ser_3-Thr_8-Leu_{14} appended to cluster of differentiation 46 protein (CD46) *(117)* revealed much about this spacer region. According to those facts, the spacer region does not contain any consensus sequence. However, the length (6-14 amino acids) and the relative hydrophilicity of this region is important for

both GPI-T recognition and consequent GPI anchoring *(111,115-117,121,122)*. In addition, spacer region may have a role in locating the ω site to the active site of GPI-T*(122)*.

1.1.2c The Hydrophobic Region

The C-terminal hydrophobic region is the third key element of the GPI-T signal sequence. The overall hydrophobicity and the length of this region are critical parameters for the proprotein substrate to be recognized and anchored by GPI-T *(123-126)*. Truncations and point mutations that diminished the hydrophobicity of the C-terminal region both eliminated GPI anchoring *(57,117,124,125)*. The remarkable ability of the Ser_3-Thr_8-Leu_{14} to direct GPI anchoring further revealed that hydrophobicity is the driving feature of this region *(117,127)*. In addition to the importance of this region for GPI-T to recognize the proprotein substrate, it is also involved in targeting the propeptide to GPI-T. For this purpose, during the GPI transamidation, the C-terminal hydrophobic region temporally anchored to the inner leaflet of the ER membrane. This attachment facilitates the proper orientation of the ω region residues at the active site of GPI transamidase *(122,127)*.

Overall, the complete GPI-T signal sequence is not a consensus sequence but rather a pattern of small, hydrophilic and hydrophobic residues. However, amino acid variations in the GPI signal sequence of GPI-APs and along with active site variations in GPI-T likely contribute to the apparent substrate and species specificity exerted by GPI-T *(128-131)*. In addition to the role of this signal sequence for directing the attachment of precursor proteins to the GPI anchor, GPI-T signal

sequence also have a role in regulating the confirmation and function of its precursor proteins *(132)*. This phenomenon was investigated using Als5 protein of *Candida albicans,* a GPI anchoring protein. The study revealed that the Als5 proteins with and without GPI signal sequence acquire two different confirmations with functional variations *(132)*.

1.2 The GPI Transamidase Complex

The discovery of GPI anchors and GPI-APs was followed by an array of investigations to elucidate the GPI anchoring process and to identify the enzyme that mediates it. Evidence suggesting that the putative enzyme is a transamidase arose from a series of *in vivo* and *in vitro* experiments *(103-105,133-136)*. These findings revealed that the enzyme, now called GPI transamidase or GPI-T, proceeds via formation of an activated carbonyl intermediate, like a protease. The intermediate is susceptible to immediate nucleophilic attack by a GPI anchor (or a suitable nucleophile donor under artificial conditions) and reaction happens without any energy source. Further, the process required only a single enzyme confirming that GPI-T is indeed a transamidase.

GPI-T is localized in the ER as multimeric protein complex *(137)*. There are five protein components that make up the GPI-T complex (Figure 1.6) *(1,138)*.

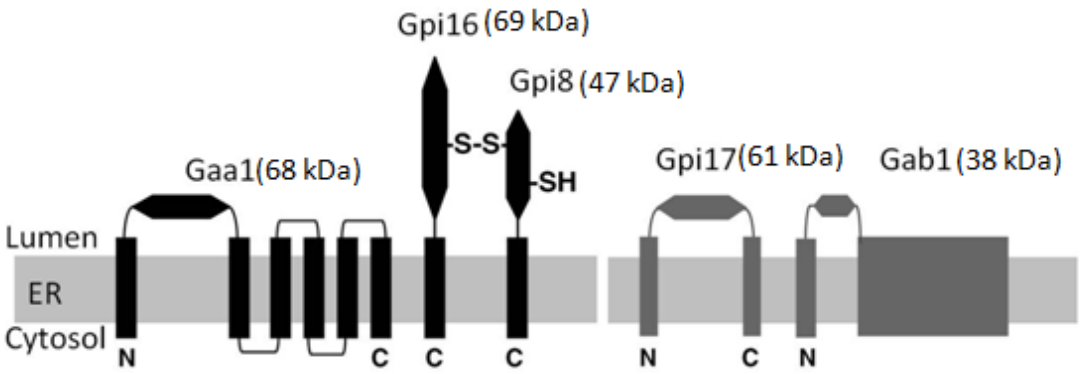

Figure 1.6 The GPI-T complex. The predicted transmembrane domains for each subunit are shown as rectangles spanning the ER membrane bilayer, which is represented in light grey. The subunits in black are found in all eukaryotes, whereas the subunits in dark grey are found in humans and yeast, but not in trypanosomes.

The subunits Gpi8, Gpi16, Gaa1, Gpi17, and Gab1 are found in yeast and their respective homologues, PIG-K, PIG-T, GPAA1, PIG-S and PIG–U, are found in humans *(1)*. The subunits, Gpi8, Gpi16, and Gaa1, are ubiquitous in eukaryotes, however, Gpi17 and Gab1 are absent from trypanosomes *(139)*, where they are replaced by two unique subunits - TTA1 and TTA2 *(139)*. TTA1 and TTA2 have no sequence homology to Gpi17 and Gab1. However, they possess similar membrane topologies.

1.2.1 The Subunits of GPI-T

Identification of the GPI-T subunits was challenging and utilized a combination of genetic, molecular biology and biochemical approaches. Gaa1 and Gpi8 were the first subunits identified. Co-immunoprecipitation experiments lead to the identification of rest of the GPI-T subunits including Gpi17, Gab1 and Gpi16 *(138,140,141)*. In *S. cerevisiae* the subunits Gaa1 and Gpi16 co-immunoprecipitate with GST tagged Gpi8 forming a heterotrimeric complex *(138)*. The subunits Gpi17

and Gab1 of *S.cerevisiae* do not interact with the heterotrimeric complex and exist as a heterodimer *(140)*. In humans expression of FLAG-GST-hGPI8 lead to co-immunoprecipitation of subunits GPAA1, PIG-S and PIG-T *(141)*. Further, in humans it is also revealed (via mutational analysis) that the GPI-T complex to be functional it should also associate with PIG-U. Thus, in contrast to *S.cerevisiae* GPI-T, human GPI-T exists as a heteropentamer.

The gene *GPI8*, which encodes for Gpi8, was first identified from *Saccharomyces cerevisiae* using a temperature-sensitive (TS) mutant strain *(142)*. This strain is unable to express GPI anchored proteins on the cell surface but produced full-length GPI anchors. However, when transformed with yeast chromosomal DNA, GPI anchoring activity was restored and the complementing gene was identified as *yGPI8 (143)*. In yeast, deletion of this gene is indicating that GPI anchoring is an essential function in yeast *(143)*.The human homologue of *GPI8, hGPI8* was isolated using a similar genetic approach to that of *yGPI8 (143)*. The class K mutant strain, lacking a functional *hGPI8* gene, efficiently expressed mature GPI anchors but was unable to produce GPI-APs *(144,145)*. *yGPI8* was able to restore GPI anchoring activity in the class K cell line, indicating that *yGPI8* and *hGPI8* are homologues *(145)*. A forward genetic approach was used to identify the corresponding *GPI8* gene in trypanosomes. Mutation of trypanosomal *GPI8* was not lethal; however, it affected pathogenesis *(146)* due to the lack of GPI anchored protein procyclin. In *T.brucei* GPI anchored procyclin act as a protease-resistant protective coat against enzymes secreted from the midgut of tsetse fly. This protection is important for *T.brucei* survival and to establish infections *(14,146,147)*.

In yeast and humans, Gpi8 is a type I transmembrane protein with a large lumenal domain and a single transmembrane (TM) domain *(138,143,145)*. In protozoans, Gpi8 is soluble and does not contain a TM domain *(148,149)*, hinting that the Gpi8 TM domain is not involved in Gpi8's function *(150)*. Gpi8 is a 47 kD protein with 25–28% sequence homology to a family of cysteine proteases, especially to that of C13 family *(138,151)*. In addition, the active site of Gpi8 shows weak sequence similarity to caspases, especially to caspase-1 *(151)*. Recent work by our group demonstrated that Gpi8 has organizational similarity to caspases as well as it undergoes homodimerization *(152)*. The enzymatic contribution of Gpi8 towards GPI transamidation was investigated using several reporter assays *(150,153-155)*. The production of GPI-anchored VSG was restored in Gpi8-depleted *T. brucei* ER membranes by the addition of recombinant *Leishmania mexicana* Gpi8 *(150)*, indicating the direct contribution of Gpi8 towards GPI anchoring of proproteins. Gpi8's role in the proteolytic processing of proprotein substrates was confirmed in an *in vitro* fluorescence assay, which utilized a fluorogenic peptide substrate acetyl-S-V-L-N-aminomethyl-coumarine *(153)*. Recombinant TbGpi8 was able to process this synthetic substrate, causing an increase in coumarine fluorescence. Gpi8 was also observed to be physically associated with precursor protein substrate prominiPLAP in an assay performed with semi-permeabilized K562 cells**.** This association was not observed when the assay performed with *GPI8* knockdown class K mutant cell line *(155)*.

The active site of Gpi8 was preliminarily identified based on its sequence homology to cysteine proteases (the C13 family of cysteine proteases and caspase-

1). These proteases carry a cysteine:histidine catalytic dyad and use a general acid/base catalytic mechanism to cleave substrate proteins *(156,157)*. All forms of eukaryotic Gpi8, including yGpi8, hGpi8 and LmGpi8, had conserved cysteine and histidine residues *(148,151,158)*. The conserved residues were investigated using mutagenic analysis to identify the putative Cys:His pair for catalysis. For instance, yGpi8 contains two conserved cysteine residues (C85 and C199) and two histidine residues (H57 and H54) *(151)*. These residues were individually mutated to alanine and analyzed for their ability to promote GPI anchoring activity in *GPI8* depleted cell lines or in TS strains. The expression of yGpi8, containing C199A or H57A point mutations, did not have GPI anchoring activity, suggesting that these positions make up the putative catalytic dyad. Similarly, in human cells, mutation at the potential amino acids C92, H164 and C206 revealed that H164 and C206 comprised the catalytic dyad *(158)*. In trypanosomes, conserved residues H174 and C216 are responsible for catalysis *(148)*. These results revealed that Gpi8 is the catalytically active subunit of GPI-T. However, it is catalytically inert in the absence of other GPI-T subunits *(152)*.

The gene encoding Gaa1, *GAA1,* was first identified from a temperature sensitive *S. cerevisiae* strain using similar methods as described for yGPI8 *(159)*. These strains were unable to incorporate metabolically labeled GPI (containing [^{3}H] inositol) onto Gas1p, a known GPI-AP. Complementation with a plasmid carrying *yGAA1* restored GPI anchoring activity and mature Gas1-GPI was detected by SDS-PAGE. Based on these evidences, Gaa1 is important to incorporate GPI anchor to

GPI anchoring proteins. The corresponding human *(158,160,161)* and trypanosomal *(139) GAA1* were identified based on sequence similarities to that of *yGAA1*.

Gaa1 is an ER-oriented protein with several C-terminal transmembrane domains (TM), a large lumenal domain and a single N-terminal transmembrane domain (Figure 1.6) *(149)*. Yeast Gaa1 is a 70 kD protein with six TM domains, while human Gaa1 is a 68 kD protein with seven TM domains *(149)*. The structure-function relationship of different Gaa1 domains were analyzed using C-terminally truncated human Gaa1 mutants *(162,163)*. According to these studies, the large lumenal domain of Gaa1 is sufficient to interact with other subunits in the GPI-T complex. However, the assembled GPI-T complex was functionally defective in the absence of the C-terminal TM domains of Gaa1. Immunoprecipitation studies also revealed that this GPI-T complex could still interact with proprotein substrates but not with the GPI anchor *(162)*. Further experiments revealed that the last TM domain of Gaa1 likely interacts directly with the GPI anchor. This interaction is important as it facilitate recruitment of GPI to GPI-T in order to participate in GPI transamidation. A conserved proline residue in this last Gaa1 TM domain has been proposed to act as a dynamic hinge during requirement of the GPI anchor *(163)*.

In 2001, two new GPI-T subunits, named Gpi16/PIG-T and Gpi17/PIG-S were identified from yeast and humans *(138,141)*. The expression of a glutathione-*S*-transferase (GST) tagged *GPI8* in a GPI8 knockout *S. cerevisiae* strain enabled affinity purification and characterization of GPI-T *(138)*. SDS-PAGE analyses of this protein complex, followed by silver nitrate staining, revealed three distinct bands *(138)*. Tryptic digestion followed by mass spectroscopy identified these bands

correspond to proteins GST-Gpi8, Gaa1, and a new protein YHR188c, which was later named Gpi16 in yeast. In a similar manner, the expression and affinity purification of *FLAG-GST-hGPI8* in *GPI8*-depleted class K mutant cells led to the co-precipitation of four proteins *(141)*. The proteins co-precipitated with Gpi8 include Gaa1 and two new proteins. The two new proteins were later named PIG-S and PIG-T *(141)*.

Gpi16/PIG-T is a type 1 transmembrane protein with an N-terminal ER localizing sequence, a large lumenal domain, and a C-terminal transmembrane *(138)*. Yeast Gpi16 is a 69 kD protein *(138)*. Its homologues from other eukaryotic organisms have a similar hydrophobicity profile with amino acid lengths that vary from 531-639 amino acids *(141,164)*. Treatment of Gpi16 with endoglycosidase H (Endo H) caused a decrease in observed mass revealing that Gpi16 is a glycoprotein with two N-glycosylation sites *(138)*. Mutational studies with human *GPI8* and *PIG-T (the human GPI16 homolog)* revealed the existence of a disulfide linkage between these two subunits *(164)*. Upon expression of *GST- GPI8*^{C92S} in *GPI8*-deficient class K mutant cells, co-immunoprecipitation of PIG-T with Gpi8 was disrupted. Similarly the mutant *PIG-T*^{C182S} did not interact with Gpi8 indicating the existence of a disulfide linkage between Cys192 of Gpi8 and Cys182 of PIG-T. This disulfide bond might form a funnel that gates the access of proteins to the active site of Gpi8 *(164)*. However, GPI-T containing either *GPI8*^{C92S} or *PIG-T*^{C182S} in *ΔGPI8* or *ΔPIG-T* mutant cell lines, respectively, was capable of producing trace amounts of mature, GPI-anchored miniPLAP *(164)*. Hence, this covalent interaction is important, but not essential for GPI anchoring activity. Further Gpi16 is involved

in stabilizing the GPI-T as depletion of Gpi16 led to reduced expression of GPI-T subunits, Gaa1 and Gpi8 *(141)*.

Gpi17 is a 61 kD, glycosylated transmembrane protein *(140)*. Its large soluble domain is lumenally oriented *(140)* and flanked by two transmembrane domains so that both the N and C termini of Gpi17 are cytosolically oriented *(140)*. In humans, PIG-S (the human GPI17 homolog) is associated with the rest of the GPI-T subunits in stoichiometric ratios *(141)*. In contrast, no stoichiometric level association is observed between yeast Gpi17 with subunits Gpi8, Gaa1 and Gpi16 *(140)*.

Even though the exact functions of Gpi16/PIG-T and Gpi17/PIG-S are not known, these two subunits are essential to the GPI anchoring process *(141)*. Depletion of either subunit causes accumulation of GPI anchor and proprotein, indicating a dramatic reduction in GPI-T activity. Gpi16 is sensitive to depletion of other GPI-T subunits *(140)*. Further Gpi16 and Gpi8 depend on each other for stability *(138)*. In contrast, Gpi17/PIG-S stability and its GPI anchoring function is slightly affected only with Gaa1 depletion *(140)*. These observations suggest that Gpi17 might not be part of the catalytically functional unit of yeast GPI-T.

PIG-U/Gab1 is the fifth GPI-T subunit. PIG-U was first identified from a chemically mutated Chinese hamster ovary (CHO) cell line that was deficient in cell surface expression of GPI anchored proteins *(165)*. Transfection with genes corresponding to any of the known human GPI-T subunits did not restore the GPI anchoring activity. This observation indicated the need for another subunit. Complementation with a rat cDNA expression library led to the identification of the complementing gene *PIG-U* and hence the fifth subunit of GPI-T. Nearly

simultaneously, the corresponding yeast subunit Gab1 was identified from a yeast strain defective in cellular morphogenesis *(166)*.

Gab1 is a 38 kD, highly hydrophobic protein with several transmembrane domains and a very small putative soluble domain (~50 amino acids). The number of estimated TM domains varies between 8 and 10. Due to the high hydrophobicity of Gab1 and its sequence similarity to that of fatty acid elongase, it has been speculated that Gab1 might be involved in recognizing the fatty acid in the GPI anchor, presenting it to the active site of Gpi8 *(165)*. This was supported by the fact that in humans, the GPI-T complex can assemble in the absence of PIG-U, but it is non-functional in GPI anchoring of proprotein substrates *(165)*.

With the identification of the subunit Gab1, we now able to predict the structural arrangement of GPI-T complex to a certain extent. In humans expression, and two step affinity purification of *FLAG-GST-hGPI8* revealed that the subunits, PIG-T, GAA1, PIG-U and PIG-S co-immunoprecipitate with PIG-K confirming human GPI-T is a pentamer. In contrast, yeast GPI-T complex composed of two sub complexes a heterotrimer *(138)* and a heterodimer *(140,166)*. In trypanosomes, GPI-T consists of five subunits. Three of the trypanosomal subunits are homologues to subunits Gpi8, Gaa1 and Gpi16 while Gab1 and Gpi17 are replaced with two unrelated subunits TTA1 and TTA2 *(139)*. Overall, the subunits Gpi8, Gaa1 and Gpi16 are found in all forms of GPI-T. Therefore, we can speculate that these subunits are the core components of GPI-T complex. However, in the absence of experimental data with a pure soluble form of GPI-T we cannot draw conclusions about the GPI-T structure.

1.2.2 The Mechanism of GPI Transamidation

Gpi8/PIG-K is the catalytically active subunit and its sequence homology to cysteine proteases led to propose the mechanism of GPI transamidation. Mutagenetic studies revealed that Gpi8/PIG-K contains conserved cysteine and histidine residues that are essential for activity and presumably comprise the catalytic dyad *(148,151,158)*. In addition, different experiments revealed that the Gpi8 is physically interacting with the proprotein substrate via a thioester intermediate *(150)*. For instance, the conversion of pro-VSG to VSG-hydrazine by *L. mexicana* His-tagged Gpi8 in a cell free system was abolished by treatment with the thiol alkylating reagent iodoacetamide providing evidence for the formation of a thioester intermediate *(150)*. These results supported the similarity between mechanisms of cysteine protease with that of GPI-T. The only difference is that GPI-T uses the GPI anchor instead of water to complete the reaction (Figure 1.7).

According to the proposed mechanism, the histidine residue acts as a base to deprotonate the cysteine thiol. The thiolate nucleophilically attacks the carbonyl carbon of the ω amino acid, forming a thioester and releasing the C-terminal signal sequence. Consequently, a second nucleophilic attack, by the free amine of the ethanolamine in the GPI anchor, cleaves the thioester bond to form an amide linkage between the GPI anchor and the protein.

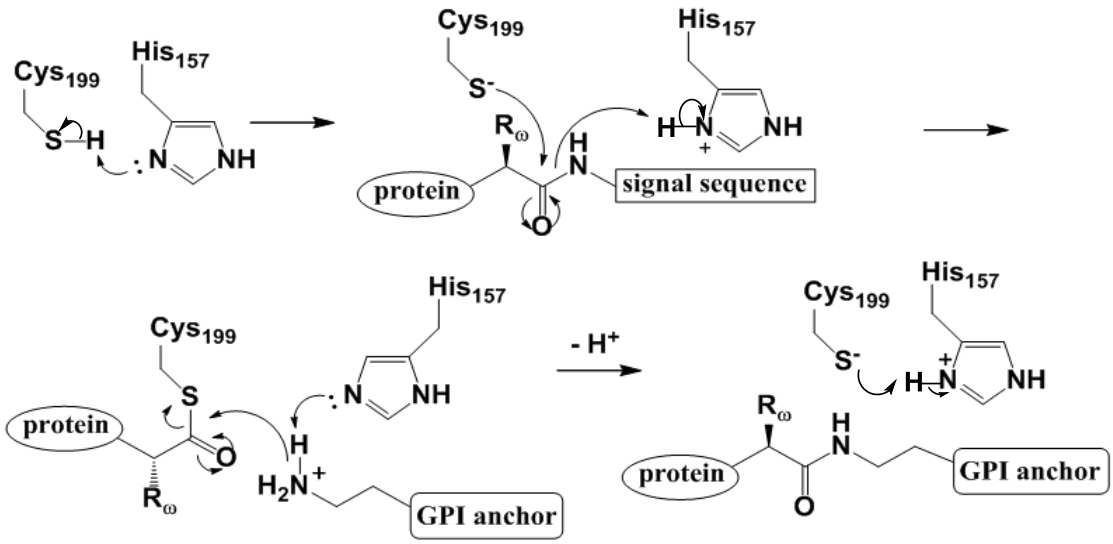

Figure 1.7 The proposed reaction mechanism for GPI-T. Deprotonation of the catalytic cysteine residue by histidine facilitates the nucleophilic attack, formation of a thioester bond and release of the C-terminal GPI-T signal sequence. A secondary nucleophilic attack by the free amine of EtNP cleaves the thioester bond and forms a new amide bond between the protein and the GPI anchor.

1.3 The GPI Anchored Proteins (GPI-APs)

In eukaryotes, proteins can associate with the extracellular membrane via different means. GPI anchoring of proteins offers one method that is distinct from lipidation or the addition of transmembrane domains GPI anchoring proteins are co-translationally translocated to the ER lumen as preproproteins. At ER the N-terminal ER localizing signal sequence is cleaved by signal peptidase. The resulted proprotein then undergo GPI transamidation at the inner leaflet of the ER to produce GPI anchored proteins *(107-110)*. GPI-APs are typically transported through the

secretory pathway to the extracellular membrane and perform a diverse set of physiological functions as detailed below.

1.3.1 Intracellular Transport of GPI-APs

GPI-APs attached to the inner leaflet of the ER membrane, exit the ER and are transferred to the extracellular membrane via the Golgi network. During this journey, the GPI anchor plays a major role as a sorting signal. First, it functions as an ER exit signal *(167-169)*. Next, in the Golgi, it acts as a sorting signal in combination with other sorting signals from the attached protein to direct the GPI-APs to different domains of the cell membrane. In order to act as a signal, the GPI anchor in GPI-APs undergoes two structural modifications *(170)*. These include the removal of the acyl chain linked to the inositol ring of the GPI anchor (a reaction catalyzed by inositol deacylase) and the removal of the EtNP attached to the second mannose in the anchor *(171,172)*. Inability to perform either of these modifications lead GPI-APs to accumulate in the lumen of the ER followed by degradation.

GPI-APs with suitable export signals leave the ER at ER-exit sites (ERES) and are transported to the Golgi via coat protein complex II (COPII) vesicles *(173)*. GPI-APs lack transmembranes; as a result, there is no direct loading of GPI-APs to COPII vesicles. Hence, cargo receptors (p24 family protein complex) are needed *(174)*. These receptors first interact with GPI-APs at ERES. Then these GPI-AP loaded cargo receptors concentrate into COPII vesicles. Upon transportation to the cis-Golgi compartment the cargo receptors load GPI-APs into the golgi complex and then they dissociate from the GPI-APs, a process that is mediated by pH changes.

The cargo receptors are then recycled back to ERES via coat protein complex I (COPI) vesicles *(173)* to initiate another cycle.

The sorting mechanisms in the trans Golgi network determine the final destinations of different GPI-Aps (apical *vs*. basolateral domains of the plasma membrane) *(175-177)*. However, this process remains poorly understood. Most GPI-APs are ultimately localized to the apical domains of the plasma membrane *(177)*. Originally it was suggested that the GPI anchors of GPI-APs act alone as apical sorting signals *(175,176)*. Later it was shown that at trans Golgi network fatty acid remodeled GPI-APs are recruited to the lipid micro domains/lipid rafts. This lipid raft/GPI-AP combination may act as an apical sorting signal *(178)*. Here, saturated fatty acid chains in the PI of the GPI anchor interact with ceramides in the lipid rafts. Recently it was shown that recruitment of GPI-APs to lipid rafts further facilitate the oligomerization of GPI-APs via its protein domains and hence provide a combined effect for apical sorting machinery operated within the trans golgi network *(179,180)*. It has also been proposed that the N-glycans and O-glycans on GPI-APs also can act as apical sorting signals to direct GPI-APs from the Golgi to plasma membrane *(181,182)*. However there exist contradictory opinions towards the roles of these glycans *(183)*.

In fungi, certain GPI-APs are ultimately covalently integrated into the cell wall *(7)*. For instance, in *S. cerevisiae,* the first mannose (Man_1) residue, immediately adjacent to the GlcN-PI in the GPI anchor, forms a new glycosidic linkage with β1-6 glucan in the yeast cell wall *(184)*. This process removes the GlcN-PI of the GPI anchor. As a result, the cell wall anchored protein has a common core structure of

protein-CO-NH-$(CH_2)_2$-PO_4-(Man_4)-Man_3-Man_2-(EtNP)-Man_1-glucan. Certain amino acids N-terminal to the ω site residue participate in determining whether or not a fungal GPI-AP remains in the plasma membrane or is transferred to the cell wall. Basic amino acids close to and upstream of the ω site direct the GPI-APs to the plasma membrane *(185,186)*. However, the presence of valine, isoleucine, or leucine at ω-4 or ω-5 and tyrosine or asparagine at ω-2 directs yeast GPI-APs to the cell wall *(186)*. In addition, serine/threonine rich regions further upstream to the ω site also favor cell wall integration of yeast GPI-APs *(187)*.

1.3.2 Functions of GPI-APs

In eukaryotic organisms GPI-APs perform a wide variety of roles as enzymes, structural components *(188,189)*, complement regulators *(190)*, adhesion molecules *(191)*, receptors *(192,193)*, signaling molecules,*(194-196)* etc. In yeast, GPI-APs are important to maintain cell wall stability and cell morphology. The *S. cerevisiae* protein Gas1p is a β1, 3-glucan specific transglucosidase that is essential for cell wall assembly *(188)*. Further many GPI-APs are attached to the yeast cell wall and contribute to maintain stretch resistance and osmotic stability *(189)*. GPI-APs also function as cell surface receptors, including nutrient uptake receptors, toxin receptors, etc. In humans, the uptake of folate is performed by GPI anchored folate receptors. However, the folate receptors also function as receptors for viruses such as Ebola virus (EBV) *(192)*. In parasitic protozoa, the high density of GPI-anchored glycoproteins acts as a protective coat to protect parasites against the immune responses from the host *(8)*. GPI-APs are engaged in mediating the immune

response. For instance, the GPI anchored protein DAF regulates the T cell mediated immune response. DAF also acts as complement regulator, to prevent complement activation and hence to protect cells from complement attack *(197)*.

1.4 The Role of GPI-T in Disease Progression

GPI-T mediates important post-translational modifications in eukaryotic organisms to produce GPI-APs. In addition to this primary role, GPI-T is also involved in disease progression, especially in relevance to cancer. In humans, the non-catalytic GPI-T subunits, PIG-U, GPAA1 and PIG-T, have been identified as oncogenic *(9-11,198)*. Overexpression and copy number variations have been observed for these subunits in a wide variety of cancer tissue samples including breast, bladder, ovarian, colon, lung, head and neck cancers *(11,198)*. These subunits may be involved in cancer progression as individual subunits or as a group with variable composition. For instance, PIG-U was identified as oncogenic in human bladder cancer *(11)*. In addition, overexpression of PIG-U with other oncogenic GPI-T subunits, Gaa1 and PIG-T induced tumorigenesis and invasion of human breast cancer in mice, suggesting a combined contribution of these subunits *(10,198)*. However, despite these observations, GPI-T's role in cancer progression is not yet resolved.

GPI-T also plays a very important role in pathogenic diseases. In parasitic protozoa, the VSG is presented at the outer leaflet of the cellular membrane via its GPI anchor. VSG helps parasites evade the host immune system *(199)*. Because parasitic protozoan carry two different GPI-T subunits instead of Gab1 and Gpi17

(TTA1 and TTA2), these differences could be useful to develop therapeutic agents against pathogenic diseases such as African sleeping sickness and leishmaniasis *(199,200)*. GPI-T also has a role in prion disease pathogenesis. GPI-anchored normal prion proteins (PrP^{c}) are located on the host cell surface. These PrP^{c}s interact with aggregates of disease associated prion proteins (PrP^{sc}) *(201)*. This interaction converts normal host cell PrP^{c} to pathogenic PrP^{SC}, leading to the progression of prion and related diseases *(201)*. However, contradictory evidence from cell free assays and transgenic mice studies reveal that non-GPI-anchored PrP^{c} can also be converted to PrP^{sc} *(202-204)*. Hence, this phenomenon needs to be further investigated.

1.5 Dissertation Research Summary

This dissertation describes our efforts towards understanding various aspects of *S. cerevisiae* GPI-T and its transamidation reaction. In this research, for the first time in the GPI-T field, a pure solubilized form of *S. cerevisiae* GPI-T was used (instead of crude microsomes) in an *in vitro* assay to characterize GPI-T.

Chapter 2 details the development and optimization of a *in vitro* kinetic fluorescence resonance energy transfer (FRET) assay for GPI-T. A time dependent fluorescence response was observed upon incubating the proprotein substrate with pure, solubilized *S. cerevisiae* GPI-T in a nucleophile-dependent manner. Various optimization experiments were used to further enhance the observed fluorescence response. In addition, experiments were conducted to identify and analyze GPI-T cleaved assay products.

Chapter 3 explains the use of this FRET assay for GPI-T to characterize various aspects of GPI transamidation. Experiments were performed to understand the effect of identity elements in the GPI signal sequence towards peptide substrate recognition by GPI-T. The assay was also utilized to investigate the species-specific substrate selectivity of GPI-T Further; the new assay was utilized to identify cofactors and inhibitors affecting the catalytic activity of GPI-T.

Chapter 2

Development and optimization of an *in vitro* FRET assay to characterize the *Saccharomyces cerevisiae* GPI-T

2.1 INTRODUCTION

The formation of glycosylphosphatidylinositol (GPI) anchored proteins (GPI-APs) is an important post-translational modification mediated by GPI-T. Many methods including *in vivo*, *in vitro* and computational analyses are being utilized to elucidate various aspects of GPI-T and its transamidation reaction *(103,104,111,112,114,115,119,120,123,131,137-143,145,146,148,150,151,153,154,158-162,165,166,205-214)*. Experiments based on these methods facilitated the identification of the GPI-T subunits *(138-143,145,146,148,151,158-162,165,166,205)(20)* and defined the protein substrate parameters *(111,119,131,206,208)* the GPI anchoring mechanism *(103,104,111,114,120,137,150,153,154,209-215)*, etc. However, the majority of these experiments used qualitative approaches. So far, only one quantitative *in vitro* assay has been developed to characterize GPI-T *(153)*. However this assay is accompanied with serious limitations (refer to section 2.1.2.b). To date no one has successfully reconstituted GPI anchoring activity *in vitro* using a pure solubilized GPI-T. Further, quantitative assays to kinetically analyze the catalytic activity of GPI-T have not been reported. As a solution to this ongoing problem, this chapter describes the development and optimization of the first high-throughput, *in vitro* fluorescence resonance energy transfer (FRET) assay to characterize the catalytic activity of GPI-T.

2.1.1 *In Vivo* Assays for GPI-T

Most of the *in vivo* assays developed so far have been based on genetic methods *(139,142,143,145,146,148,151,158-161,165,166,205)*, co-immunoprecipitation *(138,140,141,162)*, flow cytometry *(165)* and immunofluorescence microscopy *(124)* (see Chapter 1). The major drawback of these *in vivo* assays is the inability to study GPI transamidation alone without impact or contribution from other cellular components. This issue limits the types of experimental questions that can be addressed. The following sections present brief descriptions of the *in vivo* assay methods that have been most successfully applied to the study of GPI transamidation.

2.1.1a The PreproPLAP Assay

In vivo assays were conducted with placental alkaline phosphatase (PLAP), a human GPI anchored protein, to elucidate various aspects of GPI-T catalysis. COS cells were transfected with wild type and mutant cDNA copies of the *ALPP* gene (encoding PLAP). GPI anchoring of the expressed PLAP protein was analyzed by SDS-PAGE, Western blots and for its sensitivity to phosphatidylinositol specific phospholipase C (PI-PLC). PLAP was used to identify the key identity elements in the GPI-T signal sequence, amongst other significant discoveries *(111,119,206,208)*. Overall, these experiments revealed that the C-terminal GPI-T signal sequence is not a consensus sequence and the amino acid composition can vary as long as it meets general charge, hydrophobicity and length requirements.

2.1.1b The Invertase Assay

Recently, a novel *in vivo* assay was developed by members of the Hendrickson group to investigate GPI-T and the possibility of species specificity *(131)*. The C-terminal GPI signal sequence of two human GPI-APs, the campath-1 antigen (CA26) and the urokinase-type plasminogen-activated receptor (UP30) and an *S. cerevisiae* GPI-AP, Yapsin 2 (Y21), were appended individually onto the C-terminus of the yeast secretory protein invertase (INV) (Figure 2.1, *(131)*).

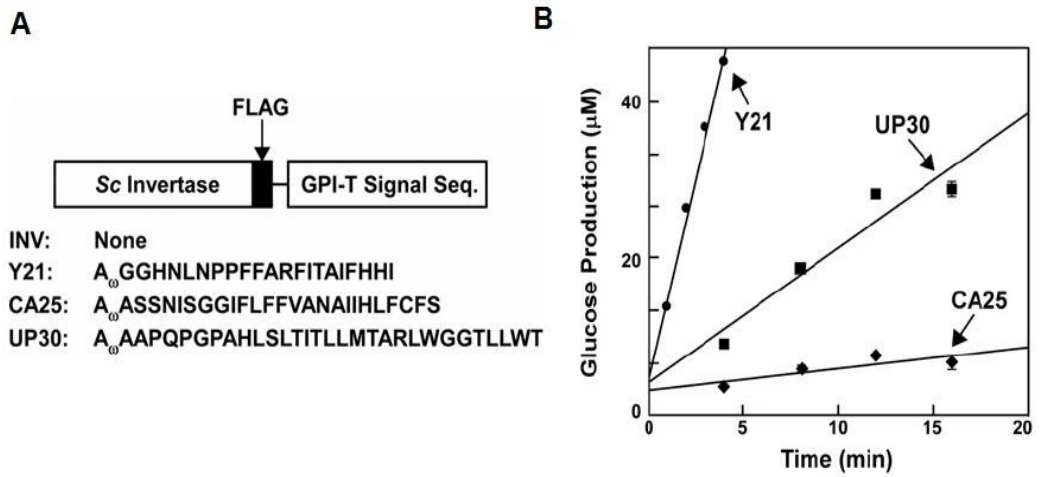

Figure 2.1 Species specificity of *S. cerevisiae* GPI-T. (A) Strategy to produce invertase reporter proteins as substrates for *S. cerevisiae* GPI-T. The C-terminus of full-length soluble invertase (INV) was modified by appending GPI-T signal sequences from yeast Y21, human CA25 and human UP30 separately. (B) An *in vitro* colorimetric assay was used to measure the *S. cerevisiae* cell surface expression of invertase (INV-Y21, INV-CD52 and INV-UP30). The construct INV-Y21 demonstrated the highest level of cell surface invertase activity, consistent with yeast GPI-T favoring the fungal Y21 signal sequence. Figure courtesy of Dr. Rachel Morissette

Cell (*S. cerevisiae*) surface expression levels of GPI anchored INV were monitored using a colorimetric assay and biochemical partitioning. This assay demonstrated that GPI anchoring of human-INV constructs were diminished

compared to that of INV with the yeast GPI signal sequence. Although only a small number of signal sequences were tested, these results suggested that GPI-T has some ability to recognize sequences according to species.

2.1.2 *In Vitro* GPI-T Assays

In vivo assays contributed greatly to our understanding of GPI-T and its transamidation reaction as detailed in section 2.1.1. and as reviewed in Chapter 1. However, *in vivo* experiments performed in intact cells obscure a mechanistic view of the GPI-T reaction, due to the complicated nature of the cellular environment. To overcome this challenge, several efforts have been made to develop cell free methodologies to study the catalytic activity of GPI-T *(103,104,111,114,120,137,150,153,154,209-215)*. The following sections provide brief descriptions of theses assays and how they have contributed to GPI-T research.

2.1.2a The PreprominiPLAP Assay

The preprominiPLAP assay is the most widely used in vitro assay to study GPI-T (Figure 2.2, *(114,216)*) *(103,104,114,120,137,154,211-213)*. This cell free assay was developed by coupling rough microsomes (RMs) to an *in vitro* translation system, which translates preprominiPLAP mRNA. As in intact cells, the N-terminal signal peptide is cleaved from preprominiPLAP to produce prominiPLAP, the substrate for GPI-T. The processing of prominiPLAP by GPI-T, to GPI anchored miniPLAP, is monitored by SDS-PAGE and Western blot.

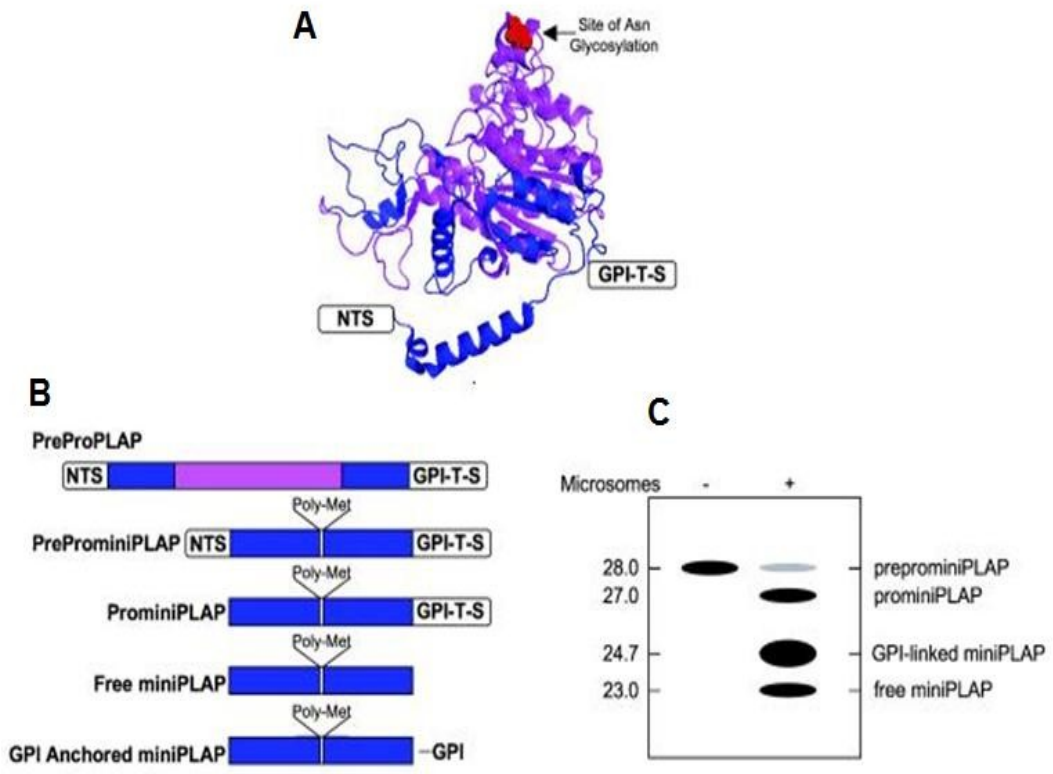

Figure 2.2 The miniPLAP assay to monitor GPI-T activity *in vitro*. (A) The crystal structure of the full length PLAP (PDB ID: 1ZEB).NTS and GPI-T-S represent the N-terminal ER localizing and C-terminal GPI-T recognition signal sequences, respectively. (B) A cartoon schematic representing the stepwise conversion of preproPLAP to different miniPLAP derivatives, including free miniPLAP and the GPI anchored, mature miniPLAP. The preprominiPLAP construct was designed by deleting a majority of the protein's internal sequence. A poly methionine (Poly-Met) region was incorporated for ^{35}S labeling. (C) A cartoon schematic of an SDS-PAGE gel showing the stepwise conversion of preprominiPLAP to different forms of miniPLAP.
Adapted with permission from Varma, Y., and Hendrickson, T., Chembiochem, (2010), 11, 623-636, with permission from John Wiley and Sons.

This miniPLAP assay was utilized extensively to investigate many aspects of the GPI transamidation reaction. Some of these findings include the analysis of the sequential conversion of the preproprotein to a mature GPI anchored protein *(103,104,114)*, the cellular localization of GPI-T *(137)*, GPI-T signal sequence requirements *(114,120,211)* and the interaction of GPI-T subunits with proprotein substrates *(154,212)*. Despite these credible efforts, the miniPLAP assay is also

accompanied with limitations such as the use of crude RMs instead of pure GPI-T and the inability to use synthetic peptide substrates. Thus, the preprominiPLAP assay remains fairly qualitative as a method to analyze GPI-T.

2.1.2b A Fluorescence Assay for GPI-T

The ability of *T. brucei* Gpi8 to mediate the transamidation reaction *(150)*, the acceptability of small nitrogen nucleophiles *(214)* and a short, synthetic peptide substrate for GPI-T were critical in the development of the first specific cell free assay (Figure 2.3,*(153)*) *(153)*.

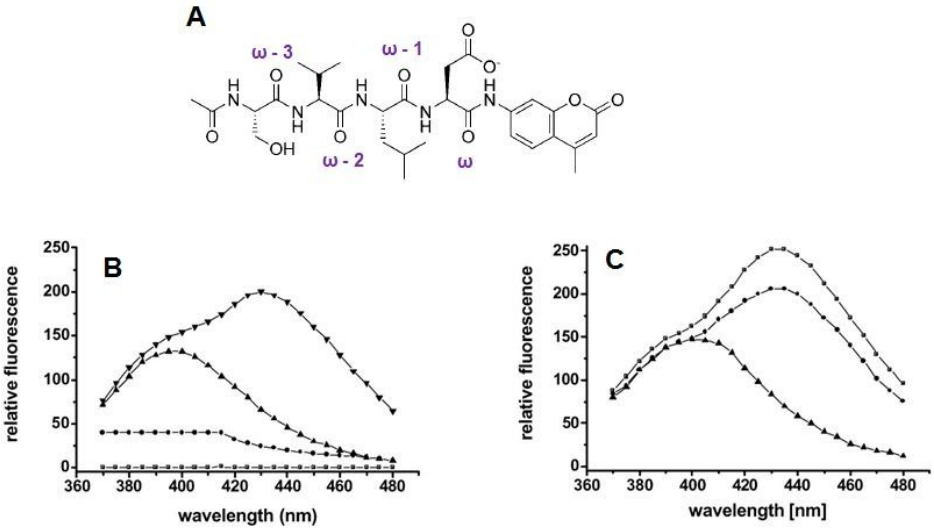

Figure 2.3 An *in vitro* assay to quantitatively characterize GPI-T activity. Incubation of a fluorescently labeled, synthetic tetrapeptide (Ac-SVLN-AMC) with trypanosomal lysates results in enhanced fluorescence with a shift in the emission maximum. (A) Ac-SVLN-AMC is based on the cleavage and anchor attachment site of VSG. (B) Incubation with trypanosomal lysates leads to cleavage of the terminal amide bond in the peptide substrate, resulting in a shift in emission maximum from 400 nm to 440 nm (▼), compared to peptide alone (▲), lysate alone (●), or buffer alone (■). (C) The addition of 10 mM hydrazine enhances AMC release (■), compared to lysate with substrate alone (●) or peptide substrate alone (▲). Incubation was for 24 hours. Adapted with permission from kang et al., *J. Cell. Sci.* (2002) *115*, 2529-2539 with permission from the Company of Biologists.

A fluorescently labeled synthetic tetra peptide (Ac-SVLN-AMC; AMC=aminomethylcoumarin), based on the ω-3 to ω region amino acids of *T. bruc*ei VSG, was used as the peptide substrate for this assay. Incubation of this peptide with either trypanosomal lysates or pure *T. brucei Gpi8* alone resulted in cleavage of the C-terminal amide bond, releasing aminomethylcoumarin. Cleavage was monitored by following the shift in fluorescence emission maximum for free AMC compared to the stating peptide. Addition of hydrazine further enhanced the fluorescence intensity, while a sulfhydryl-alkylating agent, *p*-chloromercuriphenylsulfate (pCMPSA) abolished the reaction, presumably by modifying the active site cysteine in Gpi8. Even though this assay laid the foundation for the development of more quantitative GPI-T *in vitro* assays, it is also associated with serious limitations including an apparent requirement for a long incubation period (24 hours) and the use of a minimalistic version of a proprotein substrate that lacks the GPI-T signal sequence. In theory, a significant feature of this assay is the ability to measure changes in fluorescence over time, which gives quantitative results, compared to the qualitative *in vitro* assays discussed so far. In practice, the small fluorescence change over time is expected to limit its application. In fact, the 2002 publication describing this assay *(153)* remains the only application of this method to the study of GPI-T.

2.1.3 A New High Throughput *In Vitro* FRET Assay for GPI-T

As detailed in sections 2.1.1 and 2.1.2, previous efforts to characterize the structure and catalytic activity of GPI-T were mostly limited to qualitative analyses *(129,138)*. Efforts to study GPI-T in a quantitative way have been very limited *(153)*. These discoveries alleviated the challenges faced when using co-translational systems and rough microsomes. Despite these forays, no one has yet successfully reconstituted the GPI anchoring activity *in vitro* with purified enzyme. In addition, no high throughput quantitative methods are available to analyze pure GPI-T *in vitro.* For this reason, many questions remain with respect to understanding GPI-T, its catalytic function, and its physiological roles in healthy and abnormal cells. For instance, we cannot be certain how many subunits are necessary for GPI-T to exert catalytic activity. In other words, is GPI-T the heterotrimer that can be co-purified from yeast *(138)* , or is it the heteropentamer that is isolated from human cells *(141)* ? Hence, the Hendrickson lab stepped forward to develop a high throughput *in vitro* FRET assay for GPI-T.

Our GPI-T assay was designed to measure the restored fluorescence of a fluorophore upon hydrolysis of the scissile amide bond at the ω site in a synthetic proprotein substrate. This substrate was designed so that the proprotein would have minimal fluorescence based on the presence of an appropriate quencher; upon cleavage by GPI-T, the fluorophore and quencher would be separated, enhancing fluorescence. We choose aminobenzoic acid (Abz) as the fluorophore and a 3-nitrotyrosine (Y*) as the quencher (Figure 2.4). We envisioned that incubation of this

peptide with a source of GPI-T and a nucleophile donor would result in an increase in fluorescence over time in a manner that would correlate to GPI-T activity.

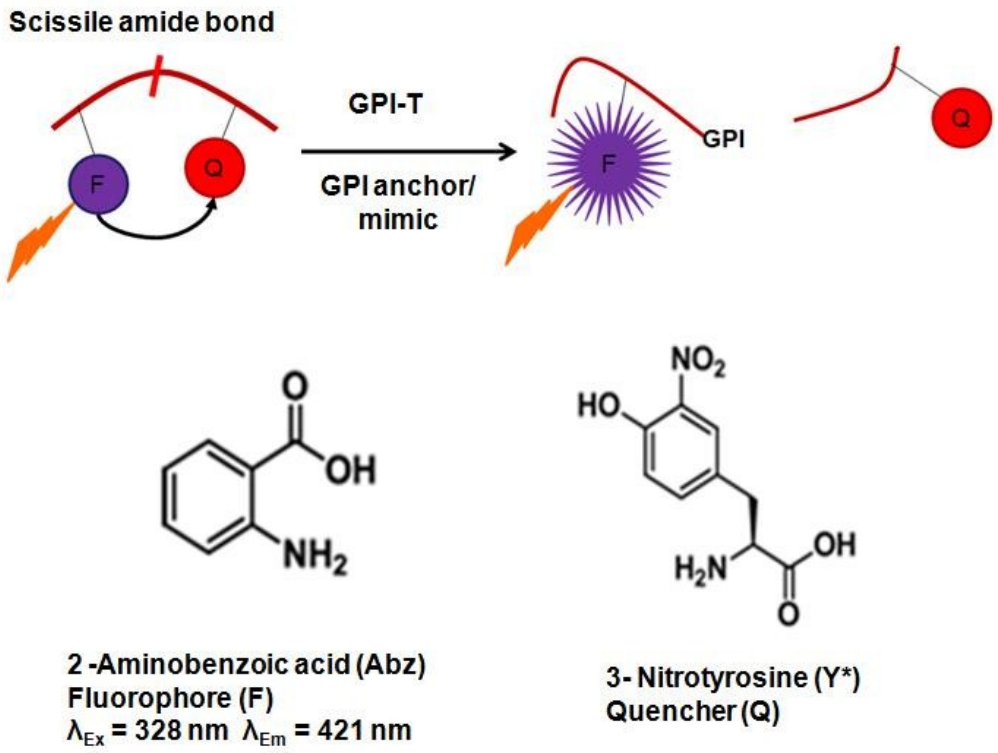

Figure 2.4 Cartoon schematic of our GPI-T fluorescence assay. GPI-T is expected to cleave the scissile amide bond in the synthetic, propeptide substrate to restore Abz fluorescence. This assay could use full-length GPI anchor or small GPI anchor mimics like hydroxylamine or hydrazine as the nucleophile donor.

2.2 RESULTS

2.2.1 Design and Synthesis of Peptide Substrates for the *In Vitro* Assay

The human Campath–1 (CD52) antigen was chosen as the basis for a synthetic peptide substrate for GPI-T. This 37 amino acid peptide is the smallest known eukaryotic substrate for GPI-T; after processing, the GPI anchored peptide is only 12 amino acids long *(217-219)* . The wild type sequence of the CD52 proprotein is shown in Table 2.1. Certain modifications were introduced into this sequence to

avoid adverse effects of N-linked glycosylation with crude microsomes and oxidation during peptide synthesis. Both Asn3 and Asn16 were changed to lysine avoid N-linked glycosylation issues and to increase the solubility of the peptide *(220)*. The C-terminal Cys35 was mutated to histidine to avoid peptide oxidation via disulfide bond formation. Cysteine was mutated to histidine, as His frequently appears in the hydrophobic region of GPI anchoring proteins*(129)*. Peptide **1** (Table 2.1) was capped with Abz and the 3-nitrotyrosine quencher was added in place of Ile17.

Peptide **1** (Table 2.1) had more than one potential ω site leading to concerns about ambiguity in product formation during our GPI-T assay. Therefore, peptide **2** (Table 2.1) was designed by replacing Thr8 and Ser15 with lysines, optimizing Ser12 as the most viable ω site. Finally, in order to evaluate the peptide products from our assay, a biotinylated version of peptide **2** (peptide **3,** Table 2.1) was also synthesized; the biotin was attached to the side chain of Lys3. For peptides **1, 2** and **3** Abz (fluorophore) was coupled to the N terminus Gly1 and Ile17 was replaced by 3-nitrotyrosine (quencher). Peptides **1** and **2** were first synthesized using automated peptide synthesis as per the standard protocols of Fmoc solid phase peptide synthesis. Peptides **2** and **3** were also synthesized by manual peptide synthesis. Digestion of peptide **1**, **2** and **3** with Trypsin revealed that peptides are internally quenched; hence sufficient to produce a readily visible fluorescence change upon incubation with GPI-T*(221)*.

Table 2.1 Peptide substrates for the GPI-T assay with pure GPI-T

Peptide	N-terminus	N-terminal seq.	ω	GPI-T Signal sequence
WT CD52	Abz	GQNDTSETSSP	S	ASSNISGGIFLFFVANAIIHLFCFS
1	Abz	GQNDTSETSSP	S	ASSNISGGIFLFFVANAIIHLFCFS
2	Abz	GQKDTSEKSSP	S	ASKN*YSGGIFLFFVANAIIHLFHFS
3	Abz	GQ**K(Biotin)**DTSEKSSP	S	ASKN*YSGGIFLFFVANAIIHLFHFS

Abz; 2-aminobenzoic acid, *Y: 3-nitrotyrosine. Bold residue indicates the site of biotin attachment. Underlined residues were modified from the native CD52 sequence as described in the text

2.2.2 Preparation of Crude Microsomes Containing GPI-T

Crude microsomes were prepared using the yeast strain YDR331W (YDC1178, Open Biosystems) which encodes Gpi8 with an appended tandem affinity purification (TAP) tag {Rigaut, 1999 #47;Puig, 2001 #48;Morissette, 2007 #710}. The TAP tag is composed of a calmodulin-binding peptide (CBP), a TEV protease cleavage site, and Protein A, which enables the two-step purification of Gpi8 and visualization by Western blot. Crude microsomal extracts were prepared based on a protocol developed by Conzelmann and coworkers *(138)*. Briefly, cells were grown to mid-log phase and lysed with liquid nitrogen; the cell lysate was centrifuged at high velocity to obtain the microsomes. Several nonionic detergents were tested to obtained the best detergent solubilized microsomes as shown in an anti-Protein A Western blot (Figure 2.5, Dr. Tamara L. Hendrickson). Igepal, triton X-100, and digitonin successfully solubilized Gpi8. Igepal was chosen as the detergent to solubilize crude yeast microsomes.

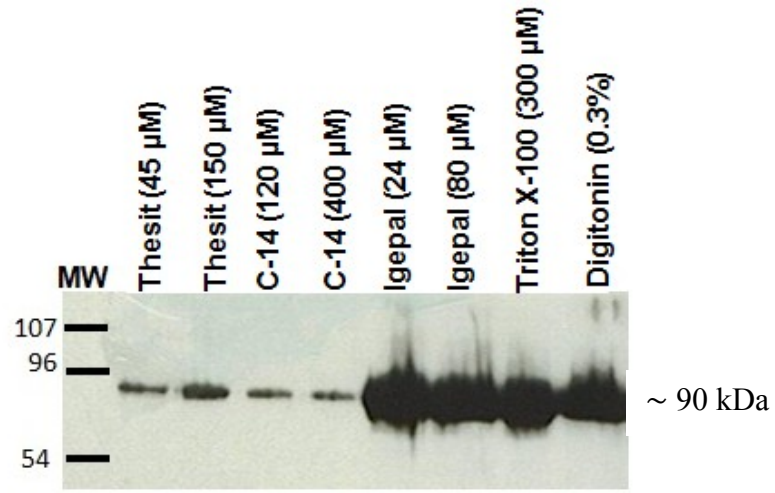

Figure 2.5 Effect of various non-ionic detergents on solubilizing *S.cerevisiae* microsomes carrying TAP tagged Gpi8. TAP-tagged Gpi8 was visualized in an anti-protein A Western blot. MW: Molecular weight markers Figure courtesy of Dr. T. Hendrickson.

2.2.3 Initial *In Vitro* Assay with Crude Yeast Microsomes

Initial assay development efforts were initiated by Dr. R. Morissette *(221)*, using solubilized, crude yeast microsomes containing GPI-T. A time-dependent increase in Abz fluorescence was observed when peptide **1** was incubated overnight in Hepes pH 7.0 buffer, with solubilized microsomes, with and without hydroxylamine (Figure 2.6, *(221)*). The observed fluorescence response was higher in the presence of hydroxylamine (NH_2OH) as predicted, suggesting that hydroxylamine is serving as a GPI anchor mimic as previously reported *(105,153)*. Thus, these results offered the first indication that this new GPI-T assay was, in fact, measuring GPI-T transamidation of the substrate peptide. An initial burst in fluorescence response was observed that was independent of hydroxylamine.

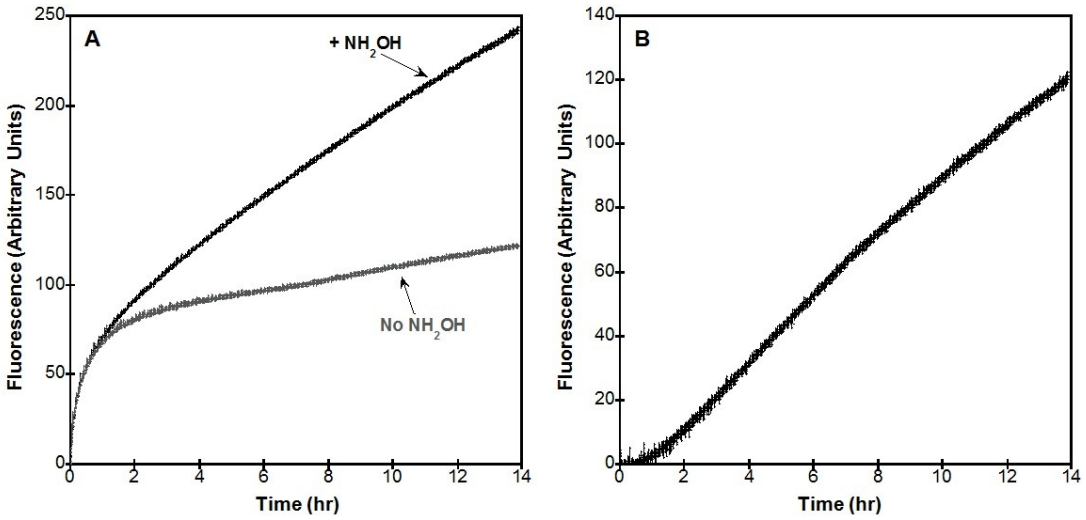

Figure 2.6 An *in vitro* GPI-T assay using solubilized microsomes. (A) A time-dependent fluorescence response was observed upon incubation of peptide **1** with crude solubilized yeast microsomes. The observed fluorescence intensity was higher for the assay with hydroxylamine (NH_2OH). (B) The nucleophile dependent fluorescence response calculated from (A). The nucleophile dependence was obtained by subtracting the signal without hydroxylamine from the NH_2OH-containing signal. Figure courtesy of Dr. R. Morissette

2.2.4 Extraction and Purification of GPI-T

The enzyme for GPI-T assay was expressed using yeast strain FBY656, kindly provided by Prof. Conzelmann *(138)*. The FBY656 strain is a *GPI8* knockout strain (*MATa ade2-1 ura3-1 leu2-3, 112 trp1-1 his3-11,15lys⁻ GPI8Δ::kanMX2*) and contains plasmid YCplac22-*GST-GPI8*, encoding for a GST tag on the N-terminus of Gpi8. Membrane solubilization and purification of the GST-tagged GPI-T complex was performed essentially as previously reported *(138)*, with only a few modifications. A cocktail of protease inhibitors was added through the membrane isolation step; after which, all inhibitors were omitted, except phenylmethylsulfonyl fluoride (PMSF) to avoid inadvertent inhibition of GPI-T. Protein elution conditions (from glutathione resin) were also optimized iteratively based on observable activity

with our FRET assay. Optimal activity was obtained when the enzyme was eluted once with buffer containing 0.3 % digitonin, 20 mM reduced glutathione (RG), and PMSF as the only protease inhibitor. Due to poor yield of purified enzyme, the concentration of GPI-T was not determined. Purified, heterotrimeric GPI-T was examined by SDS-PAGE with Silver staining (not shown) and by Western blot (Figure 2.7) with anti GST polyclonal antibodies. These analyses verified the presence of Gpi8 in this enzyme mixture but the co-purification of Gaa1 and Gpi16 was not confirmed. However, since we used the same yeast strain (FBY656) and same purification protocol published by conzelmann and co workers, who previously reported the co-precipitation of yeast Gpi16 and Gaa1 with Gpi8 *(138)* we proceeded to assay this enzyme preparation assuming that both Gaa1 and Gpi16 are present in our enzyme source in addition to GST tagged Gpi8.

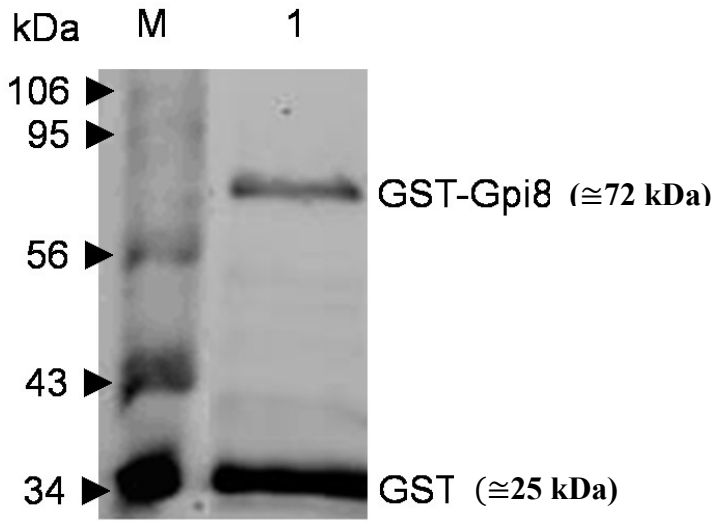

Figure 2.7 Affinity purification of GST tagged GPI-T. Western blot with anti GST polyclonal antibody revealed the presence of GST tagged Gpi8. MW - molecular weight markers Lane 1 - Elution of GST tagged GPI-T from FBY656 strain. Figure courtesy of Dilani Gamage

2.2.5 Initial *In Vitro* Assay with Affinity Purified Solubilized GPI-T

Upon obtaining affinity purified GST-tagged GPI-T, another initial *in vitro* assay was performed (Figure 2.8). Peptide **2** was incubated with affinity purified GPI-T with and without hydroxylamine in the GPI-T assay buffer, pH 7.0. This assay yielded a significant faster increase in Abz fluorescence compared to the original assay that used crude yeast microsomes, reducing the necessary assay time from hours to minutes. Further, no initial burst was observed for no hydroxylamine assay similar to that of assay with crude microsomes. Instead a slight increase in fluorescence was observed for no nucleophile assay. This slight increase in fluorescence response is probably due to the hydrolysis of the amide bond at the ω site as previously reported *(105)*.

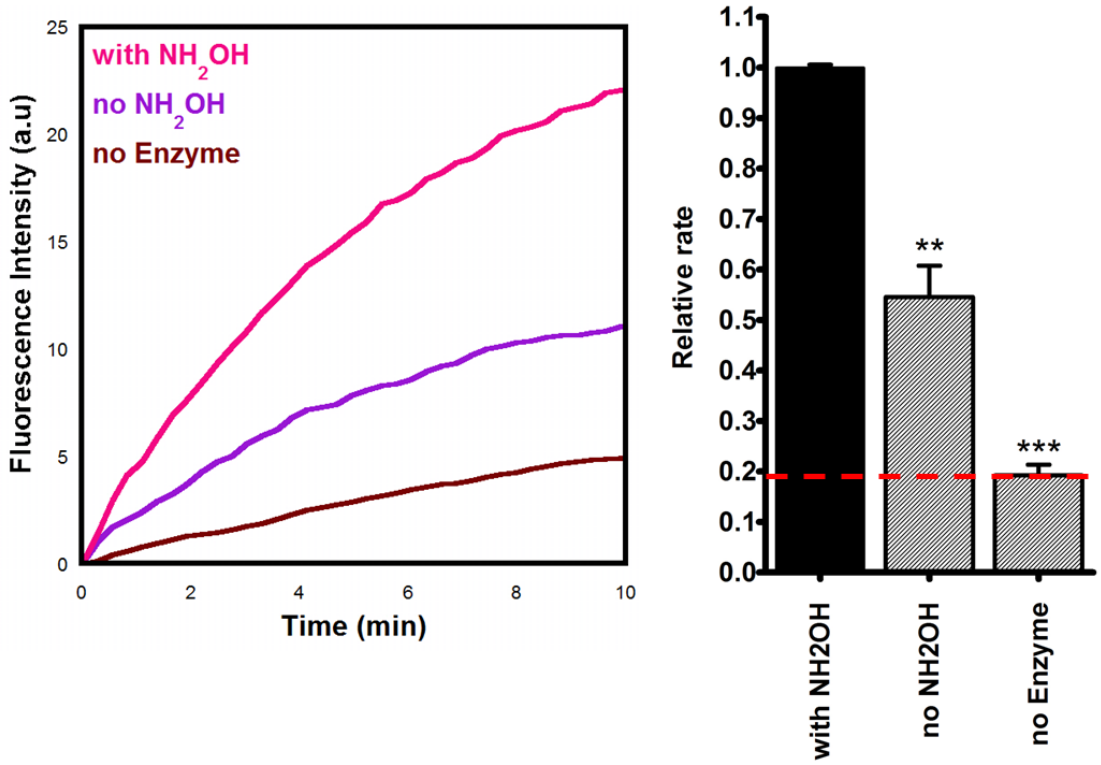

Figure 2.8. FRET assay with GPI-T. (A) Peptide **2** fluorescence increases over time in the presence of NH_2OH, indicating peptide cleavage and transamidation, presumably to produce the hydroxamide peptide product. Magenta: 10 mM NH_2OH and 10 µM peptide **2**; Maroon: 10 µM peptide **2**; Purple: No enzyme control (10 mM NH_2OH and 10 µM peptide **2**). (B) Relative rates for the data from panel (A). Fluorescence intensities were normalized with a GPI-T unit correction factor. The red dashed line indicates the background fluorescence (no enzyme assay, relative rate = 0.192±0.0216), Data above this line is considered relevant. Data represents the mean ± SD, n = 3 and P ≤ 0.05 vs. with NH_2OH assay (dark grey). Raw data can be found in Appendix A: Figure A1.

2.2.6 Assay Optimization

As mentioned in section 2.2.3, our first FRET assay was developed by Dr. R. Morissette using crude yeast microsomes, containing GPI-T *(221)*. With peptide **1**, she observed a significant, time-dependent and hydroxylamine-dependent fluorescence response suggestive of GPI-T activity. One of the major drawbacks of this assay was the requirement for a long incubation period (up to 12 hours) to

obtain a significant response. This requirement affects both enzyme viability and assay sensitivity. To overcome these problems, we performed another initial assay with affinity purified GPI-T. This assay also yielded a hydroxylamine-dependent fluorescence response over a significantly shorter time scale. Therefore we decided to use affinity purified GPI-T instead of crude microsomes to characterize various aspects of GPI-T *in vitro* with this assay.

However, prior to the characterization assays, we set out to further optimize this GPI-T assay. For optimization, several parameters were assessed, including the impact of different detergents, pH, reducing agents, nucleophiles, peptide concentration and enzyme amount. In addition, modifications to the enzyme purification process and fluorimeter setup were performed to obtain optimized Abz fluorescence over time. These experiments are described in detail in the following sections.

2.2.6a The Effect of Different Detergents on GPI-T Activity

Detergents are important to solubilize transmembrane proteins and crude microsomes and they provide a mechanism to separate membrane-bound proteins from soluble proteins. Our initial GPI-T assay with affinity-purified GPI-T was performed using digitonin as the solubilizing detergent. However, the GPI-T assay performed with crude yeast microsomes used igepal CA-630 (also known as nonidet P-40) as the detergent (Refer to Figure 2.5) *(221)*.

Hence, we tested igepal CA-630 alone or in combination with digitonin to determine which detergent yielded optimal results in terms of enzyme yield and

activity. In contrast to the assay with crude yeast microsomes, peptide **2** precipitated out of solution in the igepal solubilized assay, leading to a turbidity-induced decrease in apparent fluorescence. The addition of 0.1% digitonin with igepal CA-630, slightly lowered the turbidity of the assay buffer, but activity was most robust in 0.1% digitonin alone (Figure 2.9.). Therefore, we concluded that 0.1% digitonin is the best for our assay, at least with peptide **2** as the substrate.

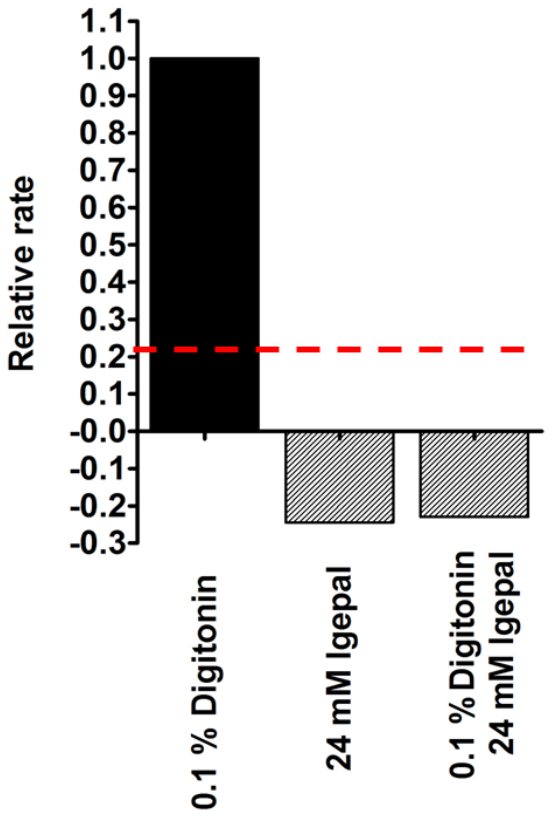

Figure 2.9 The effect of igepal and digitonin on GPI-T activity. The negative relative rates are due to precipitation of peptide **2** over time, which impacts the observed fluorescence. The red dashed line indicates background fluorescence (relative rate = 0.192±0.0216). Data above this line was considered relevant to GPI-T transamidation. Experiments were run in duplicate. Relative rates were calculated with respect to the 0.1% Digitonin assay (dark gray) and data represents the mean.

2.2.6b The Effect of Digitonin Concentration on GPI-T Activity

Next, experiments were conducted to optimize the digitonin concentration in the assay buffer (Figure 2.10). We tested the impact of different digitonin concentrations on GPI-T activity. producing a robust fluorescence response in our GPI-T assay in terms of GPI-T activity. At low (0.05% w/v) and high (0.3% w/v) concentrations, peptide **2** precipitated from solution, increasing turbidity of the assay buffer and prohibiting any quantitative assessment of GPI-T activity. The intermediate digitonin concentrations (0.1% w/v and 0.2% w/v) yielded optimal GPI-T activity, while alleviating peptide precipitation and turbidity issues. Since 0.1% w/v digitonin resulted in the highest GPI-T activity, we decided to use 0.1% w/v as the optimized digitonin concentration for our assay.

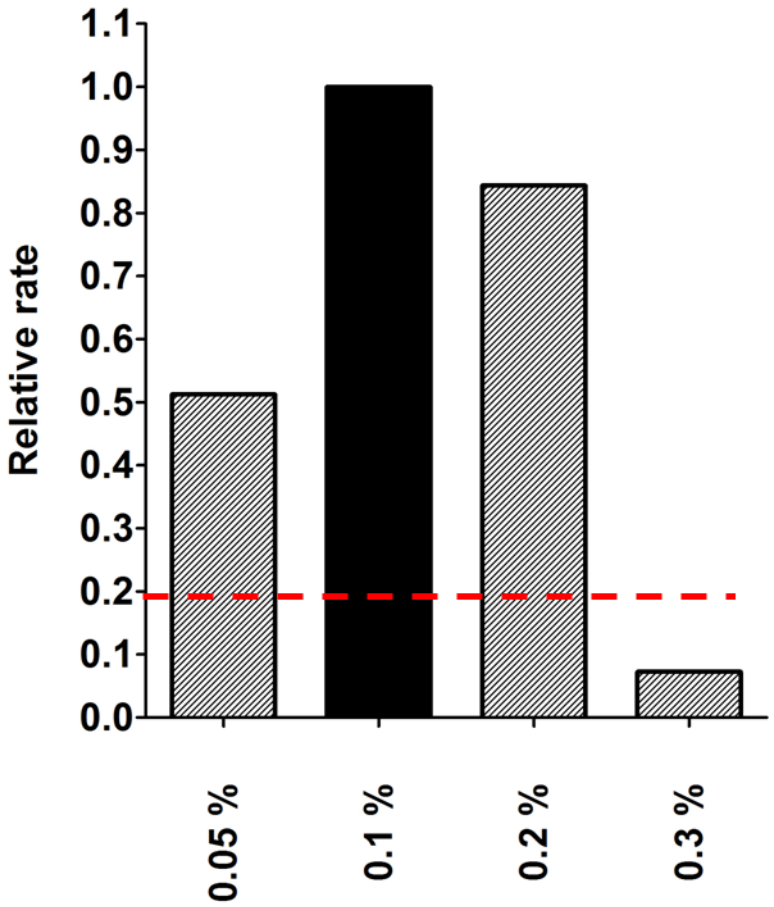

Figure 2.10 Optimization of digitonin concentration. Optimal GPI-T activity was observed with 0.1% digitonin in assay buffer. The red dashed line indicates background fluorescence (relative rate = 0.192±0.0216). Data above this line was considered relevant to GPI-T transamidation. Experiments were run in duplicate. Relative rates were calculated with respect to the 0.1% Digitonin assay (dark gray) and data represents the mean without SD. Raw data can be found in Appendix A: Figure A3.

2.2.6c The Effect of pH on GPI-T Activity

Reaction pH can also be a key factor for enzyme activity. Therefore, we used different pH buffer systems (varying from pH 6.0 to 9.0) to find the optimized pH for GPI-T activity (Figure 2.11). A pH of 7.0 yielded the best GPI-T relative rates.

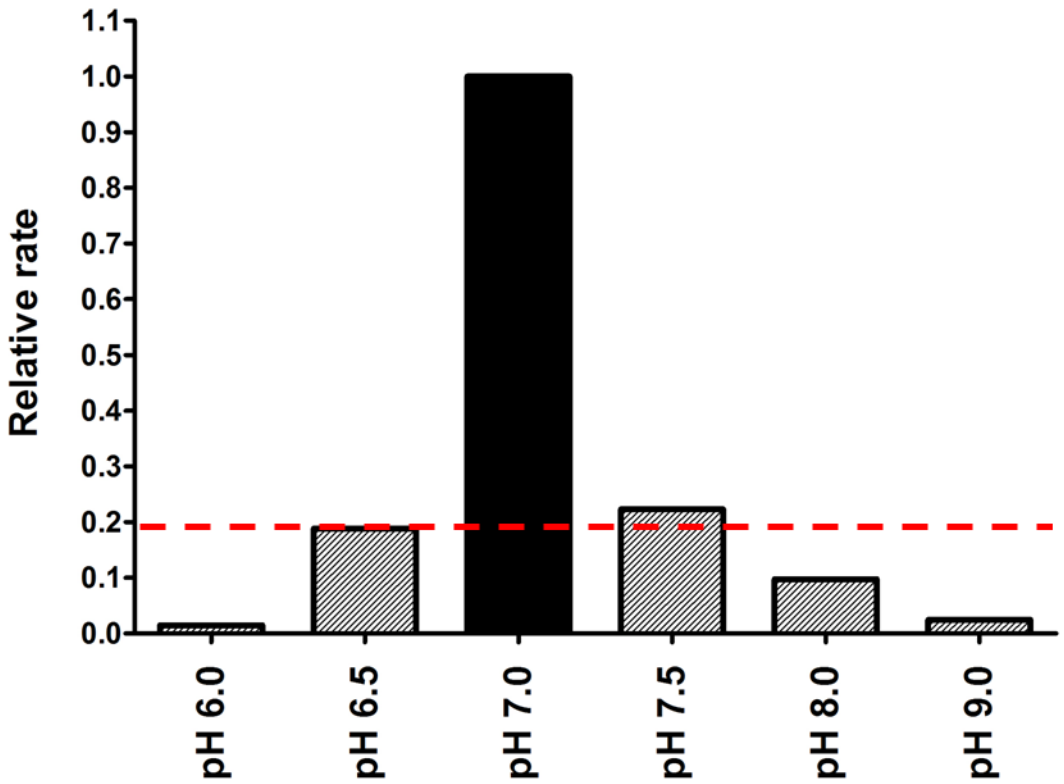

Figure 2.11 Effect of pH on GPI-T activity. pH 7.0 was chosen as the optimal pH for the assay buffer. Each experiment was run only once, fluorescence intensities were normalized with unit correction factor prior to initial rate calculation. Relative rates were calculated with respect to the optimal rate observed at pH 7.0 (dark gray). The red dashed line indicates background fluorescence (relative rate = 0.192±0.0216). Data above this line was considered relevant to GPI-T transamidation. Raw data can be found in Appendix A: Figure A4.

2.2.6d The Effect of Reducing Agents on GPI-T Activity

The catalytically active subunit of GPI-T, Gpi8 contains an apparent cysteine histidine catalytic dyad; hence, it is important to maintain a reducing environment in our *in vitro* assay. Therefore the impacts of dithiothreitol (DTT, 1 mM) and reduced glutathione (RG, 20 mM) were analysed (Figure 2.12).

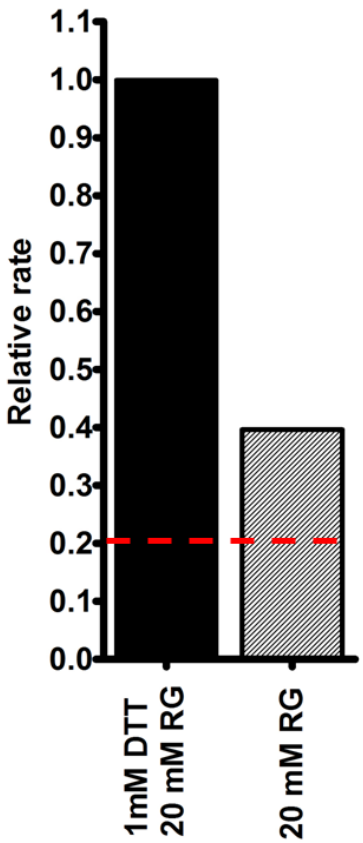

Figure 2.12 The effect of reducing agents on GPI-T activity. DTT (1 mM) enhances the GPI-T activity in the prescence of RG (20 mM). Data represents the mean of duplicate assays. Relative rates were calculated with respect to the assay with both DTT and RG (dark gray).The red dashed line indicates background fluorescence (relative rate = 0.192$\pm$0.0216). Data above this line was considered relevant to GPI-T transamidation. Raw data can be found in Appendix A: Figure A5.

RG was assessed because it is present in our assay buffer following purification of GPI-T by glutathione affinity chromatography. The addition of DTT improved GPI-T acyivity above that of RG alone. Therefore, we decided to keep both DTT and RG in our GPI-T assay buffer.

2.2.6e Effect of Enzyme Amount on Optimal Activity of the GPI-T Assay

Because we can't accurately quantify the low levels of GPI-T in our purification preparations, we decided to optimize GPI-T based on a standard purification protocol and then to assign a unit definition to the observed transamidation rate. Similarly, to our preliminary results, the best initial rates for GPI-T were obtained when 50 µL of affinity purified GPI-T was used in a 2 mL assay (Figure 2.13). At lower enzyme concentrations, peptide precipitation overwhelmed fluorescence detection. Unexpectedly, the fluorescence signal was also ablated at high GPI-T concentrations (100 µL), perhaps due to turbidity from the enzyme preparation itself.

2.2.6f Effect of Peptide Substrate Concentration on GPI-T Activity

We also optimized the concentration of peptide **2** for our GPI-T assay (Figure 2.14) and determined that a concentration of 10 µM peptide **2** produced the highest initial rates. Peptide precipitation was observed with increasing turbidity with 20 µM of peptide **2**.

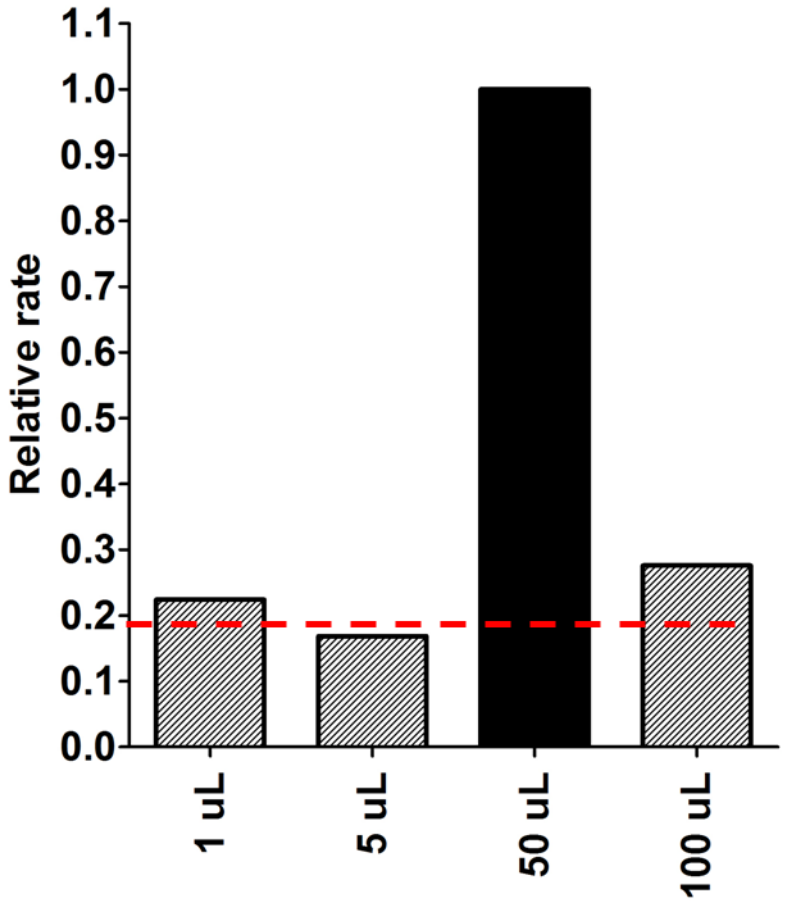

Figure 2.13 Optimizing GPI-T assay with varying amount of GPI-T enzyme. Optimal fluorescence response was observed with 50 µL of GPI-T. Data represents the mean of duplicate assays. Relative rates were calculated with respect to the assay with 50 µL of GPI-T (dark gray).The red dashed line indicates background fluorescence (relative rate = 0.192±0.0216). Data above this line was considered relevant to GPI-T transamidation. Raw data can be found in Appendix A: Figure A6.

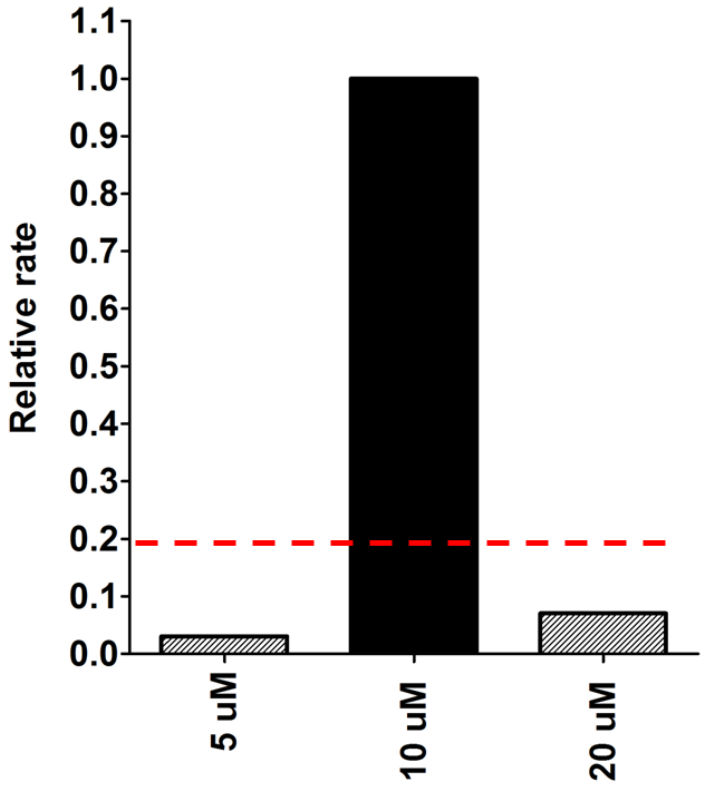

Figure 2.14 Effect of peptide 2 concentration on GPI-T activity. The assay with 10 μM of peptide **2** results the optimal activity. Data represents the mean of duplicate assays. Relative rates were calculated with respect to the assay with 10 μM of peptide **2** (dark gray).The red dashed line indicates background fluorescence (relative rate = 0.192±0.0216). Data above this line was considered relevant to GPI-T transamidation. Raw data can be found in Appendix A: Figure A7.

2.2.6g Effect of Different Nucleophiles on GPI-T Activity

The impact of different nucleophiles was also assessed. Assays discussed to this point all used 10 mM hydroxylamine as the GPI mimic/nucleophile donor. Hydrazine (N2H2) and ethanolamine phosphate methyl ester (EPME, see appendix A8 for the structure) a GPI anchor mimic synthesized by Dr Franklin John *(97)* were also tested as assay substrates to determine if either molecule is a better substrate

than NH_2OH (Figure 2.15). Compared to the no nucleophile assay, NH_2OH proved to be the best GPI anchor mimic substrate. Surprisingly, in contrast to previous literature reports *(105)*, NH_2NH_2 or based on structural similarity to EtNP group of GPI anchor, EPME were not a robust substrate to mimic GPI anchor, within the context of our assay.

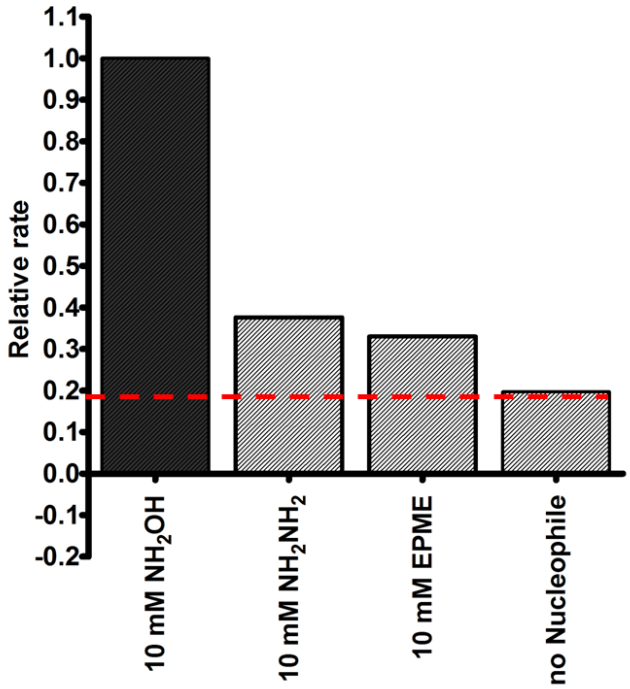

Figure 2.15 Effect of different GPI anchor mimics/nucleophiles on GPI-T activity. GPI-T assay with 10 mM NH_2OH results the highest GPI-T activity. Data represents the experiment run in once. Relative rates were calculated with respect to the assay with 10 mM of NH_2OH (dark gray). The red dashed line indicates background fluorescence (relative rate = 0.192 ± 0.0216). Data above this line was considered relevant to GPI-T transamidation. Raw data can be found in Appendix A: Figure A8.

2.2.7 Analysis of GPI-T Cleaved Hydroxylamine Attached Peptide Products

As the final step in our GPI-T assay development, we wanted to confirm that the observed fluorescence response corresponds to GPI-T-mediated transamidation of peptide **2**, while simultaneously confirming that the correct ω site was modified. To investigate this phenomenon, a biotinylated peptide substrate (peptide **3**) was used. Peptide **3,** differ from the peptide **2** only by the addition of a biotin group attached to the side chain of Lys3 (Table 2.1). The presence of biotin allows for streptavidin purification of peptide fragments after extended incubation with GPI-T. We expected that this purification would isolate peptide **3** and any N-terminal peptide products (e.g. the hydroxylamine modified 12 amino acid peptide, hydroxamate **1**, refer to table 2.2) away from GPI-T and other assay components. Next, the purified peptide mixture was was separated by high performance liquid chromatography (HPLC). In Figure 2.16, the HPLC trace for peptide **3** (peak 5 b) is shown in green. Incubation of this peptide with GPI-T led to a dramatic reduction in the concentration of peptide **3** (Figure 2.16, blue trace, peak 5a)**.** Furthermore, four new products (Figure 2.16, blue trace, peaks 1-4) were observed; each of which is a potential product from the GPI-T reaction.

Peaks 1-4 were collected and analyzed by mass spectrometry. Unfortunately, this analysis did not reveal the expected product, the hydroxamate **1** (the 12 N-terminal amino acids of peptide **3**, with Ser12 modified to a hydroxamate) (Table 2.2). Instead, mass spectroscopic analysis of peak 2 revealed presence of two products with masses close but not equal to the calculated masses of two GPI-T cleaved truncated hydroxamates of peptide **3** (refer to Table 2.2). These truncated

hydroxamates represents hydroxamate **2** with 4 N-terminal amino acids, cleaved after Asp4 and hydroxamte **3** with 7 N-terminal amino acids, cleaved after Glu7. The residues Asp4 and Glu7 also represent alternative ω sites of the peptide **3**. Efforts to optimize these mass spectrometric experiments are currently being conducted by other members of the Hendrickson research group.

Table 2.2 - GPI-T cleaved hydroxylamine attached peptide products (hydroxamates)

Hydroxamate	Sequence	Calculated MW (M+H)	Observed MW (M+H)
1	Abz -GQ**K(Biotin)**DTSEKSSPS-NHOH	1611	-
2	Abz -GQ**K(Biotin)**D-NHOH	807	809
3	Abz -GQ**K(Biotin)**DTSE-NHOH	1124	1122

Abz; 2-aminobenzoic acid, *Y: 3-nitrotyrosine. Bold residue indicates the site of biotin attachment. Underlined residues were modified from the native CD52 (Table 2.1) as described in the text

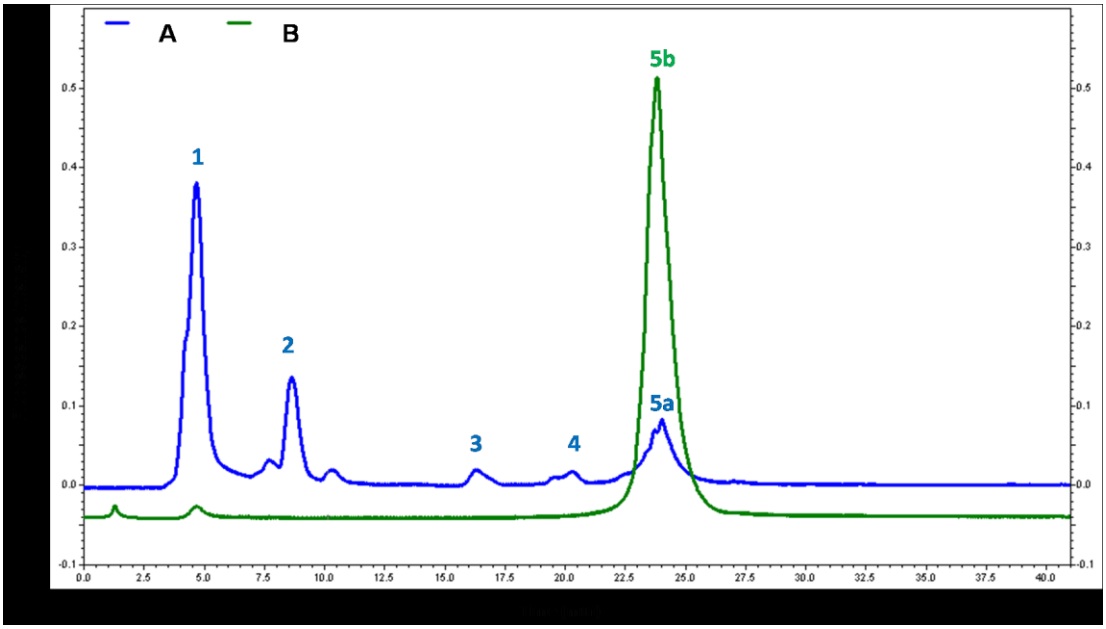

Figure 2.16 HPLC analysis of GPI-T treated peptide products. (A) HPLC trace of the purrified peptide **3** (green trace). (B) HPLC trace of assay products after strepatviadin purification (blue trace). Both traces correspond to equal starting amounts of parent peptide **3.** Clevage products on trace B (peaks 1-4) indicates new assay products were formed. Peaks 5a and 5b represents the parent peptide **3.** The labeled fractions were analyzed by ESI

2.3 DISCUSSION

In this chapter, we described the development and optimization of a high throughput *in vitro* assay to kinetically analyze GPI-T. Over three decades of GPI-T research, many assays have been developed to elucidate various aspects of GPI-T activity. These methods have remained fairly qualitative. Further, no assay successfully demonstrated the GPI-T activity *in vitro* with pure enzyme. However, with the emerging importance of GPI-T in cancer *(9-11)*, there is an urgent requirement for a high throughput, quantitative *in vitro* assay for this enzyme.

2.3.1 Initial *In Vitro* Assay with Crude Yeast Microsomes

FRET assay development was initiated by Dr. Rachel Morissette *(221)*. She demonstrated a significant nucleophile dependent fluorescence response over time upon incubating a peptide substrate with crude yeast microsomes carrying active GPI-T. These results offered the first indication that this assay was, in fact, measuring GPI-T mediate transamidation of the substrate peptide. However, this assay was associated with some limitations. An initial burst in fluorescence response was observed that was independent of the hydroxylamine nucleophile. We hypothesize that this burst is due to trace amounts of endogenous GPI anchor in the crude microsomes. The assay also required a long incubation time (hours), typical of most enzyme assays. This will affect both enzyme viability and assay sensitivity. To overcome these limitations we decided to further develop and optimize this FRET assay. Our goal was to obtain a robust nucleophile dependent fluorescence response within a short period time, using a purer form of the enzyme.

2.3.2 Initial *In Vitro* Assay with Pure GPI-T

The first hurdle to overcome was to find a suitable enzyme source for GPI-T. We chose to utilize affinity purified GPI-T, based on a purification reported by Conzelmann and colleagues *(138)*. This procedure did not provide enough enzyme to assess for concentration, but it did provide GST tagged Gpi8 enriched enzyme isolated from other microsome components. Assays with affinity purified GPI-T remained nucleophile-dependent, lacked the initial nucleophile independent activity observed with crude microsomes, and activity was quantifiable on a minute time

scale. The significant difference in initial fluorescence response observed for the assays with and without hydroxylamine is consistent with a GPI-T mediated transamidation reaction. Unexpectedly, a slight increase in fluorescence response was also observed for the peptide only control (Figure 2.7.). We do not understand this phenomenon. Furthermore, over time, the parent peptide substrate precipitated from the assay buffer in the absence of nucleophile or enzyme, causing a significant reduction in fluorescence from sample clouding

2.3.3 Optimization of *In Vitro* FRET Assay with Purified GPI-T

Upon obtaining a significant nucleophile-dependent fluorescence response over a short time scale, our next hurdle was to optimize the components of the assay buffer with the aim of further enhancing enzyme activity in our assay.

2.3.3a Digitonin is the Optimized Detergent to Solubilize GPI-T

Detergents form micelles, which loosely mimic biological membranes. These micelles are essential to extract and solubilize membrane proteins in cell free systems. The impact of digitonin and igepal on GPI-T activity was assessed, with digitonin alone providing the strongest activity (Figure 2.9). We used 0.3% w/v digitonin to purify GPI-T by glutathione affinity purification (Gpi8 was modified with a GST tag). However, this digitonin concentration induced turbidity under our assay conditions, presumably due to the limited solubility of digitonin in aqueous solution and its tendency to precipitate over time at 30 °C (the temperature used for our FRET assays). Reduction of digitonin to 0.1%-0.2% alleviated this problem (Figure

2.10.). On the other hand, further reduction in the concentration of digitonin resulted in peptide substrate precipitation and turbidity. Clearly, there is a 'Goldilocks Zone' with respect to digitonin concentration: Too little and the peptide precipitates; too much and the digitonin precipitates. In both cases, turbidity eliminated the ability to observe GPI-T transamidation of the peptide substrate.

2.3.3b DTT and RG Enhance the GPI-T Activity

Incorporation of reducing agents are necessary for GPI-T assay to prevent possible cysteine oxidation, particularly in the Gpi8 active site. Reduced glutathione was a component of our assay buffer, simply because it was used to elute GPI-T from the glutathione affinity column. Addition of DTT caused a further enhancement of GPI-T activity, suggesting that insufficient RG remained to maintain a reducing environment. We did not analyze the impact of DTT alone because of the requirement for RG during GPI-T purification.

2.3.3c Effect of Enzyme Amount and Peptide Concentration

We also optimized the impact of enzyme (Figure 2.13) and peptide (Figure 2.14) concentration. A standard enzyme concentration was selected (50 mL, see experimental section for details) for optimal activity and an enzyme unit was defined to be 3 a.u./min. Similar to our digitonin experiments, peptide solubility limited the applicability of lower enzyme amounts. Unfortunately, this result highlights some of the difficulties faced when studying GPI-T. A 5 L cell culture yields only 1 mL of affinity purified enzyme (in 50%) glycerol. Thus, the number of assays that can be

conducted with a single preparation is severely restricted. Unexpectedly, the fluorescence signal was also ablated with higher concentrations of GPI-T, perhaps due to effects of one or more of the components in the enzyme preparation (*e.g.* glycerol, digitonin, etc.). A similar trend was observed with different peptide concentration. Here again the fluorescence response was relatively low at both low and high peptide concentrations, indicating an insufficient amount of substrate and excess precipitation, respectively.

2.3.3d Effect of Different GPI Anchor Mimics

As the final assay optimization step, we tested different GPI anchor mimics as substrates in our assay. Hydroxylamine and hydrazine were chosen as potential nucleophile donors due to published evidence that these compounds are suitable nucleophiles for GPI-T in *in vitro* translational assays, in the absence of GPI anchor *(105)*.However, hydroxylamine proved to be the best substrate with minimal activity with either EPME or hydrazine (Figure 2.15). While at first glance the negative results with EPME were surprising because this compound's similarity to the GPI anchor, EPME is not as potent a nucleophile as hydroxylamine (which is activated by the alpha effect) *(224)*. Unfortunately, only limited quantities of EPME were available so this potential substrate was only assayed once.

With these optimization steps, we have developed the first high throughput *in vitro* assay to kinetically analyze the catalytic activity of GPI-T. We are now positioned to characterize aspects of GPI-T that were previously inaccessible. Some of these efforts will be discussed in detail in chapter 3. In total, these optimization

experiments highlight the challenges that have limited GPI-T assay development over the past 20+ years.

2.3.4 Analysis of GPI-T Hydrolyzed Peptide Products

As discussed in section 2.2.4, efforts were made to isolate and mass spectrometrically analyze peptide products from our GPI-T assay. The aim of this experiment was to verify that the fluorescence response is due to the GPI transamidation reaction, producing a hydroxamate peptide. As shown in Figure 2.16, we observed the formation of new products and the loss of starting peptide , when a GPI-T assay was analyzed by HPLC. To our surprise, we did not observe the expected 12 amino acid length hydroxamate **1** by mass spectrometry. Instead, we observed the formation of truncated hydroxamates **2** and **3** with little variations between calculated and observed masses (Table 2.2). We believe these truncated hydroxamates are formed by GPI-T mediated transamidation. Asp4 and Glu7 are weak alternative ω sites present within the sequence of peptide **3**, in addition to the most probable ω site, Ser 12. May be the presence of biotin tag perturbs the identification of Ser12 ω site by GPI-T. Despite the fact that we did not observe the desired product, these results confirm GPI-T activity. Unfortunately, our method of product isolation was not without weaknesses and requires further optimization. We purified the peptide products by streptavidin affinity in order to separate these products from GPI-T and components of our assay buffer. Even with this purification step, the presence of digitonin complicated mass spectral analysis. To resolve this matter, alternative purification scenarios will need to be considered. For example,

the streptavidin and HPLC purification methods can be optimized. Alternatively, the assay mixture could be extracted with a mixture of chloroform and methanol to remove the digitonin. Current efforts in the Hendrickson group are focused on resolving this issue. In the near future, results from these experiments will presumably confirm that we have successfully reconstituted GPI-T *in vitro* and have demonstrated catalytic activity.

2.4 EXPERIMENTAL PROCEDURES

2.4.1 Materials and General Instrumentation

Peptide synthesis reagents were purchased from Advanced ChemTech, including N-α-(9-fluorenylmethoxycarbonyl) (Fmoc)-protected amino acids, *tert*butoxycarbonyl(Boc)-2-Abz, Fmoc-Ser (tBu)-Wang resin, N, N-Diisopropylethylamine (DIPEA), N-methyl-2-pyrrolidinone (NMP), O-Benzotriazole-N, N, N’ ,N’-tetramethyl-uronium-hexafluoro-phosphate (HBTU). HPLC grade acetonitrile (ACN), dichloromethane, acetic anhydride, and EZ-Run pre-stained Rec protein ladder were purchased from Fisher Bioreagents. Glutathione Sepharose 4B resin was purchased from GE-Amersham Biosciences. The rabbit anti-GST polyclonal antibody, and Goat anti Rabbit IgG (Hilyte plus 647 labeled) were purchased from Genescript and AnaSpec, Inc, respectively. The protease inhibitor cocktail was purchased from Roche Biosciences. Piperidine, digitonin, reduced glutathione and all other chemicals were purchased from Sigma-Aldrich and used without further purification. Centricon centrifugation devices were purchased from Millipore Corporation.

Peptides were synthesized both manually and using a Prelude peptide synthesizer (Protein Technology, Inc.), based on standard solid phase Fmoc synthesis protocols. The glass peptide synthesis vessel for manual peptide purification was purchased from ChemGlass Lifesciences. HPLC purification was performed using a System Gold HPLC (Beckman Coulter, Inc.). Reversed phase analytical columns were from Agilent Inc., and included a Zorbax SB-C3 (4.6 x 250 mm, 5 µm) used for initial analysis, and a semi-preparative column Zorbax 300SBC3 (21.2 x 250 mm, 7 µm) for bulk purification. A Zorbax SB-C18 analytical column was used for HPLC purification of GPI-T cleaved assay products. A BioFlo 110 fermentor (New Brunswick Scientific, Inc.) was used for fermentation growths. Fluorescence assays were performed on a Varian Cary Eclipse Fluorometer with a Peltier multicell holder (Agilent Inc.). Mass spectra of peptides were obtained by using either electrospray mass spectrometry (ESI) or matrix assisted laser desorption/ionization time of flight mass spectrometry (MALDI-TOF) in Dr. S. Trimpin's lab, Department of Chemistry, Wayne State University.

2.4.2 Buffers and Solutions

Homogenization buffer: 50 mM Tris HCl, pH 7.5 ,1 mM $MgCl_2$,1 mM $MnCl_2$. Cell resuspension buffer: 50 mM Tris HCl, pH 7.5, 1 mM $MgCl_2$, 1 mM $MnCl_2$, 1 mM dithiothreitol (DTT), 1 mM phenylmethylsulfonylfluoride (PMSF), protease inhibitor cocktail (pepstatin A, leupeptin, chymostatin, antipain and aprotinin). Membrane buffer: 50 mM Tris HCl, pH 7.5, 1 mM $MgCl_2$,1 mM $MnCl_2$, 1 mM DTT, 35% glycerol, 1 mM PMSF, protease inhibitor cocktail. Transmembrane (TM) buffer: 50

mM Tris HCl, pH 7.4 ,0.2 M mannitol, 0.1 M NaCl, 1 mM MgCl2, 1 mM CaCl2, 1 mM MnCl, 1 mM DTT, 1 mM PMSF and protease inhibitor cocktail. Glycerol TM (GTM) buffer: 50 mM Tris HCl, pH 7.4, 0.2 M mannitol, 0.1 M NaCl, 1 mM MgCl2, 1 mM CaCl2, 1 mM MnCl2, 1 mM DTT, 1 mM PMSF, protease inhibitor cocktail, and 10% glycerol. Column wash buffer: 50 mM Tris HCl, pH 7.4, 0.2 M mannitol, 0.1 M NaCl, 1 mM MgCl2, 1 mM CaCl2, 1 mM MnCl2, 1 mM DTT, 1 mM PMSF, protease inhibitor

cocktail, and 0.3% digitonin. Elution buffer: 50 mM Tris HCl, pH 7.4, 0.2 M mannitol, 0.1 M NaCl, 1 mM MgCl2, 1 mM CaCl2, 1 mM MnCl2, 1 mM DTT, 1 mM PMSF, 0.3% digitonin, and 20 mM reduced glutathione. Optimized assay buffer: 50 mM Tris HCl, 0.2 M mannitol, 0.1 M NaCl, 1 mM MgCl2, 1 mM CaCl2, 1 mM MnCl2, 1 mM DTT, 1 mM PMSF, 0.1% digitonin, and 20 mM reduced glutathione. On a technical note, it is important to prepare the digitonin buffer several days before GPI-T purification to allow sufficient time for maximum solubility. Further, during the buffer preparation digitonin should solubilize in required amount of water and heat to 95 °C to enhance the solubility. Fmoc cleavage solution: 20% piperidine, 80% NMP. Activator solution: 200 mM HBTU, 400 mM DIPEA (2.5 mL). Peptide cleavage solution: Anisole, thioanisole and trifluoroacetic acid (1: 2: 27 v/v/v).

2.4.3 Yeast Strain and Growth Conditions

Yeast strain FBY656 (MATa ade2-1 ura3-1 leu2-3, 112 trp1-1, his3-11, 15lys-GPI8Δ:kanMX2, containing YCplac22-GST-GPI8) was obtained from Professor Andreas Conzelmann *(138)*. Briefly, a single colony of FBY656, chosen from a –Trp

SD plate, was used to inoculate 50 mL YPD medium; the culture was incubated overnight at 37 °C in an incubator with shaking. The overnight culture was used to inoculate 250 mL YPD medium, which was incubated overnight at 30 °C with shaking. The 250 mL culture was used as an inoculum for a 5 L fermentation using the same growth medium at 30 °C with appropriate dissolved oxygen and pH controls. Preautoclaved antifoam A (100 µL/L) was used to prevent foam formation during fermentation. The FBY656 cells were collected by centrifugation when they reached mid-log phase.

2.4.4 Automated Peptide Synthesis

Peptide **2** was synthesized on a Prelude peptide synthesizer using presubstituted Fmoc-Ser(tBu)-Wang resin (100-200 mesh, 0.10 g, 0.6 mmol/g). The amino acids were coupled using HBTU chemistry as per the protocols obtained from the peptide synthesizer manual. Each amino acid was coupled three times in the presence of activator solution unless otherwise noted. Certain amino acids required three to four coupling reactions due to the high hydrophobicity of certain regions of the peptides. Before deprotection of each Fmoc protecting group, the resin was capped with acetic anhydride. The peptides were cleaved from the resin by mixing with 1.5 mL peptide cleavage solution and rotating for 2 hours on a wheel at room temperature. The cleaved peptides were precipitated with cold ether. The resultant precipitate was lyophilized and purified by reversed phase HPLC. HPLC fractions were tested by ESI or MALDI-TOF to verify the identity of desired peptide. The pure peptide fractions were lyophilized and stored dry or as a 1 mM DMSO

stocks at -20 °C.

2.4.5 Manual Peptide Synthesis

Peptides **2** and **3** were also synthesized manually. Pre-substituted Fmoc-Ser (tBu)-Wang resin (100-200 mesh, 0.10 g, 0.6 mmol/g) was used for both peptides and the amino acids were coupled using HBTU chemistry as per the standard protocols of solid phase Fmoc peptide synthesis. A Kaiser test was performed after deprotection and after coupling of each amino acid. Based on the results of the Kaiser test the amino acid coupling time scale was varied. The peptides were cleaved ,purified and stored as described in section 2.4.4

2.4.6 Extraction and Purification of the GST-tagged GPI-T Complex

2.4.6a Preparation of Microsomal Membranes and Solubilization of Membrane Proteins

This process was performed as per the protocols of Conzelmann *et al.(138)*. Briefly, FBY656 cells (from a 5 L culture) were harvested, pelleted, and washed in homogenization buffer. Next, the cell pellet was lysed with liquid nitrogen and the resulting homogenate was resuspended in cell resuspension buffer and clarified by centrifugation at 820g for 8 minutes. The membrane fraction was isolated by centrifugation at 60,000g for 1 hour. The supernatant was saved for gel analysis and the pellet was resuspended in the same buffer and centrifuged again for 1 hour at 60,000g. The pellet was resuspended in a small amount of membrane buffer (~1 mL for cells from a 5 L culture) sufficient to obtain a membrane suspension. The

membrane suspension was frozen in liquid nitrogen and stored at -80 °C. The frozen membrane suspension was thawed gently on ice, mixed with TM buffer, and treated with 0.2 mg/mL DNAse for 45 minutes at 25 °C with shaking. Digitonin was added to the mixture until the final concentration was 1.5 % w/v; this mixture was agitated at 4 °C for 45 minutes and pelleted at 60,000 g for 1 hour. The supernatant (the solubilized membrane protein mixture) was diluted to 0.3% digitonin with TM buffer and immediately used for affinity purification.

2.4.6b Affinity Chromatography Purification of GST- GPI-T Heterotrimeric Complex

All purification steps were conducted at 4 °C unless otherwise noted. The solubilized membrane protein mixture was diluted to 10 mL with TM buffer and mixed with 1 mL glutathione sepharose 4B resin. The mixture was incubated overnight on a wheel; then the supernatant (unbound fraction) was removed and the protein-bound resin was washed three times with 10 mL column wash buffer for 15 minutes followed by 1 hour for sedimentation. The supernatants from each wash were preserved for gel analysis. The bound protein was first eluted (Eluate 1) by adding 1 mL of elution buffer (TM buffer + 0.3 % digitonin + 20 mM reduced glutathione) and then eluted a second time (Eluate 2) with another 1 mL of elution buffer, containing 100 mM reduced glutathione. The resin was incubated with each elution solution for 30 minutes with gentle agitation, followed by 30 minutes sedimentation. Each supernatant (eluted protein) was carefully removed and concentrated using Centricon centrifugation devices (Millipore Corp., Bedford, MA).

For each 5 L enzyme prep the eluted protein samples were concentrated to 500 µL and combined with another 500 µL 50 % glycerol before stored at -20 °C.

2.4.6c Detection of GST-Gpi8

Affinity purified GPI-T was loaded onto a 10% polyacrylamide gel for SDS–PAGE analysis. The gel was stained with silver nitrate to detect the presence of GST-Gpi8, Gpi16 and Gaa1, as per the manufacturer's instructions. The presence of GST-tagged Gpi8 was also confirmed by Western blotting with anti-GST antibody. Rabbit anti-GST polyclonal antibody was used as the primary antibody. Goat anti-Rabbit IgG (Hilyte plus 647 labeled) was used as the secondary antibody. Western blotting was performed as per the protocols provided by the manufacturer of the antibodies.

2.4.7 Fluorescence Assay

All peptides used for the assay were prepared as 1 mM DMSO stocks, sterile filtered, aliquoted in 20 µL fractions, and stored at -20 °C. Assay buffers were prepared in advance as large-scale stock solutions and stored at 4 °C. For each assay, the required amount of peptide and buffers were taken out 15 minutes prior to the experiment and equilibrated at room temperature for 10 minutes and then at 30 °C for 5 minutes. Freshly prepared 1 mM DTT and 1 mM PMSF were added to the assay buffers, mixed well and filtered with 0.45 µM sterile filters immediately before each assay. Each peptide was mixed with 1.93 mL assay buffer with or without nucleophile substrate. Fluorimeter settings were set to the following parameters:

excitation wavelength: 321.0 nm; emission wavelength: 417.0 nm; excitation slit width: 10 nm; emission slit width: 5 nm; temperature: 30 °C. Assays were initiated by the addition of 50 µL of a typical GPI-T enzyme preparation. Assays were mixed throughout the kinetic run using small magnetic stir bars. Fluorescence emission was monitored over time at 10-second intervals.

2.4.8 Analysis of GPI-T Cleaved Hydroxylamine Attached Peptide Products.

The fluorescence assay was performed with biotinylated peptide **3** and GPI-T for 3 hours at 30 °C using the fluorimeter parameters specified in section 2.5.6. For each assay, 0.05 mg of peptide **3** was incubated with 100 µL GPI-T with 10 mM hydroxylamine. Twenty assays were performed simultaneously, utilizing a total of 1 mg peptide **3** and 2000 µL GPI-T obtained from 2 enzyme purifications that were pooled together. Assay samples were frozen at -80 °C immediately after the incubation period. Once all samples were obtained, the frozen samples were thawed back to room temperature and mixed with protease inhibitor cocktail. Meanwhile the streptavidin sepharose resin was washed with assay buffer without digitonin. The assay samples were pooled and mixed with this resin (1.5 mL bed volume). The mixture was incubated at room temperature for 1 hour with agitation. The supernatant was removed and the resin bound peptide was washed with 6 mL H_2O. The resin was resuspended in 2 mL H_2O , and incubated at 70 °C for exactly 2 minutes to reversibly broken the biotin-streptavidin interaction *(225)*. The supernatant, carrying peptide 3 and any biotinylated peptide fragments, was removed immediately to prevent rebinding to the resin. The samples were

lyophilized and analyzed by HPLC using a 40-100% ACN/H_2O gradient over 41 minutes. The fractions were collected and analyzed by ESI.

2.4.9 Methods to Calculate GPI-T Activity

Each fluorescence assay was run in two or three independent experiments, each using a different batch of GPI-T to account for variability between preparations. An arbitrary GPI-T unit of 3 a. u./min (a. u. = arbitrary units) was defined and fluorescence intensities were normalized with a unit correction factor. The unit correction factor was calculated separately for each individual enzyme batch . In order to do so, for every enzyme batch purified, first, a standard assay was performed with 10 mM NH_2OH, 10 μM peptide **2,** and 50 μL enzyme. The fluorescence intensity obtained over the first 5 minutes of this assay was divided by 15 a.u./5 min scale (based on defined GPI-T unit 3 a.u./min) to obtain a unit correction factor for that particular batch of enzyme. For instance, if an enzyme batch produced fluorescence intensity of 30 a.u during the first 5 minutes of the assay, then the unit correction factor for that particular enzyme batch would be 2. This unit correction factor was used to normalize fluorescence intensity values for comparison between different enzyme preparations. Next, initial rates were calculated for the fluorescence data normalized with the unit correction factor. Data for initial rate determinations was varied from experiment to experiment based on the linear range of fluorescence change over time (refer to initial rate calculation data in appendix A). Next, each initial rate value for a particular experiment was divided by the average initial rate (averaged from triplicate or duplicate assays) of

the standard assay to obtain relative rates. Standard assay (represented in dark gray in vertical bar graphs) has a relative rate of ≅ 1 and the other assays were adjusted accordingly. For example, in Figure A1 (B) of Appendix A, the highest initial rate was obtained for the assay with NH_2OH. The assay was run in triplicate and the three initial rates (3.01, 3.05 and 2.97 a.u./min) were averaged to obtain a mean initial rate (3.01 a.u./min). This value was used to divide all the initial rate values (2.87, 3.06 and 3.15 a.u./min) obtained for assay with NH_2OH to obtain relative rate values (1.00, 1.02 and 1.05). The mean±SD value of the three relative rates (=0.999±0.00666) corresponding to with NH_2OH assay were represented in a vertical bar graph. For the same data set, the assay without hydroxylamine and no enzyme gave lower initial rates (1.51, 2.01, and 1.41 a.u./min and 0.702, 0.485 and 0.553 a.u/min respectively). Each initial rate is first divided by the average initial rate of with NH_2OH assay, 3.01 a.u/min, to obtain relative rate values. For no NH_2OH assay relative rates are 0.502, 0.668 and 0.468 and the mean±SD value of three relative rates was equal to 0.546±0.0619. For no enzyme assay the relative rates are 0.233, 0.161 and 0.184 and the mean±SD value of three relative rates was equal to 0.192±0.0216. obtained to obtain relative rates (0.54, 0.60 and 0.48) for no NH_2OH assay. The mean±SD values of with NH_2OH, no NH_2OH and no enzyme assays were represented in a vertical bar graph as shown in Figure 2.7. In this way, assays from different enzyme purifications and using different substrates and nucleophiles could be directly compared. Background fluorescence was observed over time in a no enzyme control assay (10 mM NH_2OH and 10 μM peptide **2** and assay buffer).This background fluorescence (mean relative rate = 0.192) is

represented as a red dashed line in all the plots. The data above this line is considered significant and relevant to GPI transamidation.

2.4.10 Statistical Analysis

Each independent experimental trial was performed two or three times. The relative rates were expressed as the mean±SD for n≥3 and as the mean for n=2. Statistical analysis was performed using a two-way, unpaired t-test with 95% confidence interval for n≥3. P-Values<0.05 were considered statistically significant. GraphPad Prism and KaleidaGraph software packages were used to analyze and plot the data. Vertical column bar graphs, representing mean±SD of the relative rates were used for assays in triplicate. Vertical column bar graphs and scattered plots (Appendix A) were used to represent relative rates for the assays done in duplicate. Scattered plots were used specifically to represent the difference in individual relative rates from the mean in the absence of p-values and error bars.

2.5. Acknowledgement

Thanks are extended to Dilani Gamage, Dr. Ellen Inutan and Dr. Sarah Trimpin for ESI analysis of peptides; Dr. Rachel Morissette for peptide **2**; Dr. Tamara Hendrickson for Gpi8 solubilization experimental data; Dr. Franklin John for EPME and Dr. Yug Varma and Megan Ehrenwerth for guidance in enzyme purification and peptide synthesis and purification.

Chapter 3

Enzymatic Characterization of the Catalytic Activity of *S. cerevisiae* GPI-T

3.1 INTRODUCTION

GPI-T is an important enzyme for eukaryotic organisms. Several *in vivo* and *in vitro* assays have been developed to investigate GPI-T (see chapter 2). The limitations of these assays prevented detailed kinetic analyses and mainly reported qualitative information*(111,112,115,119,123-125,131,139,142-146,148,151,158-161,165,166,208)*. However, with emerging research on GPI-T, especially in the medicinal field *(9-11,198-200)*. there is an urgent requirement for a kinetic analysis of this enzyme and for rapid methods to screen GPI-T inhibitors. Consequently, our new *in vitro* assay becomes an indispensable tool to characterize GPI-T. This chapter describes our efforts towards characterizing GPI-T's catalytic activity by investigating its peptide substrate recognition requirements, species specificity, GPI-T inhibitors, and the possibility of cofactor involvement in catalysis.

3.1.1 Recognition of the C-terminal GPI-T Signal Sequence by GPI-T

The C-terminal GPI-T signal sequence contains three key identity elements: the ω site, the hydrophilic spacer region and the hydrophobic region *(57,111,112,115,124,125,226)*. The requirements for these regions were discussed in detail in Chapter 1 and are briefly summarized in the following sections.

3.1.1a Sequence Requirements for the ω-Site Region

The ω site amino acid is always a relatively small, hydrophilic amino acid such as Ser, Gly, Ala, Asp, Cys, Leu and Val.*(111,112,114,115)* Deletion of this residue or replacement with a larger amino acid eliminates GPI anchoring *(115)*. These results confirmed that ω site residue is a key determinant used by GPI-T to identify appropriate substrate proteins. Amino acid specificity at the ω+1 and ω+2 residues is also important for an effective GPI transamidation reaction. Any amino acid other than proline is acceptable at the ω+1 site.*(119)* However, ω+2 site requirements are more stringent; this site should always contain a small amino acid such as Gly, Ala and Ser for an effective GPI transamidation.*(119,120,227)*

3.1.1b Hydrophilic Spacer Region Requirements

The spacer region does not contain a consensus sequence and is composed of a stretch of mostly hydrophilic amino acids *(116,118,121,122)*. Relative hydrophilicity and the length of this region are important determinants in the overall GPI-T signal sequence. Furukawa and coworkers showed that truncation of the eight amino acid spacer region in bovine 5′-nucleotidase (a GPI anchored protein) to four amino acids abrogated GPI anchoring *(122)*. However, elongation with alanines back to 14 amino acids restored GPI anchoring. This spacer region may also have a role in maintaining the proprotein in a unique conformation for introduction into the active site of GPI-T *(118)*.

3.1.1c C-terminal Hydrophobic Region Requirements

The C-terminal GPI-T signal sequence ends with a hydrophobic stretch of amino acids. Like the hydrophilic spacer, this hydrophobic region does not contain a consensus sequence but its relative hydrophobicity and length govern GPI anchoring efficiency of substrate proteins *(57,123-125)*. For instance, compared to wild type PLAP, which has a 23 amino acid GPI-T signal sequence, PLAP mutants truncated to a 17 amino acid signal sequence were not GPI anchored and were translocated to the cytosol. Further, extension of these PLAP mutants with hydrophobic residues restored GPI anchoring, while extension with hydrophilic residues did not. Similar results were obtained with *S. cerevisiae* Gas1p*(57)* and human DAF *(124)*. The hydrophobic domain may also contribute to proper orientation of the ω residue in the GPI-T active site by temporarily anchoring the substrate protein to the inner leaflet of the ER membrane where GPI-T is localized *(127)*.

3.1.2 Species Specificity of GPI-T

As described in section 3.1.1, GPI-T substrate proteins contain C-terminal signal sequences with a pattern of hydrophilic and hydrophobic residues. However, even within these minimal sequence requirements, GPI-T exerts apparent species specificity *(128-131)*. Presumably, structural variations in the GPI-T active site and/or the GPI-T signal sequences between different organisms lead to species-specific selection of substrate proteins *(128,130,131)*. For example, the gene encoding human growth hormone (hGH), a soluble protein, was modified to append

three different GPI-T signal sequences onto its C-terminus; the anchoring efficiency of each of these recombinant proteins was quantified. The signal sequences came from *T. brucei* VSG, human DAF, and *P. berghei* circumsporozoite protein (CS). Only the human DAF sequence imparted GPI anchoring in mammalian COS cells. Sequence analyses suggested that the parasitic ω region is incompatible with mammalian GPI-T machinery due to structural variations within the ω residue-binding pocket of mammalian GPI-T *(128)*. GPI-T species specificity was also probed by the Hendrickson lab, by appending two human and one yeast GPI-T signal sequences onto the C-terminus of the yeast secretory protein invertase (INV) *(131)*. The human sequences were derived from the campath-1 antigen (CA25) and the urokinase-type plasminogen-activated receptor (UP30), and the fungal sequence was from the *S. cerevisiae* GPI-AP, yapsin 2 (Y21). They demonstrated that the yeast sequence produced the highest levels of GPI-anchored INV on the cell surface of *S. cerevisiae*. A series of chimeric signal sequences, combining portions of the Y21 and the CA25 sequences, pinpointed discrimination to a six-residue portion of the GPI-T signal sequence; this peptide fell within the hydrophobic region of the signal sequence.

3.1.3 Is GPI-T Activity Regulated *in vivo?*

GPI-T is associated with human diseases like cancer *(9-11,198)*. In order to develop chemotherapeutics, it is important to identify ways to control GPI-T activity, either via inhibitors or at the level of expression. Unfortunately, investigations focused on regulating GPI-T activity/expression have been limited. One limit to such

research is a lack of background information on GPI-T catalysis from a quantitative, mechanistic viewpoint. The structurally complicated nature of GPI-T and absence of high throughput quantitative assays with pure solubilize GPI-T account for this situation.

The only mechanistic information available for GPI-T stems from Gpi8's sequence and putative structural similarity to cysteine proteases *(156,157)*, especially to caspases *(143,151,152)*. The Gpi8 subunit contains a cysteine/histidine catalytic dyad similar to that of cysteine proteases *(148,151,158)*. Consistently, sulfhydryl alkylating agents like iodoacetamide inhibit GPI-T *(150,153)*.

The impact of nucleotide cofactors on GPI-T activity was also investigated. The results were contradictory *(135,136,228)* as some report that nucleotide cofactors enhance GPI-T activity while others report no impact. However, this question requires further investigation with an assay like ours, which uses affinity-purified GPI-T *(135,136,228)*. One of the goals of the research described in this chapter was to apply our FRET assay for GPI-T (introduced in chapter 2) to answer these questions.

3.2 RESULTS

3.2.1 Design and Synthesis of Peptide Substrates

In order to analyze the catalytic activity of purified GPI-T, small propeptides (Table 3.1 and Table 3.2) were synthesized based on the human campath–1 (CD52) antigen and yeast aspartyl protease (Yapsin 2). As detailed in section 2.2.1 the propeptide sequence of wild type CD52 was modified to peptide **2;** this peptide was

used to develop our GPI-T assay**.** Peptides **4** and **5** are based on peptide **2** with single ω site mutations. These peptides were designed to demonstrate that our assay shows the same ω site requirements as more established GPI-T assays. Since GPI-T only accepts small amino acid residues at the ω site, we hypothesized that peptide **4** would be, at best, a weak substrate for GPI-T while peptide **5** would not be a substrate. A series of peptides (**6**-**10**) were constructed to determine the sensitivity of our assay to C-terminal truncations. Dr. Rachel Morissette (Hendrickson lab alumna) synthesized peptides **2,** and **4-10** (Table 3.1).

Table 3.1 Peptide substrates to study GPI-T signal sequence variations

Peptide	**N-terminus**	**N-terminal seq.**	**ω**	**GPI-T Signal sequence**
WT CD52		GQNDTSETSSP	S	ASSNISGGIFLFFVANAIIHLFCFS
2	Abz	GQKDTSEKSSP	S	ASKN*YSGGIFLFFVANAIIHLFHFS
4	Abz	GQKDTSEKSSP	D	ASKN*YSGGIFLFFVANAIIHLFHFS
5	Abz	GQKDTSEKSSP	R	ASKN*YSGGIFLFFVANAIIHLFHFS
6	Abz	GQKDTSEKSSP	S	ASKN*YSGGIFLFFVANAIIHL
7	Abz	GQKDTSEKSSP	S	ASKN*YSGGIFLFFVANA
8	Abz	GQKDTSEKSSP	S	ASKN*YSGGIFLFF
9	Abz	GQKDTSEKSSP	S	ASKN*YSGGIFL
10	Abz	GQKDTSEKSSP	S	ASKN*YS

Abz; 2 - aminobenzoic acid, *Y: 3-nitrotyrosine. Underlined residues were modified from the native, wild-type sequence for CD52, as described in Chapter 2.

Yapsin 2 was selected to analyze the species specificity of GPI-T, in comparison to peptide **2** (which is based on the human CD52). Among different *S. cerevisiae* GPI anchored proteins *(117,229)*, we chose Yapsin 2 due to the predicted synthetic accessibility/solubility of its C-terminal GPI-T signal sequence. The native signal sequence also has useful positions to introduce the Abz fluorophore (on the side chain of Lys25) and the 3-nitrotyrosine quencher (in place of Phe14). The *N*-terminal threonine was acetylated to avoid attachment of an extra Abz group. Dilani Gamage (current Hendrickson lab member) synthesized peptide **11** based on the amino acid sequence of WT Yapsin 2 (Table 3.2).

Table 3.2. Peptide substrate based on a fungal substrate for GPI-T

Peptide	**N-terminus**	**N-terminal seq.**	**ω**	**GPI-T Signal sequence**
WT Yapsin 2		TRKE	N	GGHNLNPPFFARFITAIFHHI
11	Ac	TRK(Abz)E	N	GGHNLNPP*YFARFITAIFHHI

Abz; 2 - aminobenzoic acid, *Y: 3-nitrotyrosine. Underlined residues were modified from the wild-type sequence as described in the text

3.2.2 Extraction and Purification of GPI-T

GPI-T was purified as described in section 2.2.3 of Chapter 2.

3.2.3 The Effect of ω Site Identity on Substrate Recognition by GPI-T

Amino acid specificity at the ω site of the GPI-T signal sequence has been analyzed qualitatively using both in cell and cell free assays *(111,112,114,115,120,227)*. However, none of these experiments were quantitative

and relied on endogenous or crude microsomes as the source of GPI-T. We decided to quantitatively analyze the impact of amino acid specificity at the ω site using our new GPI-T assay (Figure 3.1). Three CD52 peptides with variations at the ω site were tested as substrates for GPI-T (Table 3.1). Peptide **2** contains the wild-type Ser12 at the ω site, while peptides **4** and **5** contain Asp12 and Arg12, respectively. Consistent with previous results *(111,112,114,115)* and bioinformatic analyses *(5,6,230)*, peptide **2** was the best substrate for GPI-T. These results offer further evidence that our assay is monitoring GPI-T directly.

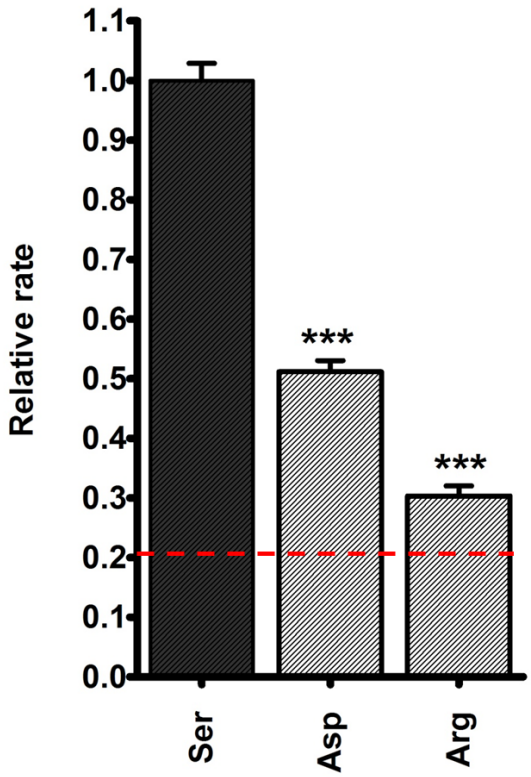

Figure 3.1. Effect of the identity of the ω site amino acid on substrate recognition by GPI-T. Peptide **2**, with serine at the ω site, yields the highest initial rate of transamidation. The red dashed line indicates background fluorescence (relative rate = 0.192±0.02). Data above this line was considered relevant to GPI-T transamidation. Data represent the mean ± SD, n = 3 and $P<0.05$ compared to peptide **2** (ω = serine, dark gray). For raw assay data, see Appendix B, Figure B1.

3.2.4 The Importance of the Length of the GPI-T Signal Sequence on Substrate Recognition

The overall hydrophilic and hydrophobic profile as well as the length of the GPI-T signal sequence are key parameters that determine transamidation efficiency.*(57,111,112,115,124,125,226)* Lack of these elements converts a substrate protein into a non-substrate *(231)*. Therefore, in accordance with this information, we used our *in vitro* assay to analyze the impact of signal sequence length on substrate activity. A series of truncated analogs of peptide **2 (**peptides **6** - **10**, Table 3.1) were used for this purpose. None of the shortened peptides were robust substrates for GPI-T, when compared to full-length peptide **2** (Figure 3.2). In fact, the loss in GPI-T activity correlated with the length of each truncation; the longest peptide was the best substrate and the shortest two peptides were not substrates at all (within the sensitivity limits of our assay).

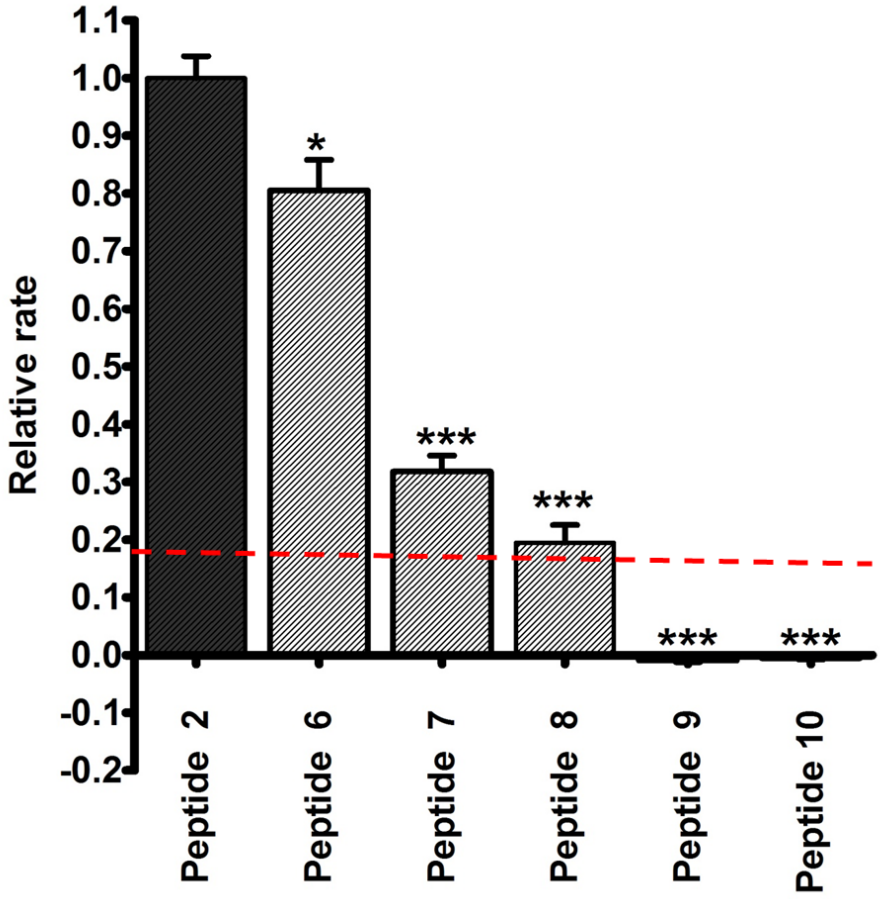

Figure 3.2 Effect of the length of the C-terminal GPI-T signal sequence on substrate recognition by GPI-T. Peptide **2** the wild-type GPI-T signal sequence yielded the highest initial rate of transamidation. GPI anchoring activity diminished as the length of the signal sequence was shortened. The red dashed line indicates background fluorescence (relative rate = 0.192±0.0216). Data above this line was considered relevant to GPI-T transamidation. Data represent the mean ± SD, n = 3 and $P \leq 0.05$ compared to peptide **2** (dark gray).

3.2.5 Species Specific Substrate Selectivity of GPI-T

GPI-T appears to have different affinities towards peptide substrates from different species *(128,130,131)*. To investigate this phenomenon further, we used our *in vitro* FRET assay to examine the species-specific substrate specificity of GPI-T with two peptide substrates. Our assay development has been based on a human

peptide substrate for GPI-T, peptide **2**; but our GPI-T was purified from *S. cerevisiae*. We hypothesized that a fungal peptide substrate would be a stronger substrate for the fungal GPI-T. We chose to test a yeast peptide substrate (peptide **11**) based on the C-terminus of the aspartyl protease Yapsin 2 (Table 3.2) because of synthetic accessibility and the fact that this signal sequence was a robust substrate for GPI-T when tested with our in vivo invertase assay *(131)*. Activity was compared to our standard CD52 substrate peptide **2** (Table 3.1). Each peptide was separately assayed with pure GPI-T. Since both Yapsin 2 and GPI-T are from *S. cerevisiae*, we expected peptide **11** be the stronger substrate. However, the fluorescence response produced with peptide **11** was negligible, even at higher peptide concentrations (Figure 3.3.). Efforts to optimize assay conditions for this substrate were ineffective (not shown).

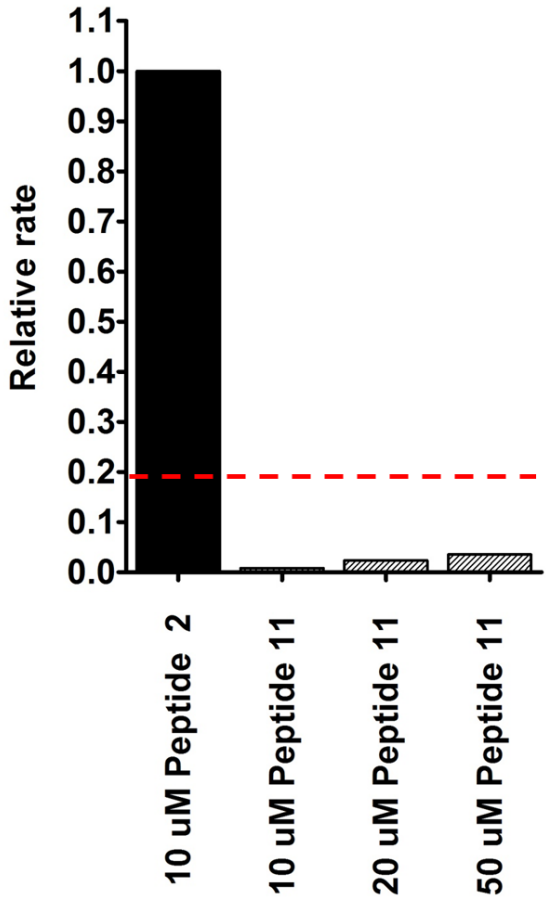

Figure 3.3 Species specific substrates and GPI-T. *S. cerevisiae* GPI-T was incubated with different concentrations of peptide **11** versus peptide **2** in the presence of 10 mM NH_2OH and *S. cerevisiae* GPI-T. Peptide **11** was not a substrate under the assay conditions tested. The red dashed line indicates background fluorescence (relative rate = 0.192±0.0216). Data above this line was considered relevant to GPI-T transamidation. Data represents the mean of experiments run in duplicate. See Appendix B, Figure B3 for raw data.

3.2.6 Effect of Transition Metal Ion Cofactors on the Catalytic Activity of GPI-T

To our knowledge, the possibility that GPI-T requires a metal cofactor has never been evaluated. Given that some caspases bind metal ions *(232-240)*, we hypothesized GPI-T might also require a transition metal for activity or regulation. To test this hypothesis, we compared GPI-T activity in the presence of various transition metals (Figure 3.4.).

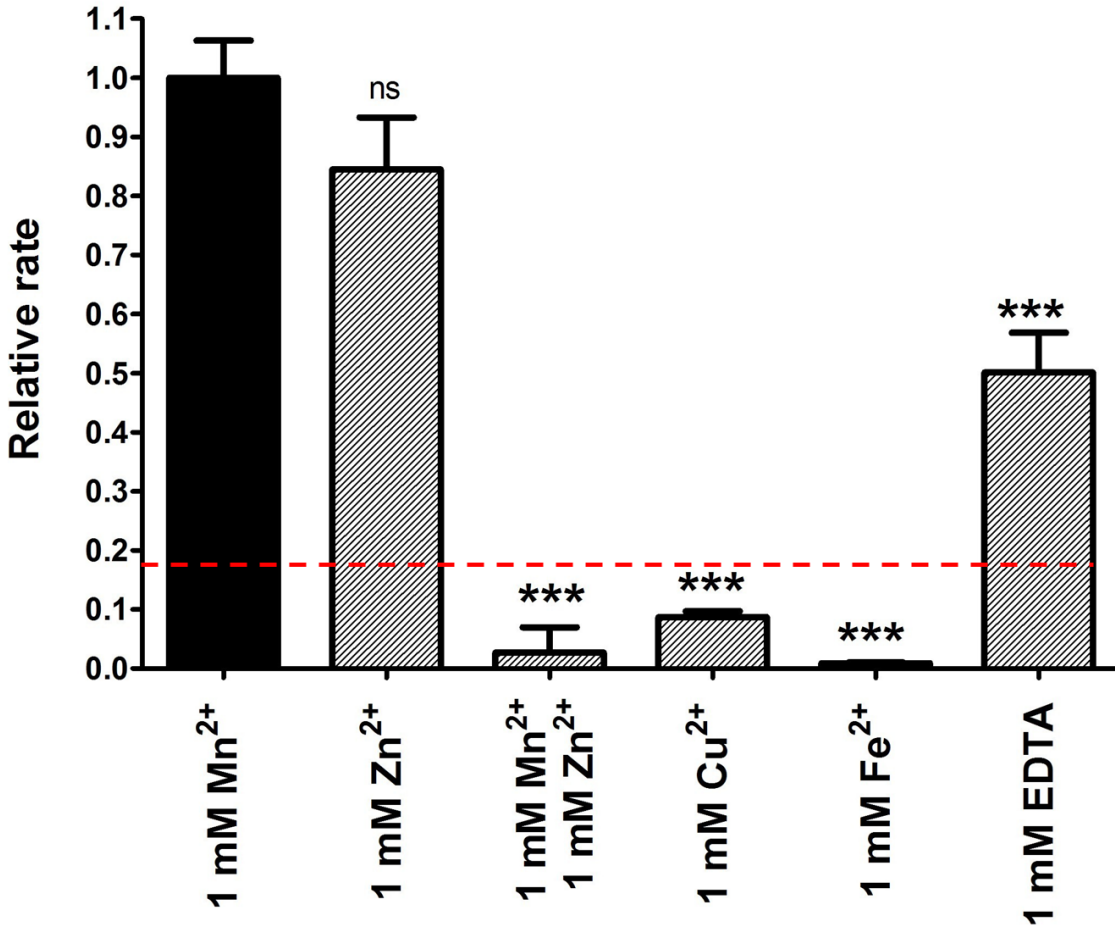

Figure 3.4 Effect of different transition metals on GPI-T activity. GPI-T activity was measured with peptide **2** and 10 mM NH_2OH in the presence of different metal ions, each at 1 mM concentrations, and GPI-T. EDTA (1 mM) was used in a control assay. The red dashed line indicates background fluorescence (relative rate = 0.192±0.0216). Data above this line was considered relevant to GPI-T transamidation. Data represent the mean ± SD, n = 3 and P≤ 0.05 compared to the assay with 1 mM Mn^{2+} as the transition metal (dark gray). ns: not significant. See Appendix B, Figure B4 for raw data.

The presence of Mn^{2+} and Zn^{2+} enhanced GPI-T activity, compared to the EDTA control; each of the three other metals tested inhibited GPI-T activity. These results suggest that the catalytic activity of GPI-T is metal-dependent. Surprisingly, however, a combination of Mn^{2+} and Zn^{2+} ablated enzyme activity, a result that requires further analysis before precise conclusions can be made.

3.2.7 The Effect of Leupeptin, a Cysteine Protease Inhibitor, on GPI-T Activity

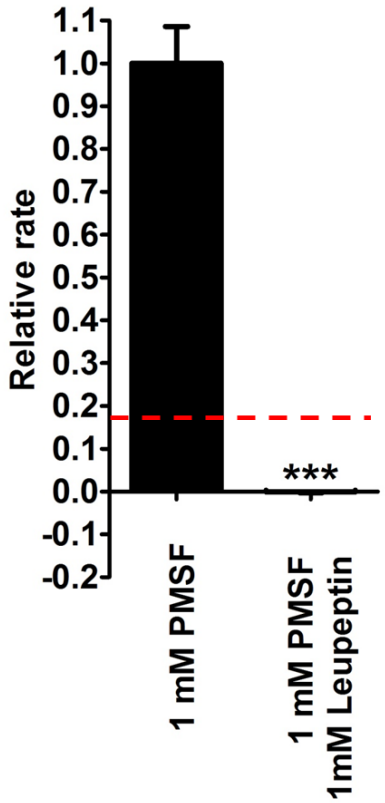

Figure 3.5 Effect of Leupeptin, a cysteine protease inhibitor, on GPI-T activity. GPI-T activity was measured with peptide **2** and 10 mM NH_2OH in the presence of different protease inhibitors, each at 1 mM concentrations. Presence of 1 mM leupeptin completely abolish the GPI-T catalytic activity. The red dashed line indicates background fluorescence (relative rate = 0.192 ± 0.0216). Data above this line was considered relevant to GPI-T transamidation. Data represent the mean ± SD, n = 3 and $P \leq 0.05$ compared to assay with 1 mM PMSF as the protease inhibitor (dark gray). See Appendix B, Figure B5 for raw data.

As mentioned above, Gpi8, the active site subunit of GPI-T, has sequence homology to caspases and other cysteine proteases *(152,156,157)*. Thus, we hypothesized that cysteine protease inhibitors might inhibit the active site of Gpi8. We confirmed this hypothesis by testing the impact of leupeptin, a cysteine protease

inhibitor, on GPI-T activity (Figure 3.5.). As expected, leupeptin inhibits GPI-T activity.

3.2.8 Effect of Nucleotides on Catalytic Activity of GPI-T

The impact of ATP and GTP on GPI anchoring has been examined and reported with contradictory results *(135,136,228)*. However, these assays were performed in an *in vitro* translation system with crude GPI-T. Thus, we reassessed the impact of ATP and GTP using our new *in vitro* assay (Figure 3.6.). The fluorescence response for the control assay (without either NTP) was significantly higher than those with either ATP or GTP (Figure 3.6a). The ATP assay showed an initial rate that was similar to the control assay; however this assay plateaued at a significantly lower level, indicating that less peptide substrate was processed. The relative rate data in Figure 3.6b is based only on the initial rate and does not take the relative plateau levels into account (Shown in Figure 3.6a). In total, these data demonstrate that neither GTP nor ATP have any role in enhancing GPI-T activity; however, they may play some sort of regulatory role as both nucleotides diminished overall transamidation activity.

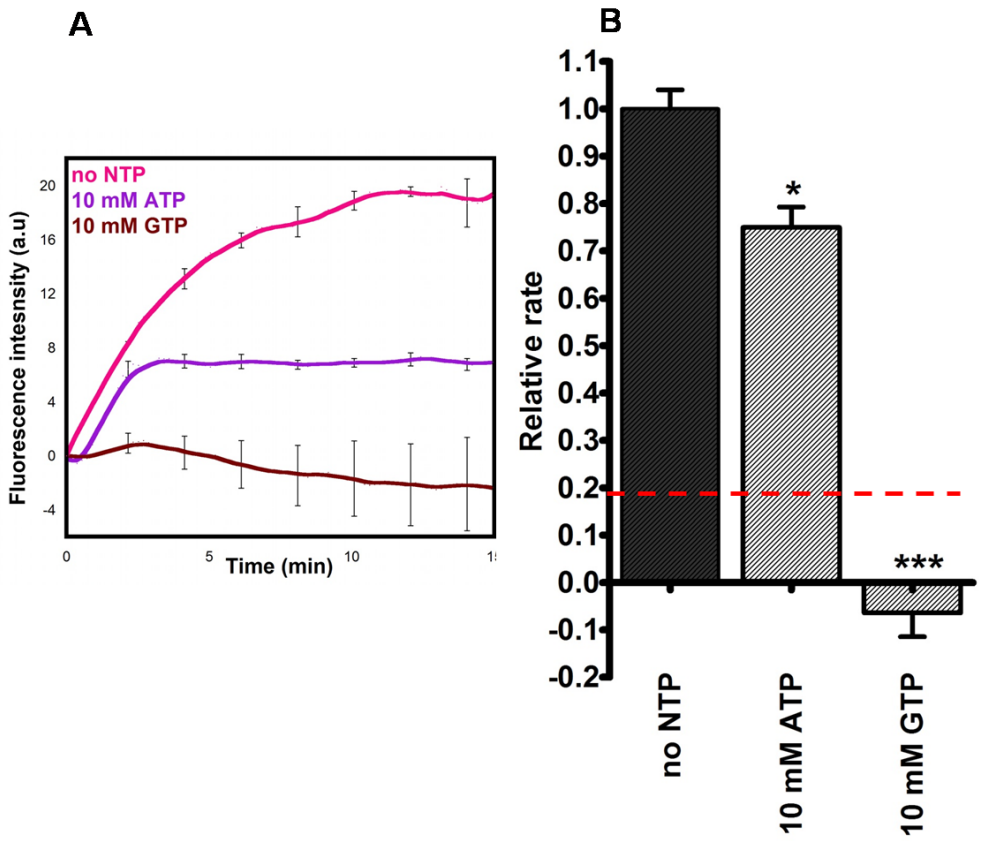

Figure 3.6 Effect of nucleotides on the catalytic activity of GPI-T. GTP and ATP did not enhance GPI-T activity with peptide **2** as the substrate. (A) GPI-T activity in terms of fluorescence response. Activity was measured with 10 μM peptide **2** and 10 mM NH_2OH with different nucleotides, each at 10 mM concentrations, and GPI-T. A no NTP assay was performed as a control. Magenta: no NTP; Purple: 10 mM ATP; Maroon: 10 mM GTP. Error bars indicate the standard deviation (SD, n=3). (B) Relative rates were calculated from the initial rate data in A. The red dashed line indicates background fluorescence (relative rate = 0.192 ± 0.021). Data above this line was considered relevant to GPI-T transamidation. Data represent the mean ± SD, n = 3 and P ≤0.05 compared to assay with no NTP (dark gray).

3.3 DISCUSSION

The lack of quantitative tools and the complexity of GPI-T has limited the type of studies that could be conducted to better understand this enzyme. Especially, investigations on the catalytic activity of GPI-T with a more quantitative, mechanistic approach have been missing. However, our *in vitro* assay for GPI-T, described in Chapter 2, offers a new approach to look at GPI-T. In this chapter we describe the use of this assay to investigate certain aspects of GPI-T catalysis, including peptide substrate recognition, species specificity and ways to regulate GPI-T catalytic activity.

3.3.1 Our *in vitro* GPI-T Assay Distinguishes Between Different ω site Residues

For our first efforts to characterize GPI-T with our assay, we decided to confirm previous observations made with GPI-T *in vivo* or in crude *in vitro* translation systems. As detailed in Chapter 1 and section 3.1.1a, the ω amino acid should be a relatively small amino acid (e.g. Ser, Gly, Ala, Asp, Asn and Cys) *(111,112,114,115)*. We designed three peptide substrates for this experiment with variations at the ω site (Ser12, Asp12, and Arg12). As expected, Ser12 was the strongest ω site, followed by Asp12, and then Arg12 (see Figure 3.1)..Our results were consistent with previous findings as the highest GPI-T activity was observed with the Ser12 ω site. GPI anchoring was lower with Asp12 and nearly eliminated with Arg12. These results provide further support that our new assay is specific for GPI-T activity, rather than for any non-specific protease contaminant.

3.3.2 Length of the GPI-T Signal Sequence is Important for Peptide Substrate Recognition by GPI-T

As described in Chapter 1 and section 3.1.1c above, the hydrophobicity profile and the length of the GPI-T signal sequence are critical parameters for GPI-T substrate recognition *(57,111,112,115,124,125,226,231)*. We tested the length of the C-terminal GPI-T signal sequence using our *in vitro* assay as a continuation of our assay validation process and to investigate GPI-T catalytic activity further. A series of C-terminally truncated peptides (peptide **6-10**, Table 3.1) were tested as substrates for GPI-T. Transamidation activity was completely abolished for peptides lacking most of the hydrophobic region of the GPI-T signal sequence. In fact, only peptide **6**, the peptide with the shortest truncation, showed any substrate activity when assayed with GPI-T, compared to that of peptide **2**. Overall, these results confirmed the contributions of the key identity elements, ω region and hydrophobic region, for GPI-T recognition of substrate peptides.

In 2007, an *in vivo* GPI-T assay developed by the Hendrickson group revealed that the replacement of the CD52 (Table 3.1) sequence FVANAI with Yapsin 2 (Table 3.2) sequence ARFIT enhanced CD52 transamidation *(131)*. For the moment, we have not synthesized peptides to demonstrate the impact of this sequence perturbation *in vitro.* We believe that such a replacement will further enhance the GPI-T activity of our model peptide substrate.

3.3.3 Species-Specific Substrate Selectivity of GPI-T

GPI-T appears to exert different affinities towards peptide substrates from different species *(128,130)*. To investigate this phenomenon further, we used our *in vitro* assay to compare two GPI-T substrates from different species. Transamidation of the yeast peptide substrate based on Yapsin 2 (peptide **11**,Table 3.2) was compared to that of our standard peptide substrate based on the human CD52 (peptide **2**). We expected to observe optimal activity with the yeast peptide substrate, peptide **11**, because our assay uses the homologous yeast GPI-T. However, the fluorescence response produced with **11** was negligible even at higher concentrations (Figure 3.3), despite efforts to optimize assay conditions. This poor substrate behavior may be due to the shorter N-terminal region upstream of the ω site in peptide **11**. Peptide **2** contains eleven residues N-terminal to the ω site; this sequence reflects the entire CD52 wild-type sequence, following ER processing of the N-terminal signal peptide. In contrast, peptide **11** only contains four amino acids N-terminal to the ω-site. Further, the peptide **11** sequence only represent a short fragment of the full-length Yapsin 2 propeptide which is 384 amino acids long. In the future, a longer Yapsin 2 peptide substrate, with an extended C-terminal GPI-T signal sequence, needs to be tested.

3.3.4 External Modulators of GPI-T Activity

Due to the highly complicated nature of GPI-T and lack of high throughput assays, we still do not have a clear picture of GPI-T structure or catalytic activity. For the first time in GPI-T history, we have a high throughput *in vitro* assay that uses

pure, solubilized GPI-T. Further, we recognize the similarities between Gpi8, the catalytically active subunit of GPI-T, with that of cysteine proteases. As discussed in Chapter 1, Gpi8 demonstrates 25%-28% sequence homology to the C13 family of cysteine proteases, with weak sequence similarity at the active site of several caspases *(138,151)*. Mn^{2+} binds to and enhances the activity of certain caspases *(233,234,241)*. However, the impact of Zn^{2+} on caspase activity is less clear. Zn^{2+} allosterically inhibits some caspases *(236-238)*, while activating others *(242-244)*. Cu^{2+} and Fe^{2+} can also inhibit caspase activity *(239,240)*. It has also been reported that low concentrations of Zn^{2+} (10 - 50 μM) diminished the Mn^{2+} mediated induction of caspase 3 activity *(243)*. Moreover, the Hendrickson group recently demonstrated that the soluble domain of *S. cerevisiae* Gpi8 has a caspase-like domain and undergoes homodimerization similar to that of caspases *(152)*. We hypothesized that the similarities between GPI-T and caspases might include a requirement for a cofactor for activity.

3.3.4a Transition Metal Ion Cofactors Regulate the Catalytic Activity of GPI-T

We analyzed GPI-T activity in the presence of various transition metal ions as described in section 3.2.6. Our results demonstrated that Mn^{2+} and Zn^{2+} ions independently enhance the catalytic activity of GPI-T, whereas the combination of these two cations is disruptive to activity. Cu^{2+} and Fe^{2+} each reduced GPI-T activity, compared to that of EDTA control. Unfortunately, due to lack of structural insight into GPI-T, a direct explanation of these results is beyond our ability at the present time. Hence, we depend on indirect information (e.g. with respect to caspases) to

hypothesize how these metals might work with GPI-T. In fact, even speculating as to which subunit mind bind a metal cofactor is beyond our current understanding.

3.3.4b Leupeptin Inactivates GPI-T

Since Gpi8 has 25-28% sequence similarity to cysteine proteases, we investigated the impact of the cysteine protease inhibitor, leupeptin, on GPI-T activity. Indeed, Leupeptin inhibited GPI-T, presumably by modification of the nucleophilic cysteine in the active site. This observation is the first demonstration of direct inhibition of GPI-T *in vitro* (to our knowledge). GPI-T activity is not inhibited by phenylmethylsulfonyl fluoride (PMSF), a serine protease inhibitor, or by EDTA (ethylenediaminetetraacetic acid), a metalloprotease inhibitor. Overall, these results continue to strengthen the comparison between GPI-T and caspases.

3.3.4c ATP and GTP Diminish GPI-T Activity

The importance of nucleotide cofactors on GPI anchoring has been studied previously. In cell free systems, the processing of prominiPLAP to miniPLAP was enhanced when either ATP or GTP as added *(136)*. It was suggested that ATP might enhance the proper folding of proprotein substrates, while GTP might facilitate translocation of the folded proprotein to the active site of GPI-T *(136,228)*. However, in another cell free assay, in which synthetic GPI anchors were transferred to cell membranes carrying VSG, GPI addition was not enhanced by either ATP or GTP *(135)*. Due to these contradictory reports, we reassessed the impact of ATP and GTP on GPI transamidation *in vitro*.

The initial rate of transamidation of peptide **2** was highest in the absence of NTPs. However, there are significant experimental differences between our assay conditions and those published in the literature *(136)*. Among them, the use of crude soluble microsomes by others *(136)*, versus affinity purified enzyme (this work) and the use of small proteins such as preprominiPLAP *(136)*, compared to the full length CD52 peptide **2** (this work) are potentially significant. For RM assays, the possibility that other cellular components are responsible for NTP dependence cannot be ruled out. These differences may account for the observed contradictions. However, our results demonstrate that neither GTP nor ATP activates GPI-T.

3.3.5 Conclusions

In this work, we utilized our *in vitro* assay to characterize several aspects relevant to the catalytic activity of GPI-T. Our results demonstrate that this assay is an indispensable tool to investigate GPI-T from a quantitative viewpoint that was previously inaccessible. Further, this new assay opens up a plethora of experiments for future research on GPI-T. For instance, even though the Gpi8 subunit catalyzes the transamidation reaction, this subunit is not active in the absence of other GPI-T subunits *(152)*. We are now poised to assess the impact of each individual subunit on Gpi8 activity in order to identify which subunit(s) is necessary to activate Gpi8 for transamidation. Results from such experiments will solve three decades of discussions about which subunits constitute the catalytically competent GPI-T complex. For instance in yeast, GPI-T is divided in to a core heterotrimer, which likely dimerizes into a heterohexamer *(138,140)*. In humans, GPI-T can be purified

as a heteropentamer *(141,165)*, presumably leading to two copies of all five subunits (for a total of 10) in the fully formed GPI-T complex. The assay described herein will certainly contribute to elucidating the size of the core GPI-T complex.

3.4 EXPERIMENTAL PROCEDURES

3.4.1 Materials and General Instrumentation

Refer to Chapter 2 Section 2.4.1

3.4.2 Buffers and Solutions

Refer to Chapter 2 Section 2.4.2

3.4.3 Yeast Strain and Growth Conditions

Refer to Chapter 2 Section 2.4.3

3.4.4 Automated Peptide Synthesis

Peptides **2,** and **4-10** were synthesized as detailed in the Ph.D. thesis of Dr. Rachel Morissette using standard solid-phase Fmoc synthesis protocols and pre-substituted Wang resins *(221)*. Peptide **11** (synthesized by Dilani Gamage) was synthesized on a Prelude peptide synthesizer using pre-substituted Fmoc-Ile-Wang resin (100-200 mesh, 0.10 g, 0.6 mmol/g). The amino acids were coupled using HBTU chemistry using standard Prelude peptide synthesizer protocols. Each amino acid was coupled three times in the presence of activator solution unless otherwise noted. Certain amino acids required three to four coupling reactions due to the high

hydrophobicity of certain regions of the peptides. The resin was coupled with acetic anhydride before Fmoc deprotection. The peptides were cleaved from the resin by mixing with 1.5 mL peptide cleavage solution and rotating for 2 hours on a wheel at room temperature. The cleaved peptides were precipitated with cold ether. The resultant precipitate was lyophilized and purified by reversed phase HPLC. The HPLC fractions were tested by ESI or MALDI-TOF to verify the identity of desired peptide. The pure peptide fractions were lyophilized and stored dry or as a 1 mM DMSO stock at -20 $^{\circ}$C.

3.4.5 Manual Peptide Synthesis

Peptide **2** was also synthesized manually, using pre-substituted Fmoc-Ser(tBu)-Wang resin (100-200 mesh, 0.10 g, 0.6 mmol/g) and HBTU chemistry as detailed in section 2.4.5 of Chapter 2.

3.4.6 Extraction and Purification of the GST-tagged GPI-T Heterotrimeric Complex

Preparation of microsomal membranes, solubilization of membrane proteins and affinity purification of GST tagged GPI-T were performed as described in section 2.4.5 of Chapter 2.

3.4.7 Fluorescence Assay

For each assay detailed in section 3.2, fluorescence response was obtained using a Varian Cary Eclipse Fluorometer with a Peltier multicell holder (Agilent Inc.) as described in section 2.4.6 of Chapter 2.

3.4.8 Methods to Calculate GPI-T Activity

Each fluorescence assay was run in triplicate, unless otherwise noted. GPI-T activity was calculated as described in section 2.5.7 of Chapter 2.

3.4.9 Statistical Analyses

Each experiment was performed three times unless otherwise noted. The relative rates were expressed as the mean $\pm$ standard deviation for $n \geq 3$. Statistical analysis was performed using a two-way, unpaired t-test with 95% confidence interval for $n \geq 3$. P-values < 0.05 were considered statistically significant. GraphPad Prism and KaleidaGraph software packages were used to analyze and plot the data. Vertical bar graphs representing mean $\pm$ SD were used to represent relative rates. Scattered plots were also used to represent relative rates for assays run in duplicate.

3.5 ACKNOWLEDGEMENT

Thanks are extended to Dr. Rachel Morissette for peptides **2-10** and Dilani Gamage for peptide 11.

APPENDIX A

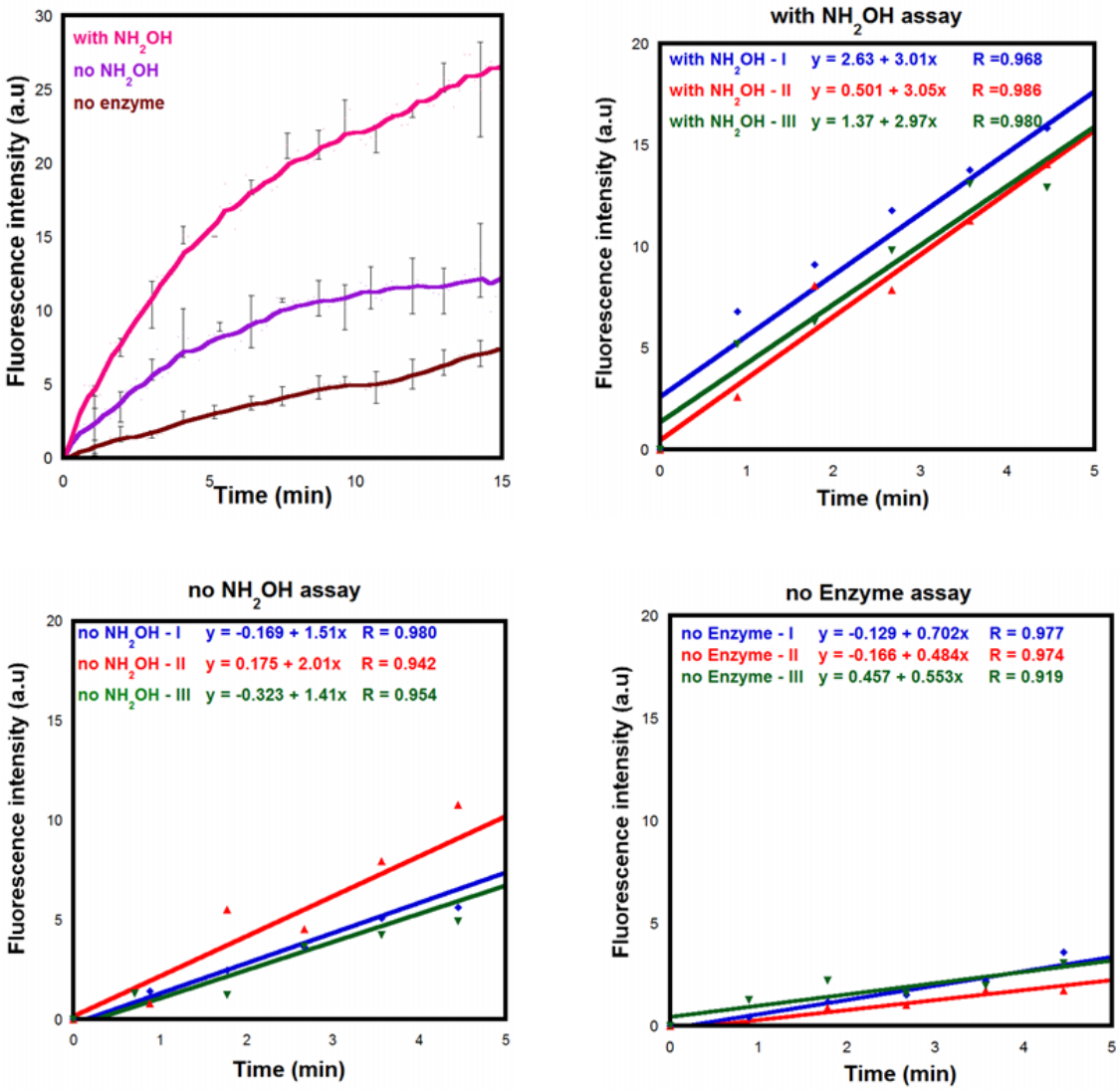

Figure A1. **Initial fluorescence assay with GPI-T.** (A) Summary of effects from enzyme and variations of nucleophile dependence on new GPI-T assay based on fluorescence response. For all assays, fluorescence intensity was normalized using the GPI-T unit definition. See text for details Magenta: 10 mM NH_2OH + 50 µL GPI-T; Maroon: 50 µL GPI-T; Purple: 10 mM NH_2OH + no GPI-T. Error bars indicate the standard deviation (n=3). Initial rates of transamidation for the assays with (B) 10 mM NH_2OH (C) no NH_2OH and (D) no enzyme assay. Refer to table A1 for experimental conditions.

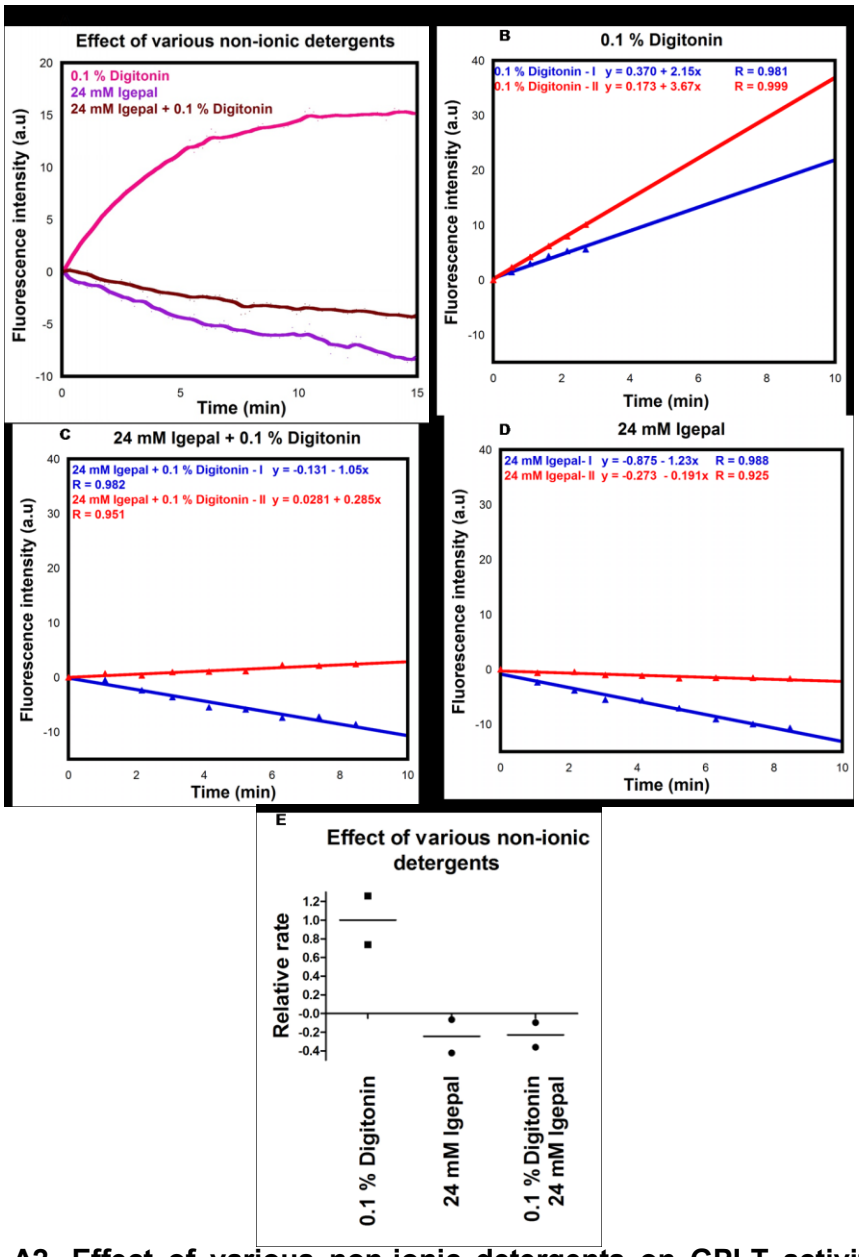

Figure A2. **Effect of various non-ionic detergents on GPI-T activity.** (A) Summary of effect of non-ionic detergents on GPI-T activity based on fluorescence response. For all assays, fluorescence intensity was normalized using the GPI-T unit definition. See text for details Magenta: 0.1 % Digitonin; Maroon: 24 mM Igepal + 0.1 % Digitonin; Purple: 24 mM Igepal. n = 2 Initial rates of transamidation for assay with (B) 0.1% Digitonin.(C) 0.1 % Digitonin and 24 mM Igepal (D) 24 mM Igepal. (E) Effect of various non-ionic detergents on GPI-T activity based on relative rates. Relative rates were calculated with respect to 0.1% Digitonin assay (■).Refer to table A1 for experimental conditions.

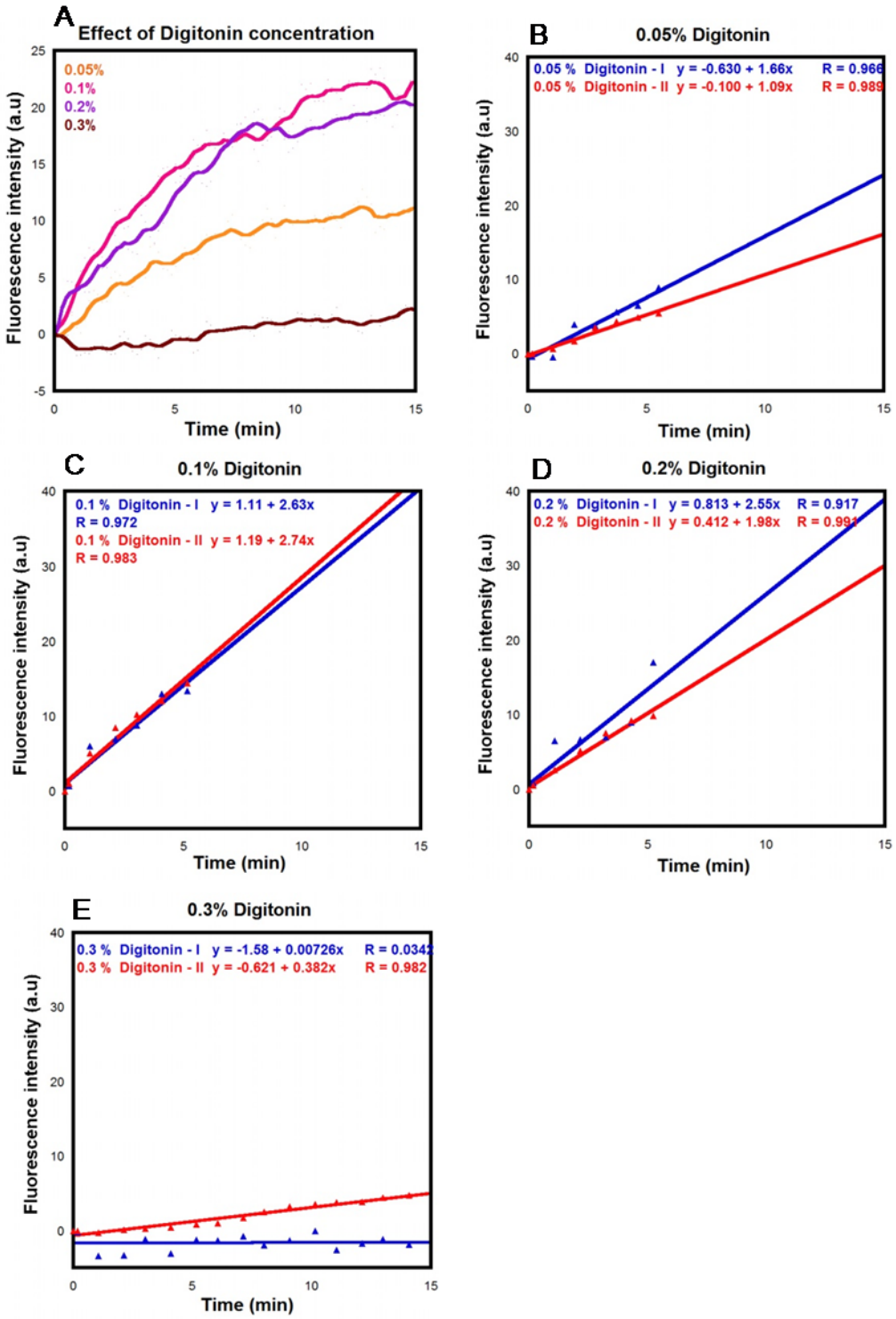

Continued on next page

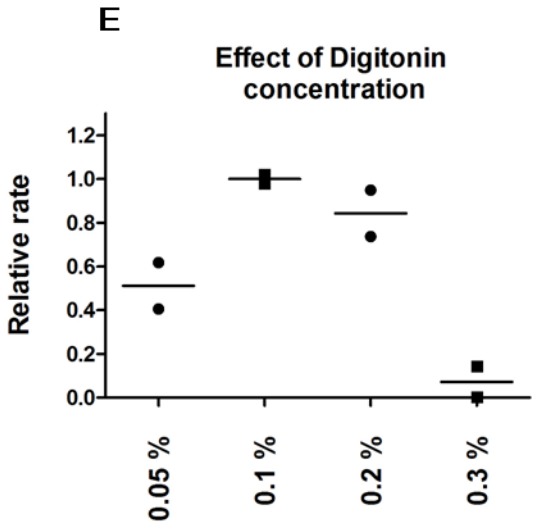

Figure A3. Effect of Digitonin concentration on GPI-T activity.(A) Summary of effect of variation in digitonin concentration on GPI-T activity based on fluorescence response. For all assays, fluorescence intensity was normalized using the GPI-T unit definition. See text for details. n = 2 Initial rates of transamidation for assay with (B) 0.05% Digitonin (C) 1% Digitonin (D) 2% Digitonin and (E) 0.3% Digitonin (E) Effect of Digitonin concentration on GPI-T activity based on Relative rates. Relative rates were calculated with respect to 0.1 % Digitonin assay (■). Refer to table A1 for experimental conditions.

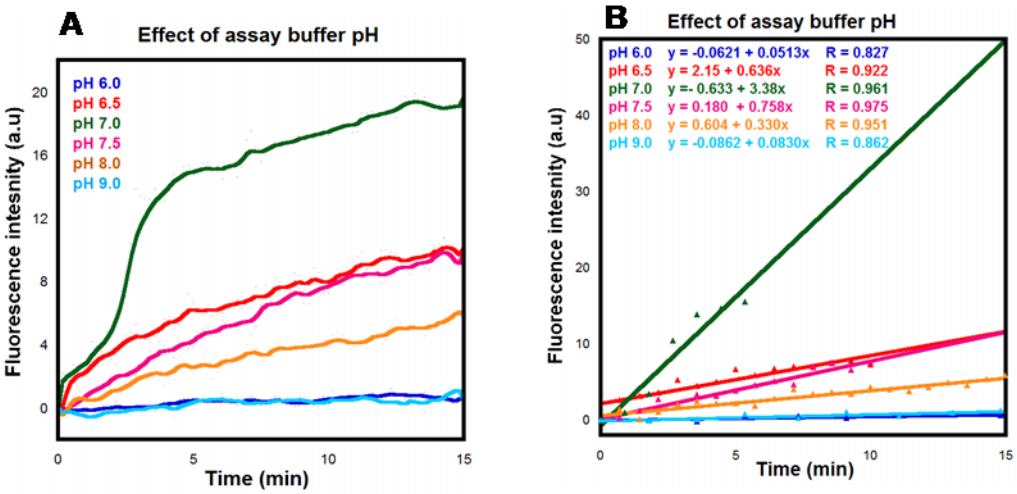

Figure A4. Effect of pH on GPI-T activity. (A) Summary of effect of variation in assay buffer pH on GPI-T activity based on fluorescence response. For all assays, fluorescence intensity was normalized using the GPI-T unit definition. See text for details. n = 1 (B) Initial rates of transamidation for assays with different pH conditions. All assays were performed with 10 mM NH_2OH, 10 µM peptide **2** and 50 µL GPI-T with varion in pH. Refer to table A1 for experimental conditions.

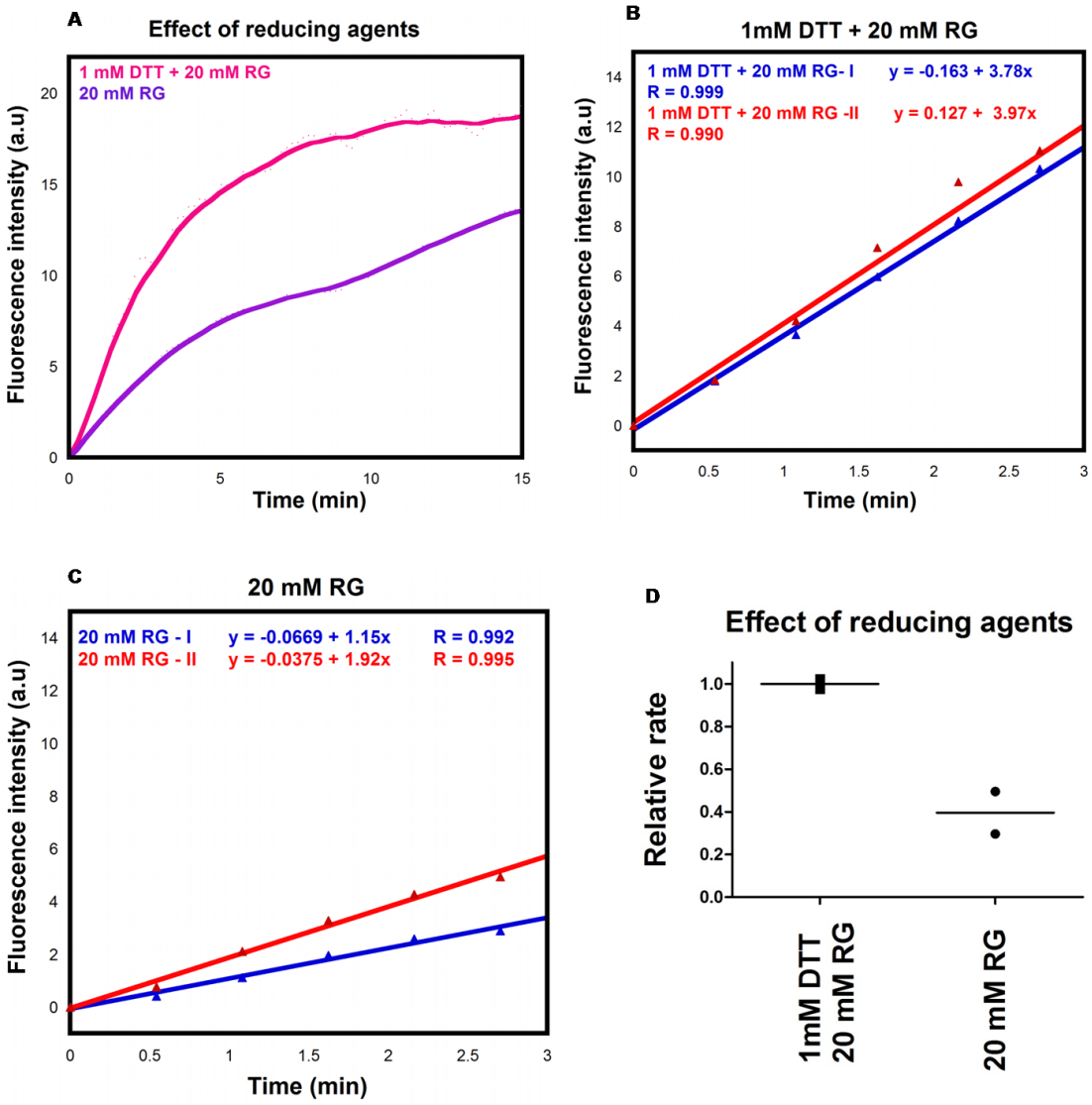

Figure A5. **Effect of reducing agents on GPI-T activity.** (A) Summary of effect of variation in reducing agents on assay buffer on GPI-T activity based on fluorescence response. For all assays, fluorescence intensity was normalized using the GPI-T unit definition. See text for details. n = 2 Initial rates of transamidation for assay with (B) 1 mM DTT and 20 mM RG and (C) 20 mM RG (D) Effect of agents on GPI-T activity based on relative rates. Relative rates were calculated with respect to assay with 1 mM DTT and 20 mM RG (■).Refer to table A1 for experimental conditions.

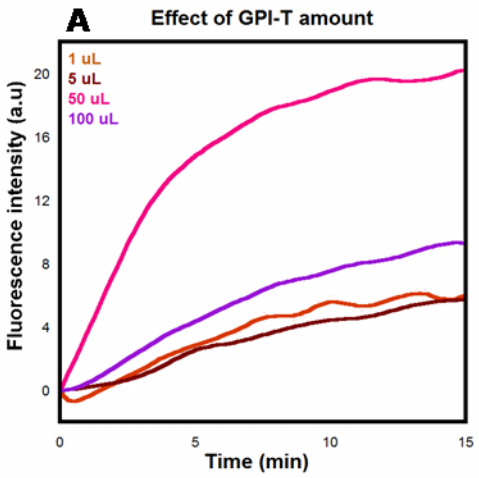

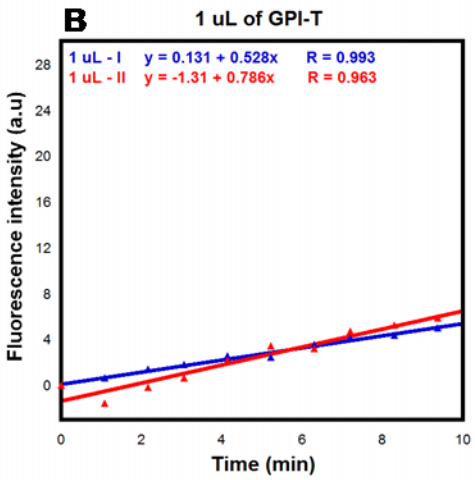

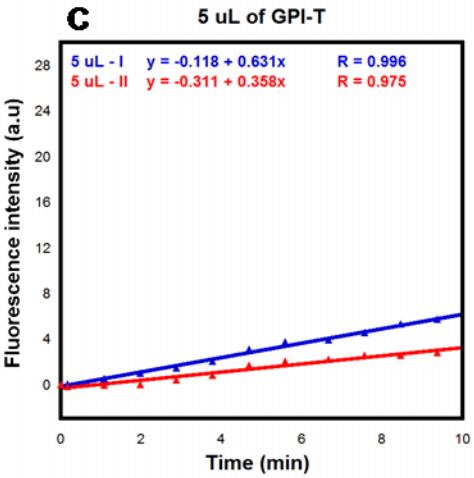

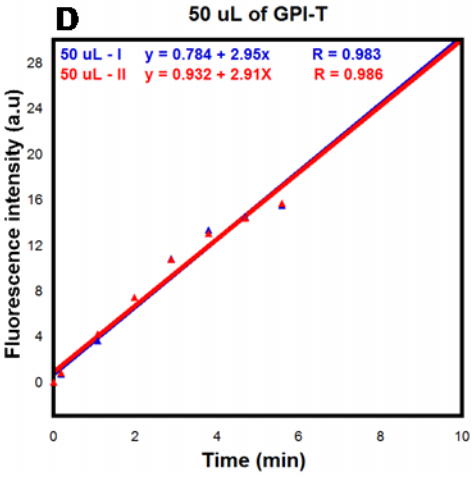

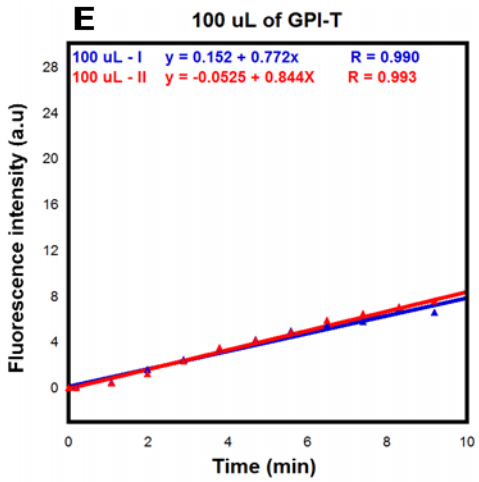

Continued on next page

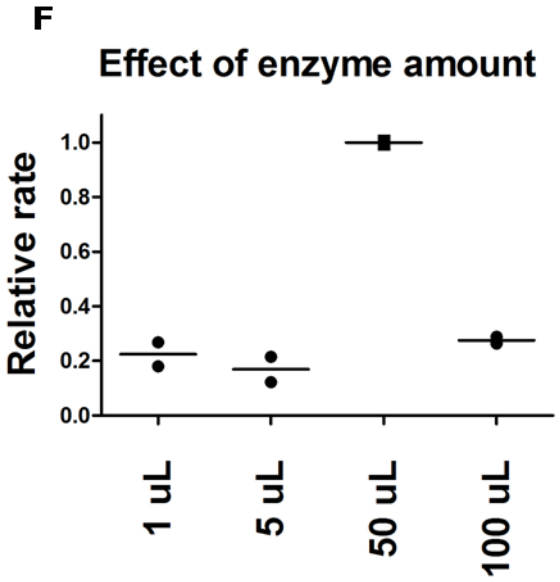

Figure A6. **Optimizing GPI-T assay with amount of GPI-T enzyme.** (A) Summary of effect of variation in enzyme amount on GPI-T activity based on fluorescence response. For all assays, fluorescence intensity was normalized using the GPI-T unit definition. See text for details. n = 2 Initial rates of transamidation for assays with (B) 1 µL GPI-T (C) 5 µL GPI-T (D) 50 µL GPI-T and (E) 100 µL GPI-T. (F) Effect of enzyme amount on GPI-T activity based on relative rates. Relative rates were calculated with respect to assay with 50 µL of GPI-T(■).Refer to table A1 for experimental conditions.

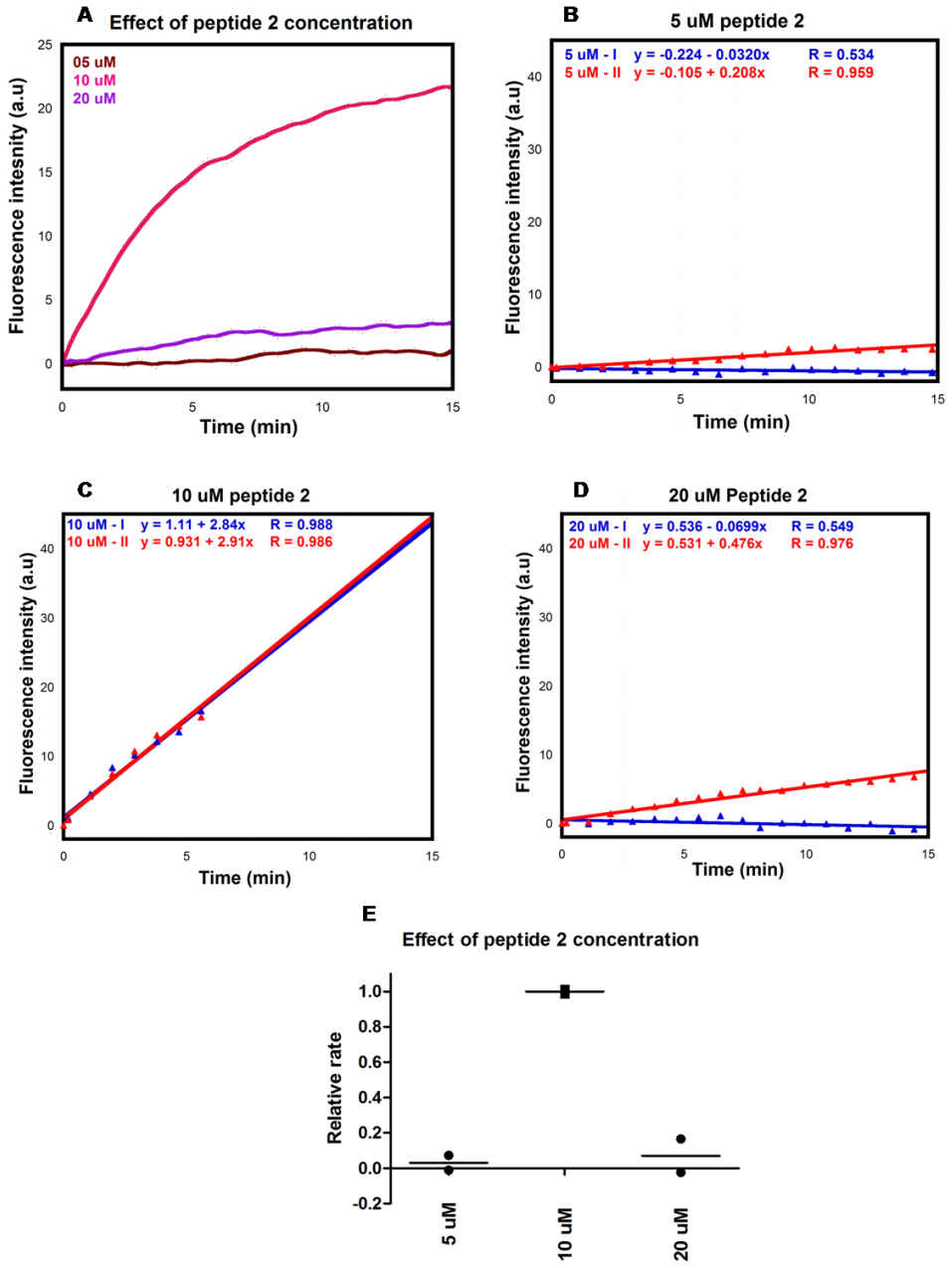

Figure A7. **Effect of peptide 2 concentration on GPI-T activity** (A) Summary of effect of variation in peptide **2** concentration on GPI-T activity based on fluorescence response. For all assays, fluorescence intensity was normalized using the GPI-T unit definition. See text for details. n = 2 Initial rates of transamidation for assays with (B) 5 μM peptide **2** (C) 10 μM peptide **2** and (D) 20 μM GPI-T (E) Effect of peptide **2** concentration on GPI-T activity based on relative rates. Relative rates were calculated with respect to assay with 10 μM of peptide **2** (■).Refer to table A1 for experimental conditions.

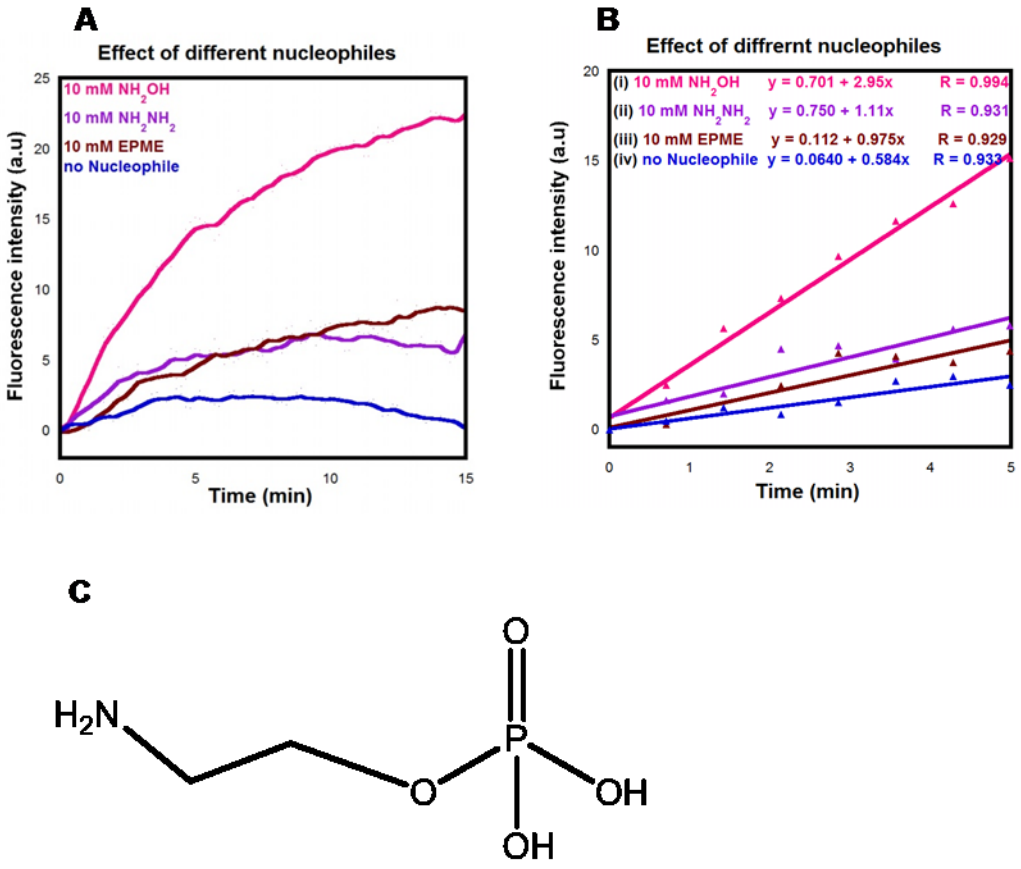

Figure A8. **Effect of different nucleophiles on GPI-T activity** (A) Summary of effect of different nucleophiles on GPI-T activity based on fluorescence response. For all assays, fluorescence intensity was normalized using the GPI-T unit definition. See text for details. n = 1 Initial rates of transamidation for assays with (B i) 10 mM NH_2OH ,(B ii) 10 mM NH_2NH_2 ,(B iii) 10 mM EPME and (B iv) no nucleophile (C) Structure of EPME. Refer to table A1 for experimental conditions.

Table A1 Experimental conditions for assays described in appendix A

Figure	**Additives**	**Changes to standard Assay/Assay buffer conditions ***
A1.C		no 10 mM NH_2OH
A1.D		No GPI-T
A2.C	24 mM Igepal	-
A2.D	24 mM Igepal	no Digitonin
A3.B	-	0.05% Digitonin
A3.D	-	0.2% Digitonin
A3.E	-	0.3% Digitonin
A5.C		no 1 mM DTT
A6.B	-	1 µL GPI-T
A6.C	-	5 µL GPI-T
A6.E	-	50 µL GPI-T
A7.B	-	5 µM peptide **2**
A7.D	-	20 µM peptide **2**
A8.B ii	-10 mM NH_2NH_2	no 10 mM NH_2OH
B8.B iii	10 mM EPME	no 10 mM NH_2OH
A8.B iv		no 10 mM NH_2OH

All experiments were performed with 10 µM peptide **2**. Experimental details for the assays performed under standard conditions (10 mM NH_2OH, 50 µL GPI-T, 10 µM peptide **2** with GPI-T assay buffer as detailed section 2.4.2 and 2.4.7) were not included in Table A.1.

APPENDIX B

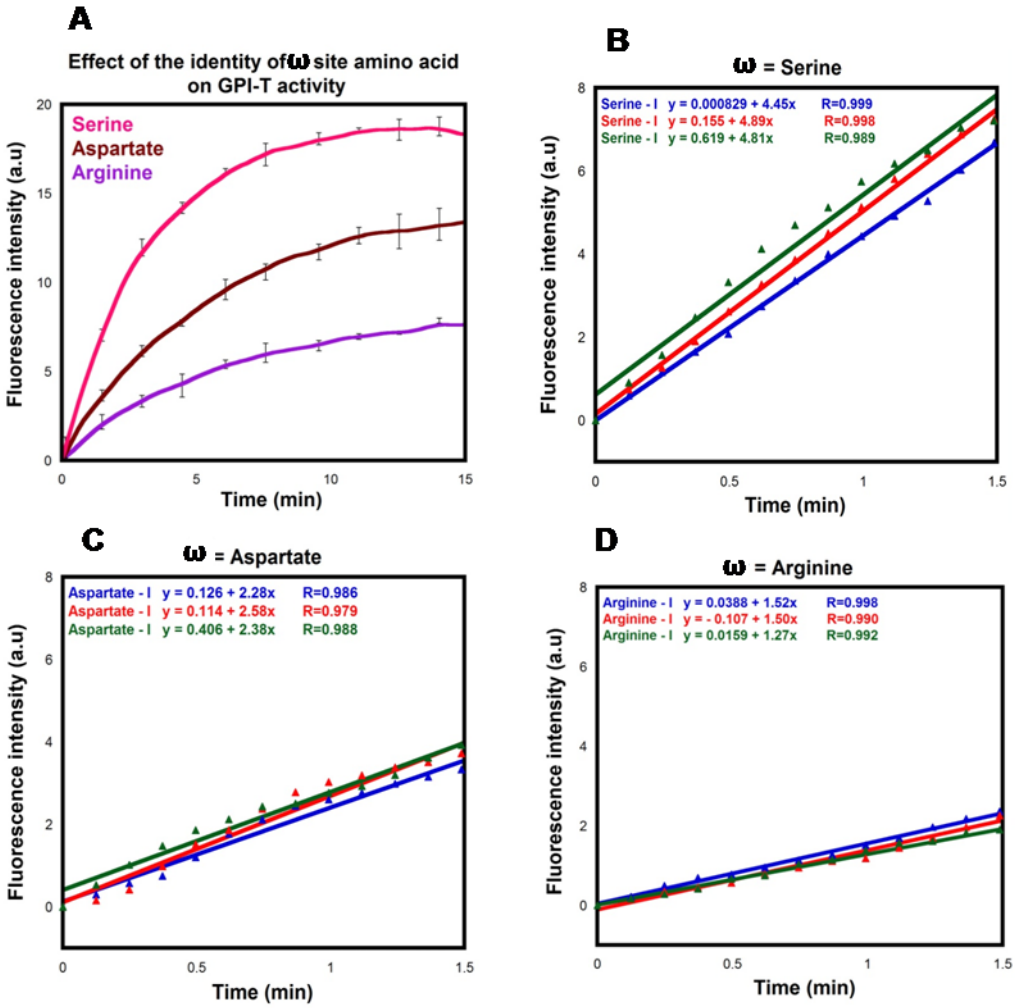

Figure B1. **Effect of the identity of the ω site amino acid on peptide substrate recognition by GPI-T.** (A) Summary of effects from variations at the ω site on GPI-T activity based on fluorescence response. For all assays, fluorescence intensity was normalized using the GPI-T unit definition. See text for details. Magenta: peptide **2** (ω = Ser); Brown: peptide **4** (ω = Asp); Purple: peptide **5** (ω = Arg). Error bars indicate the standard deviation (n=3). (B) Initial rates of transamidation for peptide **2** with ω = serine. (C) Initial rates of transamidation for peptide **4** with ω = aspartate. (D) Initial rates of transamidation for peptide **5** with ω = arginine. Refer to table B1 for experimental conditions.

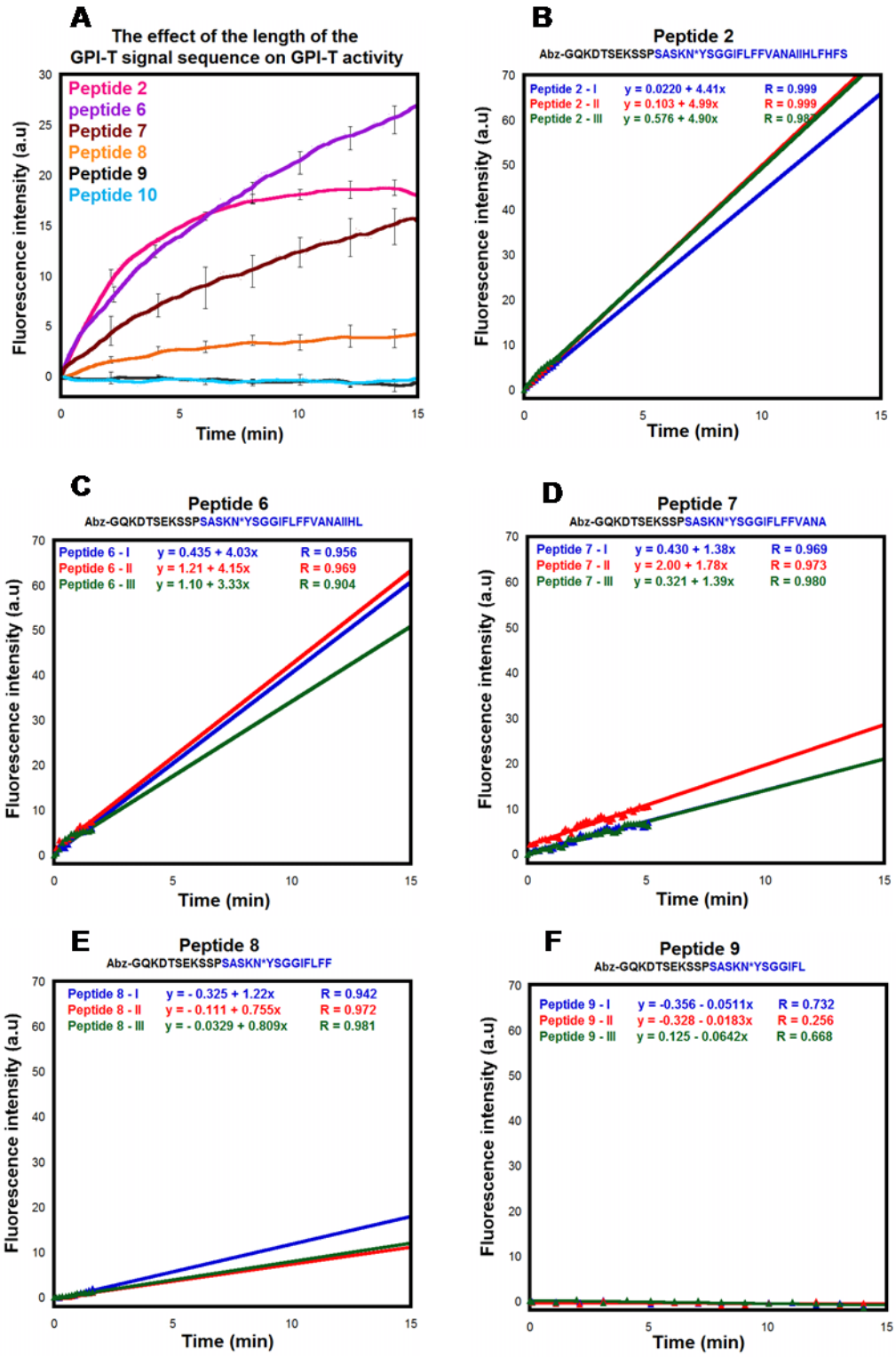

Continued on next page

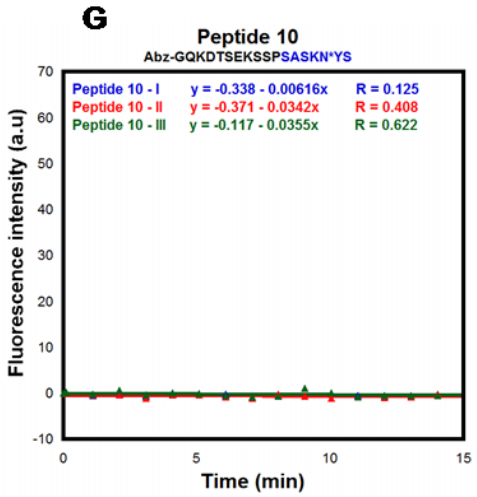

Figure B2. **Effect of the length of the C-terminal GPI-T signal sequence on GPI-T activity.** (A) Summary of effects from variations of the length of the GPI-T signal sequence on GPI-T activity based on fluorescence response. For all assays, fluorescence intensity was normalized using the GPI-T unit definition. See text for details. Magenta: peptide **2** (37 mer); Purple: peptide **6** (33 mer); Maroon: peptide **7** (29 mer); Orange: peptide **8** (25 mer); Black: peptide **9** (23 mer); Cyan: peptide **10** (18 mer). Error bars indicate the standard deviation (n=3). (B) Initial rates of transamidation for peptide **2**. (C) Initial rates of transamidation for peptide **6**. (D) Initial rates of transamidation for peptide **7**. (E) Initial rates of transamidation for peptide **8**. (F) Initial rates of transamidation for peptide **9**. (G) Initial rates of transamidation for peptide **10.** For each plot (B-G), the peptide sequence is represented at the top of plot with the hydrophobic portion highlighted in blue. Refer to table B1 for experimental conditions.

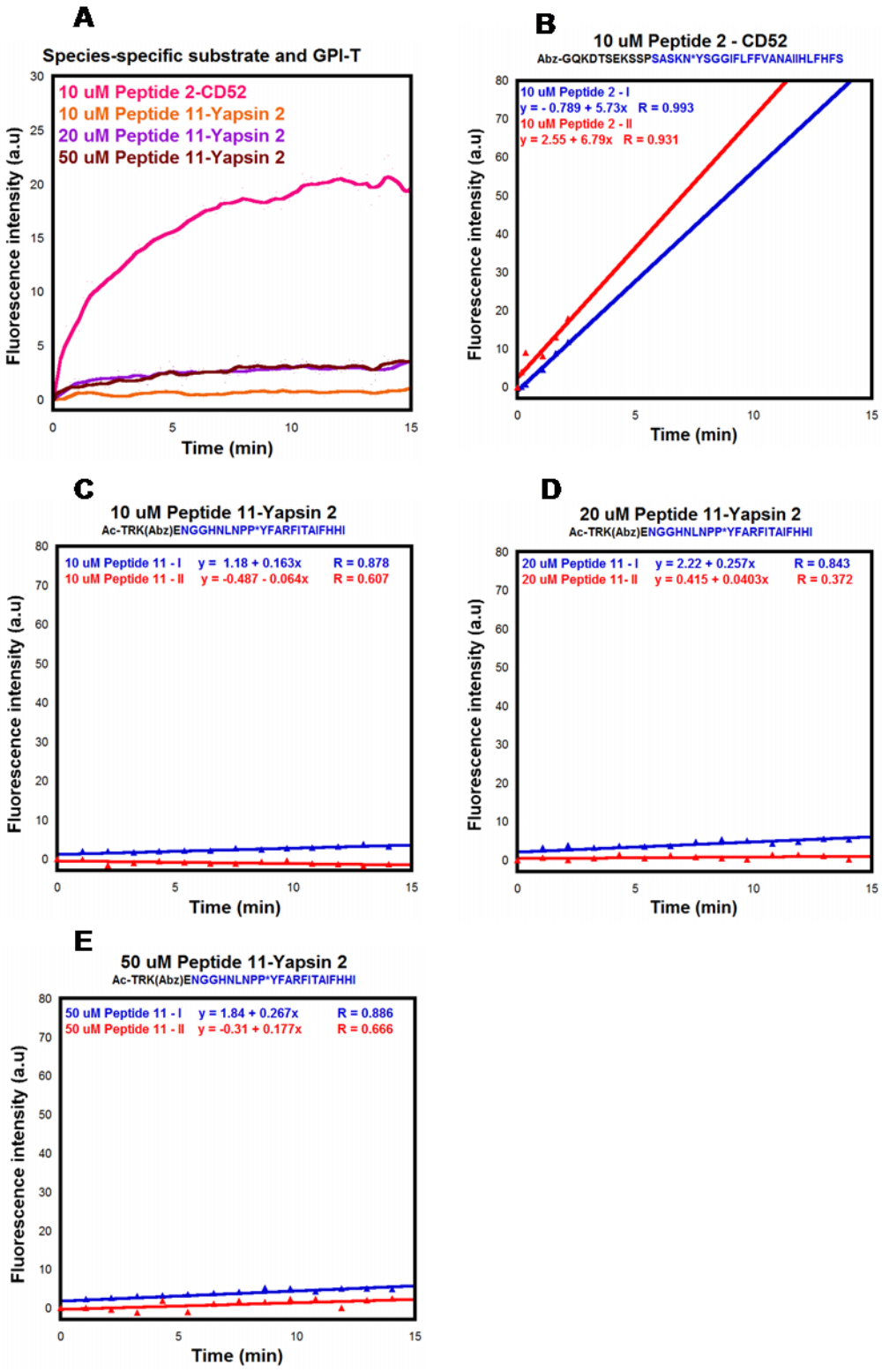

Continued on next page

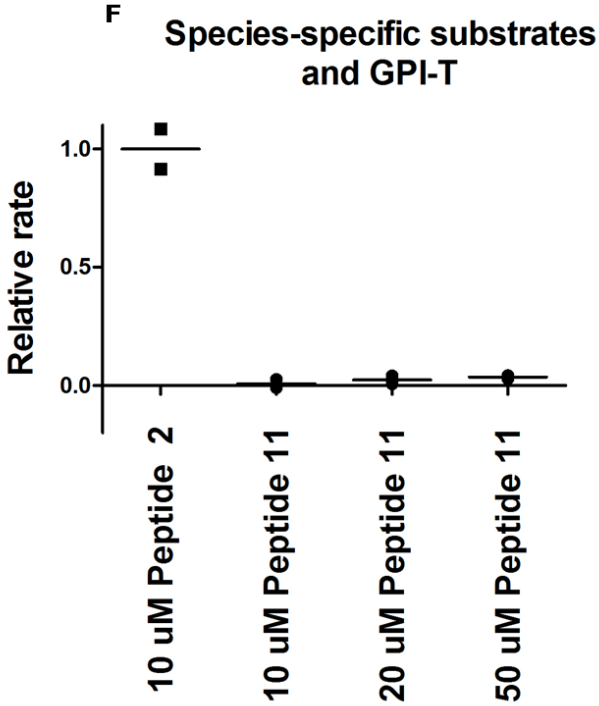

Figure B3. **Species specific substrate selectivity.** (A) Summary of effects from peptides **2** (CD52) and **11** (Yapsin 2) on GPI-T activity, based on fluorescence responses. For all assays, fluorescence intensity was normalized using the GPI-T unit definition. See text for details. Magenta: 10 μM peptide **2** (CD52); Orange: 10 μM peptide **11** (Yapsin 2); Purple: 20 μM peptide **11** (Yapsin 2); Maroon: 50 μM peptide **11** (Yapsin 2); n=2. (B) Initial rates of transamidation for 10 μM peptide **2**. (C) Initial rates of transamidation for 10 μM peptide **11**. (D) Initial rates of transamidation for 20 μM peptide **11**. (E) Initial rates of transamidation for 50 μM peptide **11**. (F) Species specificity of GPI-T in terms of relative rates. Relative rates were calculated with respect to the assay with 10 μM peptide **2** (■). For each plot (B-E), the peptide sequences is represented at the top of plot. Refer to table B1 for experimental conditions.

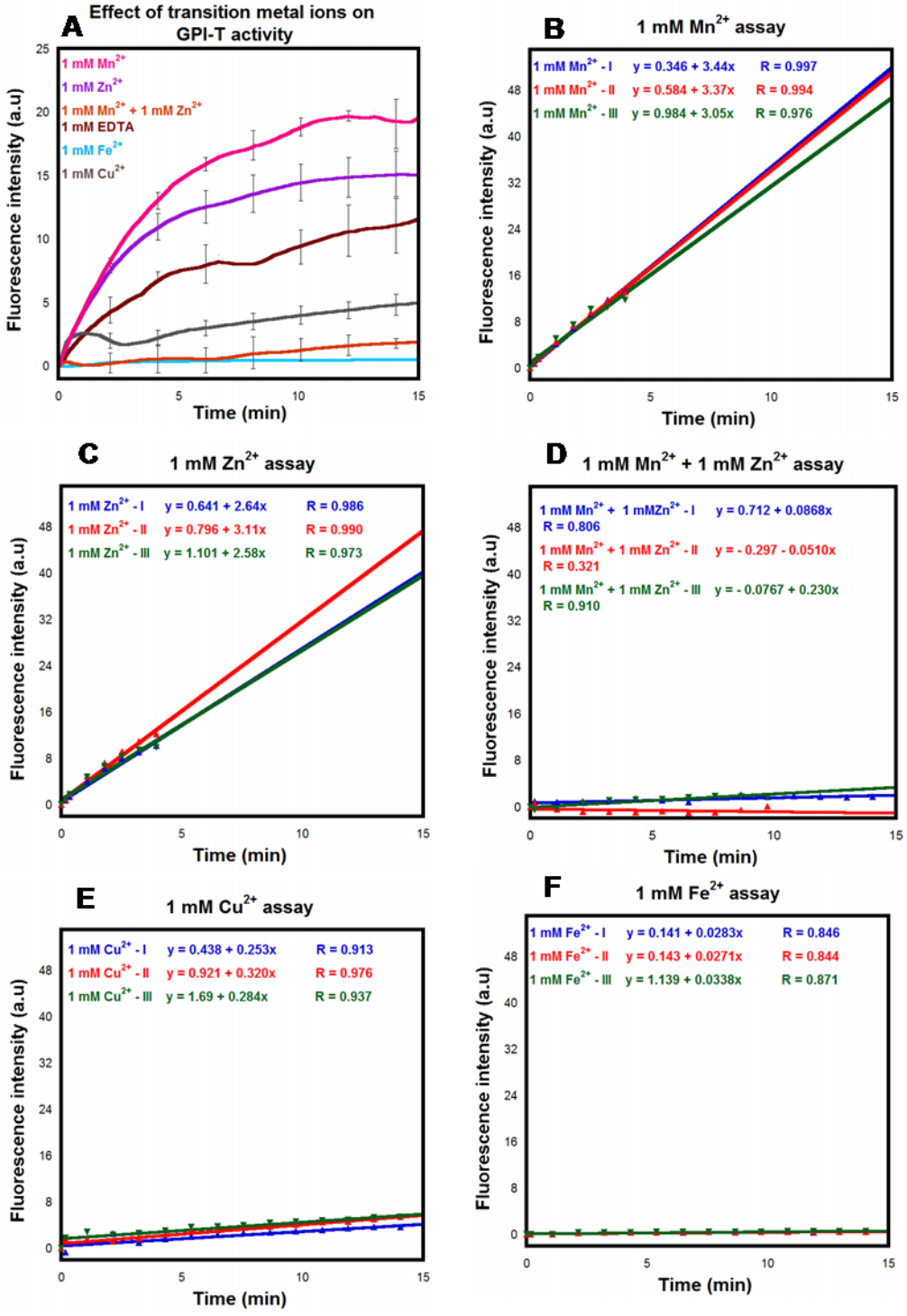

Continued on next page

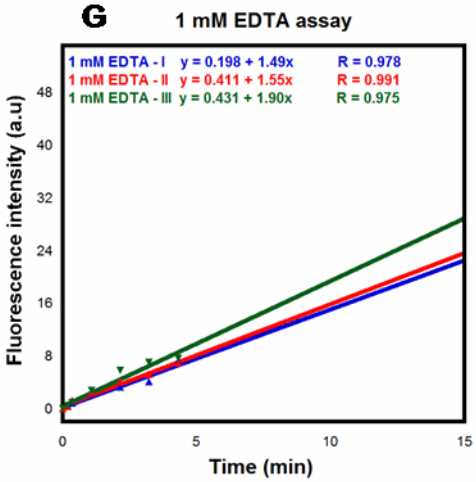

Figure B4. **Effect of transition metals on GPI-T activity.** (A) Summary of effects from different transition metals on GPI-T activity, based on fluorescence response. For all assays, fluorescence intensity was normalized using the GPI-T unit definition. See text for details. Magenta: 1 mM Mn^{2+}; Purple: 1 mM Zn^{2+}; Orange: 1 mM Mn^{2+} & 1 mM Zn^{2+}; Gray: 1 mM Cu^{2+}; Cyan: 1 mM Fe^{2+}; Maroon: 1 mM EDTA. Error bars indicate the standard deviation (n=3). (B) Initial rates of transamidation for assay with 1 mM Mn^{2+}. (C) Initial rates of transamidation for assay with 1 mM Zn^{2+}. (D) Initial rates of transamidation for assay with 1 mM Mn^{2+} + 1 mM Zn^{2+}. (E) Initial rates of transamidation for assay with 1 mM Cu^{2+}. (F) Initial rates of transamidation for assay with 1 mM Fe^{2+}. (G) Initial rates of transamidation for assay with 1 mM EDTA. Refer to table B1 for experimental conditions.

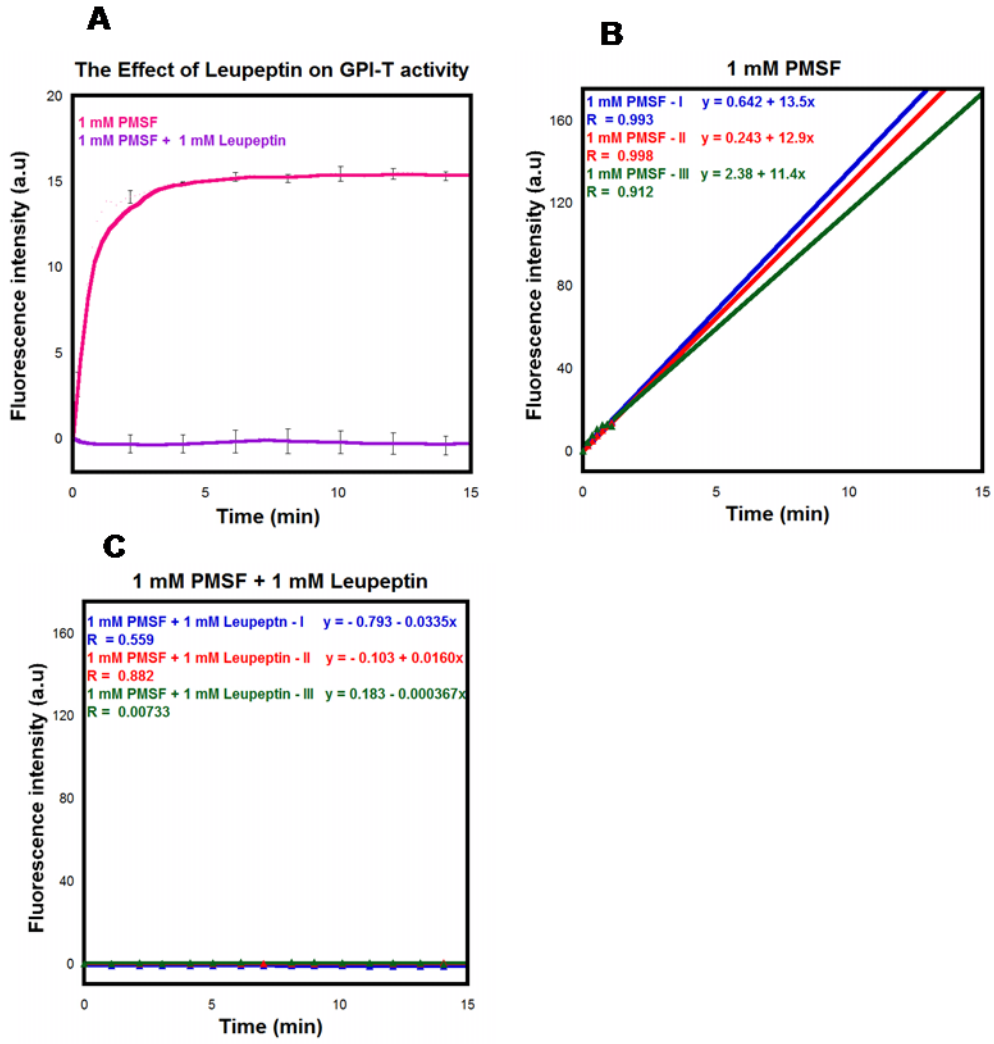

Figure B5 Effect of Leupeptin on catalytic activity of GPI-T. (A) Summary of effects from leupeptin and PMSF on GPI-T activity based on fluorescence response. For all assays, fluorescence intensity was normalized using the GPI-T unit definition. See text for details. Magenta: 1 mM PMSF; Purple: 1 mM Leupeptin + 1 mM PMSF. Error bars indicate the standard deviation (n=3). (B) Initial rates of transamidation for assay with 1 mM PMSF. (C) Initial rates of transamidation for assay with 1 mM PMSF + Leupeptin. Refer to table B1 for experimental conditions.

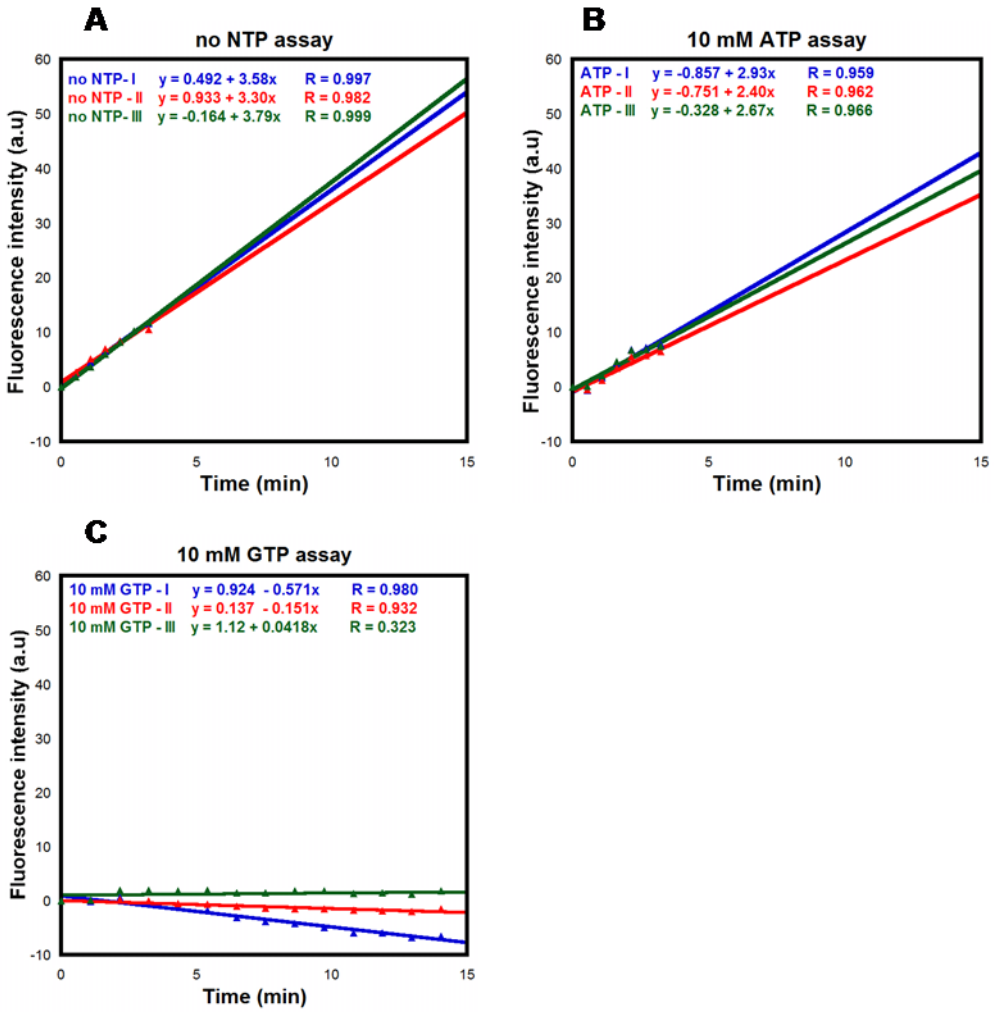

Figure B6. **Effect of nucleotides on the catalytic activity of GPI-T.** (A) Summary of effects from different nucleotides on GPI-T based on fluorescence response. For all assays, fluorescence intensity was normalized using the GPI-T unit definition. See text for details. Magenta: no NTP; Purple: 10 mM ATP; Maroon: 10 mM GTP. Error bars indicate the standard deviation (n=3). (A) Initial rates of transamidation for assay with no NTP. (B) Initial rates of transamidation for assay with 10 mM ATP. (C) Initial rates of transamidation for assay with 10 mM GTP. Refer to table B1 for experimental conditions.

Table B1. Experimental conditions for assays in appendix B

Figure	Peptide	Peptide concentration	Additive
B1.B	**2**	10 μM	-
B1.C	**4**	10 μM	-
B1,D	**5**	10 μM	-
B2.B	**2**	10 μM	-
B2.C	**6**	10 μM	-
B2.D	**7**	10 μM	-
B2.E	**8**	10 μM	-
B2.F	**9**	10 μM	-
B2.G	**10**	10 μM	-
B3.B	**2**	10 μM	-
B3.C	**11**	10 μM	-
B3.D	**11**	20 μM	-
B3.E	**11**	50 μM	-
B4.B	**2**	10 μM	1 mM Mn^{2+}
B4.C	**2**	10 μM	1 mM Zn^{2+}
B4.D	**2**	10 μM	1 mM Mn^{2+} + Zn^{2+}
B4.E	**2**	10 μM	1 mM Cu^{2+}
B4.F	**2**	10 μM	1 mM Fe^{2+}
B4.G	**2**	10 μM	1 mM EDTA

B5.B	**2**	10 μM	1 mM PMSF
B5.C	**2**	10 μM	1 mM PMSF + 1 mM Leupeptin
B6.A	**2**	10 μM	-
B6.B	**2**	10 μM	1 mM ATP
B6.C	**2**	10 μM	1 mM GTP

All experiments were performed with 10 mM NH_2OH and 50 μL GPI-T in GPI-T assay buffer (total volume 2 mL) unless otherwise noted in the last column.

REFERENCES

1. Orlean, P., and Menon, A. K. (**2007**) Thematic review series: Lipid posttranslational modifications. Gpi anchoring of protein in yeast and mammalian cells, or: How we learned to stop worrying and love glycophospholipids. *J. Lipid. Res. 48*, 993-1011.
2. Nozaki, M., Ohishi, K., Yamada, N., Kinoshita, T., Nagy, A., and Takeda, J. (**1999**) Developmental abnormalities of glycosylphosphatidylinositol-anchor-deficient embryos revealed by cre/loxp system. *Lab. Invest. 79*, 293-299.
3. Tarutani, M., Itami, S., Okabe, M., Ikawa, M., Tezuka, T., Yoshikawa, K., Kinoshita, T., and Takeda, J. (**1997**) Tissue-specific knockout of the mouse pig-a gene reveals important roles for gpi-anchored proteins in skin development. *Proc. Natl. Acad. Sci. U S A 94*, 7400-7405.
4. Leidich, S. D., Drapp, D. A., and Orlean, P. (**1994**) A conditionally lethal yeast mutant blocked at the first step in glycosyl phosphatidylinositol anchor synthesis. *J. Biol. Chem. 269*, 10193-10196.
5. Eisenhaber, B., Bork, P., and Eisenhaber, F. (**2001**) Post-translational gpi lipid anchor modification of proteins in kingdoms of life: Analysis of protein sequence data from complete genomes. *Protein Eng. 14*, 17-25.
6. Eisenhaber, B., Schneider, G., Wildpaner, M., and Eisenhaber, F. (**2004**) A sensitive predictor for potential gpi lipid modification sites in fungal protein sequences and its application to genome-wide studies for aspergillus nidulans, candida albicans, neurospora crassa, saccharomyces cerevisiae and schizosaccharomyces pombe. *J. Mol. Biol. 337*, 243-253.

7. Pittet, M., and Conzelmann, A. (**2007**) Biosynthesis and function of gpi proteins in the yeast saccharomyces cerevisiae. *Biochim. Biophys. Acta 1771*, 405-420.

8. Cross, G. A. (**1996**) Antigenic variation in trypanosomes: Secrets surface slowly. *Bioessays 18*, 283-291.

9. Nykjaer, A., Conese, M., Christensen, E. I., Olson, D., Cremona, O., Gliemann, J., and Blasi, F. (**1997**) Recycling of the urokinase receptor upon internalization of the upa:Serpin complexes. *EMBO J. 16*, 2610-2620.

10. Wu, G., Guo, Z., Chatterjee, A., Huang, X., Rubin, E., Wu, F., Mambo, E., Chang, X., Osada, M., Sook Kim, M., Moon, C., Califano, J. A., Ratovitski, E. A., Gollin, S. M., Sukumar, S., Sidransky, D., and Trink, B. (**2006**) Overexpression of glycosylphosphatidylinositol (gpi) transamidase subunits phosphatidylinositol glycan class t and/or gpi anchor attachment 1 induces tumorigenesis and contributes to invasion in human breast cancer. *Cancer Res. 66*, 9829-9836.

11. Guo, Z., Linn, J. F., Wu, G., Anzick, S. L., Eisenberger, C. F., Halachmi, S., Cohen, Y., Fomenkov, A., Hoque, M. O., Okami, K., Steiner, G., Engles, J. M., Osada, M., Moon, C., Ratovitski, E., Trent, J. M., Meltzer, P. S., Westra, W. H., Kiemeney, L. A., Schoenberg, M. P., Sidransky, D., and Trink, B. (**2004**) Cdc91l1 (pig-u) is a newly discovered oncogene in human bladder cancer. *Nat. Med. 10*, 374-381.

12. Ozeki, H., Shirai, S., Nozaki, M., Ikeda, K., and Ogura, Y. (**1999**) Maldevelopment of neural crest cells in patients with typical uveal coloboma. *J. Pediatr. Ophthalmol. Strabismus 36*, 337-341.

13. Inoue, N., Murakami, Y., and Kinoshita, T. (**2003**) Molecular genetics of paroxysmal nocturnal hemoglobinuria. *Int. J. Hematol. 77*, 107-112.

14. Nagamune, K., Nozaki, T., Maeda, Y., Ohishi, K., Fukuma, T., Hara, T., Schwarz, R. T., Sutterlin, C., Brun, R., Riezman, H., and Kinoshita, T. (**2000**) Critical roles of glycosylphosphatidylinositol for trypanosoma brucei. *Proc. Natl. Acad. Sci. U. S. A. 97*, 10336-10341.

15. Almeida, A. M., Fonseca, C. R., Prado, P. I., Almeida-Neto, M., Diniz, S., Kubota, U., Braun, M. R., Raimundo, R. L., Anjos, L. A., Mendonca, T. G., Futada, S. M., and Lewinsohn, T. M. (**2006**) Assemblages of endophagous insects on asteraceae in sao paulo cerrados. *Neotrop. Entomol. 35*, 458-468.

16. Butikofer, P., Malherbe, T., Boschung, M., and Roditi, I. (**2001**) Gpi-anchored proteins: Now you see 'em, now you don't. *FASEB J. 15*, 545-548.

17. Barboni, E., Rivero, B. P., George, A. J., Martin, S. R., Renoup, D. V., Hounsell, E. F., Barber, P. C., and Morris, R. J. (**1995**) The glycophosphatidylinositol anchor affects the conformation of thy-1 protein. *J. Cell Sci. 108 (Pt 2)*, 487-497.

18. Jones, D. R., and Varela-Nieto, I. (**1998**) The role of glycosyl-phosphatidylinositol in signal transduction. *Int. J. Biochem. Cell Biol. 30*, 313-326.

19. Robinson, P. J. (**1997**) Signal transduction via gpi-anchored membrane proteins. *Adv. Exp. Med. Biol. 419*, 365-370.

20. Low, M. G., and Saltiel, A. R. (**1988**) Structural and functional roles of glycosyl-phosphatidylinositol in membranes. *Science 239*, 268-275.

21. Brown, D. A., and Rose, J. K. (**1992**) Sorting of gpi-anchored proteins to glycolipid-enriched membrane subdomains during transport to the apical cell surface. *Cell 68*, 533-544.

22. Zurzolo, C., Lisanti, M. P., Caras, I. W., Nitsch, L., and Rodriguez-Boulan, E. (**1993**) Glycosylphosphatidylinositol-anchored proteins are preferentially targeted to the basolateral surface in fischer rat thyroid epithelial cells. *J. Cell. Biol. 121*, 1031-1039.

23. Ikezawa, H., Yamanegi, M., Taguchi, R., Miyashita, T., and Ohyabu, T. (**1976**) Studies on phosphatidylinositol phosphodiesterase (phospholipase c type) of bacillus cereus. I. Purification, properties and phosphatase-releasing activity. *Biochim. Biophys. Acta 450*, 154-164.

24. Low, M. G., and Finean, J. B. (**1977**) Release of alkaline phosphatase from membranes by a phosphatidylinositol-specific phospholipase c. *Biochem. J. 167*, 281-284.

25. Taguchi, R., and Ikezawa, H. (**1978**) Phosphatidyl inositol-specific phospholipase c from clostridium novyi type a. *Arch. Biochem. Biophys. 186*, 196-201.

26. Taguchi, R., Asahi, Y., and Ikezawa, H. (**1980**) Purification and properties of phosphatidylinositol-specific phospholipase c of bacillus thuringiensis. *Biochim. Biophys. Acta. 619*, 48-57.

27. Low, M. G., and Finean, J. B. (**1977**) Modification of erythrocyte membranes by a purified phosphatidylinositol-specific phospholipase c (staphylococcus aureus). *Biochem. J. 162*, 235-240.

28. Low, M. G., and Finean, J. B. (**1977**) Non-lytic release of acetylcholinesterase from erythrocytes by a phosphatidylinositol-specific phospholipase c. *FEBS. Lett. 82*, 143-146.

29. Low, M. G., and Finean, J. B. (**1978**) Specific release of plasma membrane enzymes by a phosphatidylinositol-specific phospholipase c. *Biochim. Biophys. Acta 508*, 565-570.

30. Chatterjee, S., and Mayor, S. (**2001**) The gpi-anchor and protein sorting. *Cell Mol. Life. Sci. 58*, 1969-1987.

31. Ferguson, M. A., Haldar, K., and Cross, G. A. (**1985**) Trypanosoma brucei variant surface glycoprotein has a sn-1,2-dimyristyl glycerol membrane anchor at its cooh terminus. *J. Biol. Chem. 260*, 4963-4968.

32. Ferguson, M. A., Low, M. G., and Cross, G. A. (**1985**) Glycosyl-sn-1,2-dimyristylphosphatidylinositol is covalently linked to trypanosoma brucei variant surface glycoprotein. *J. Biol. Chem. 260*, 14547-14555.

33. Tse, A. G., Barclay, A. N., Watts, A., and Williams, A. F. (**1985**) A glycophospholipid tail at the carboxyl terminus of the thy-1 glycoprotein of neurons and thymocytes. *Science 230*, 1003-1008.

34. Williams, A. F., and Tse, A. G. (**1985**) A glycophospholipid covalently attached to the c-terminus of the thy-1 glycoprotein. *Biosci. Rep. 5*, 999-1005.

35. Futerman, A. H., Low, M. G., Ackermann, K. E., Sherman, W. R., and Silman, I. (**1985**) Identification of covalently bound inositol in the hydrophobic membrane-anchoring domain of torpedo acetylcholinesterase. *Biochem. Biophys. Res. Commun. 129*, 312-317.

36. Roberts, W. L., and Rosenberry, T. L. (**1985**) Identification of covalently attached fatty acids in the hydrophobic membrane-binding domain of human erythrocyte acetylcholinesterase. *Biochem. Biophys. Res. Commun. 133*, 621-627.

37. Ferguson, M. A., Homans, S. W., Dwek, R. A., and Rademacher, T. W. (**1988**) Glycosyl-phosphatidylinositol moiety that anchors trypanosoma brucei variant surface glycoprotein to the membrane. *Science 239*, 753-759.

38. Homans, S. W., Ferguson, M. A., Dwek, R. A., Rademacher, T. W., Anand, R., and Williams, A. F. (**1988**) Complete structure of the glycosyl phosphatidylinositol membrane anchor of rat brain thy-1 glycoprotein. *Nature 333*, 269-272.

39. Fankhauser, C., Homans, S. W., Thomas-Oates, J. E., McConville, M. J., Desponds, C., Conzelmann, A., and Ferguson, M. A. (**1993**) Structures of glycosylphosphatidylinositol membrane anchors from saccharomyces cerevisiae. *J. Biol. Chem. 268*, 26365-26374.

40. Deeg, M. A., Humphrey, D. R., Yang, S. H., Ferguson, T. R., Reinhold, V. N., and Rosenberry, T. L. (**1992**) Glycan components in the glycoinositol

phospholipid anchor of human erythrocyte acetylcholinesterase. Novel fragments produced by trifluoroacetic acid. *J. Biol. Chem. 267*, 18573-18580.

41. Brewis, I. A., Ferguson, M. A., Mehlert, A., Turner, A. J., and Hooper, N. M. (**1995**) Structures of the glycosyl-phosphatidylinositol anchors of porcine and human renal membrane dipeptidase. Comprehensive structural studies on the porcine anchor and interspecies comparison of the glycan core structures. *J. Biol. Chem. 270*, 22946-22956.
42. Nakano, Y., Noda, K., Endo, T., Kobata, A., and Tomita, M. (**1994**) Structural study on the glycosyl-phosphatidylinositol anchor and the asparagine-linked sugar chain of a soluble form of cd59 in human urine. *Arch. Biochem. Biophys. 311*, 117-126.
43. Mukasa, R., Umeda, M., Endo, T., Kobata, A., and Inoue, K. (**1995**) Characterization of glycosylphosphatidylinositol (gpi)-anchored ncam on mouse skeletal muscle cell line c2c12: The structure of the gpi glycan and release during myogenesis. *Arch. Biochem. Biophys. 318*, 182-190.
44. Fontaine, T., Magnin, T., Melhert, A., Lamont, D., Latge, J. P., and Ferguson, M. A. (**2003**) Structures of the glycosylphosphatidylinositol membrane anchors from aspergillus fumigatus membrane proteins. *Glycobiology 13*, 169-177.
45. Kinoshita, T., Fujita, M., and Maeda, Y. (**2008**) Biosynthesis, remodelling and functions of mammalian gpi-anchored proteins: Recent progress. *J. Biochem. 144*, 287-294.

46. Paulick, M. G., and Bertozzi, C. R. (**2008**) The glycosylphosphatidylinositol anchor: A complex membrane-anchoring structure for proteins. *Biochemistry 47*, 6991-7000.

47. Sipos, G., Reggiori, F., Vionnet, C., and Conzelmann, A. (**1997**) Alternative lipid remodelling pathways for glycosylphosphatidylinositol membrane anchors in saccharomyces cerevisiae. *EMBO. J. 16*, 3494-3505.

48. McConville, M. J., and Ferguson, M. A. (**1993**) The structure, biosynthesis and function of glycosylated phosphatidylinositols in the parasitic protozoa and higher eukaryotes. *Biochem. J. 294 (Pt 2)*, 305-324.

49. McConville, M. J., and Menon, A. K. (**2000**) Recent developments in the cell biology and biochemistry of glycosylphosphatidylinositol lipids (review). *Mol. Membr. Biol. 17*, 1-16.

50. Canivenc-Gansel, E., Imhof, I., Reggiori, F., Burda, P., Conzelmann, A., and Benachour, A. (**1998**) Gpi anchor biosynthesis in yeast: Phosphoethanolamine is attached to the alpha1,4-linked mannose of the complete precursor glycophospholipid. *Glycobiology 8*, 761-770.

51. Butikofer, P., Kuypers, F. A., Shackleton, C., Brodbeck, U., and Stieger, S. (**1990**) Molecular species analysis of the glycosylphosphatidylinositol anchor of torpedo marmorata acetylcholinesterase. *J. Biol. Chem. 265*, 18983-18987.

52. Walter, E. I., Roberts, W. L., Rosenberry, T. L., Ratnoff, W. D., and Medof, M. E. (**1990**) Structural basis for variations in the sensitivity of human decay accelerating factor to phosphatidylinositol-specific phospholipase c cleavage. *J. Immunol. 144*, 1030-1036.

53. Roberts, W. L., Myher, J. J., Kuksis, A., and Rosenberry, T. L. (**1988**) Alkylacylglycerol molecular species in the glycosylinositol phospholipid membrane anchor of bovine erythrocyte acetylcholinesterase. *Biochem. Biophys. Res. Commun. 150*, 271-277.

54. Redman, C. A., Thomas-Oates, J. E., Ogata, S., Ikehara, Y., and Ferguson, M. A. (**1994**) Structure of the glycosylphosphatidylinositol membrane anchor of human placental alkaline phosphatase. *Biochem. J. 302 (Pt 3)*, 861-865.

55. Luhrs, C. A., and Slomiany, B. L. (**1989**) A human membrane-associated folate binding protein is anchored by a glycosyl-phosphatidylinositol tail. *J. Biol. Chem. 264*, 21446-21449.

56. Ferguson, M. A. J., Kinoshita, T., and Hart, G. W. (2009) Glycosylphosphatidylinositol anchors, In *Essentials of glycobiology* (Varki, A., Cummings, R. D., Esko, J. D., Freeze, H. H., Stanley, P., Bertozzi, C. R., Hart, G. W., and Etzler, M. E., Eds.) 2nd ed., Cold Spring Harbor (NY).

57. Nuoffer, C., Jeno, P., Conzelmann, A., and Riezman, H. (**1991**) Determinants for glycophospholipid anchoring of the saccharomyces cerevisiae gas1 protein to the plasma membrane. *Mol. Cell. Biol. 11*, 27-37.

58. Roberts, W. L., Myher, J. J., Kuksis, A., Low, M. G., and Rosenberry, T. L. (**1988**) Lipid analysis of the glycoinositol phospholipid membrane anchor of human erythrocyte acetylcholinesterase. Palmitoylation of inositol results in resistance to phosphatidylinositol-specific phospholipase c. *J. Biol. Chem. 263*, 18766-18775.

59. Vidugiriene, J., and Menon, A. K. (**1993**) Early lipid intermediates in glycosyl-phosphatidylinositol anchor assembly are synthesized in the er and located in the cytoplasmic leaflet of the er membrane bilayer. *J. Cell. Biol. 121*, 987-996.

60. Watanabe, R., Inoue, N., Westfall, B., Taron, C. H., Orlean, P., Takeda, J., and Kinoshita, T. (**1998**) The first step of glycosylphosphatidylinositol biosynthesis is mediated by a complex of pig-a, pig-h, pig-c and gpi1. *EMBO. J. 17*, 877-885.

61. Nakamura, N., Inoue, N., Watanabe, R., Takahashi, M., Takeda, J., Stevens, V. L., and Kinoshita, T. (**1997**) Expression cloning of pig-l, a candidate n-acetylglucosaminyl-phosphatidylinositol deacetylase. *J. Biol. Chem. 272*, 15834-15840.

62. Pottekat, A., and Menon, A. K. (**2004**) Subcellular localization and targeting of n-acetylglucosaminyl phosphatidylinositol de-n-acetylase, the second enzyme in the glycosylphosphatidylinositol biosynthetic pathway. *J. Biol. Chem. 279*, 15743-15751.

63. Vishwakarma, R. A., and Menon, A. K. (**2005**) Flip-flop of glycosylphosphatidylinositols (gpi's) across the er. *Chem. Commun. (Camb)*, 453-455.

64. Vidugiriene, J., and Menon, A. K. (**1994**) The gpi anchor of cell-surface proteins is synthesized on the cytoplasmic face of the endoplasmic reticulum. *J. Cell. Biol. 127*, 333-341.

65. Menon, A. K., and Vidugiriene, J. (**1994**) Topology of gpi biosynthesis in the endoplasmic reticulum. *Braz. J. Med. Biol. Res. 27*, 167-175.

66. Urakaze, M., Kamitani, T., DeGasperi, R., Sugiyama, E., Chang, H. M., Warren, C. D., and Yeh, E. T. (**1992**) Identification of a missing link in glycosylphosphatidylinositol anchor biosynthesis in mammalian cells. *J. Biol. Chem. 267*, 6459-6462.

67. Murakami, Y., Siripanyapinyo, U., Hong, Y., Kang, J. Y., Ishihara, S., Nakakuma, H., Maeda, Y., and Kinoshita, T. (**2003**) Pig-w is critical for inositol acylation but not for flipping of glycosylphosphatidylinositol-anchor. *Mol. Biol. Cell 14*, 4285-4295.

68. Umemura, M., Okamoto, M., Nakayama, K., Sagane, K., Tsukahara, K., Hata, K., and Jigami, Y. (**2003**) Gwt1 gene is required for inositol acylation of glycosylphosphatidylinositol anchors in yeast. *J. Biol. Chem. 278*, 23639-23647.

69. Doerrler, W. T., Ye, J., Falck, J. R., and Lehrman, M. A. (**1996**) Acylation of glucosaminyl phosphatidylinositol revisited. Palmitoyl-coa dependent palmitoylation of the inositol residue of a synthetic dioctanoyl glucosaminyl phosphatidylinositol by hamster membranes permits efficient mannosylation of the glucosamine residue. *J. Biol. Chem. 271*, 27031-27038.

70. Menon, A. K., Mayor, S., and Schwarz, R. T. (**1990**) Biosynthesis of glycosyl-phosphatidylinositol lipids in trypanosoma brucei: Involvement of mannosyl-phosphoryldolichol as the mannose donor. *EMBO. J. 9*, 4249-4258.

71. Maeda, Y., Watanabe, R., Harris, C. L., Hong, Y., Ohishi, K., Kinoshita, K., and Kinoshita, T. (**2001**) Pig-m transfers the first mannose to

glycosylphosphatidylinositol on the lumenal side of the er. *EMBO. J. 20*, 250-261.

72. Oriol, R., Martinez-Duncker, I., Chantret, I., Mollicone, R., and Codogno, P. (**2002**) Common origin and evolution of glycosyltransferases using dol-p-monosaccharides as donor substrate. *Mol. Biol. Evol. 19*, 1451-1463.

73. Ashida, H., Hong, Y., Murakami, Y., Shishioh, N., Sugimoto, N., Kim, Y. U., Maeda, Y., and Kinoshita, T. (**2005**) Mammalian pig-x and yeast pbn1p are the essential components of glycosylphosphatidylinositol-mannosyltransferase i. *Mol. Biol. Cell 16*, 1439-1448.

74. Kang, J. Y., Hong, Y., Ashida, H., Shishioh, N., Murakami, Y., Morita, Y. S., Maeda, Y., and Kinoshita, T. (**2005**) Pig-v involved in transferring the second mannose in glycosylphosphatidylinositol. *J. Biol. Chem. 280*, 9489-9497.

75. Fabre, A. L., Orlean, P., and Taron, C. H. (**2005**) Saccharomyces cerevisiae ybr004c and its human homologue are required for addition of the second mannose during glycosylphosphatidylinositol precursor assembly. *FEBS. J. 272*, 1160-1168.

76. Takahashi, M., Inoue, N., Ohishi, K., Maeda, Y., Nakamura, N., Endo, Y., Fujita, T., Takeda, J., and Kinoshita, T. (**1996**) Pig-b, a membrane protein of the endoplasmic reticulum with a large lumenal domain, is involved in transferring the third mannose of the gpi anchor. *EMBO. J. 15*, 4254-4261.

77. Sutterlin, C., Escribano, M. V., Gerold, P., Maeda, Y., Mazon, M. J., Kinoshita, T., Schwarz, R. T., and Riezman, H. (**1998**) Saccharomyces cerevisiae gpi10, the functional homologue of human pig-b, is required for

glycosylphosphatidylinositol-anchor synthesis. *Biochem. J. 332 (Pt 1)*, 153-159.

78. Grimme, S. J., Westfall, B. A., Wiedman, J. M., Taron, C. H., and Orlean, P. (**2001**) The essential smp3 protein is required for addition of the side-branching fourth mannose during assembly of yeast glycosylphosphatidylinositols. *J. Biol. Chem. 276*, 27731-27739.

79. Taron, B. W., Colussi, P. A., Wiedman, J. M., Orlean, P., and Taron, C. H. (**2004**) Human smp3p adds a fourth mannose to yeast and human glycosylphosphatidylinositol precursors in vivo. *J. Biol. Chem. 279*, 36083-36092.

80. Hong, Y., Maeda, Y., Watanabe, R., Ohishi, K., Mishkind, M., Riezman, H., and Kinoshita, T. (**1999**) Pig-n, a mammalian homologue of yeast mcd4p, is involved in transferring phosphoethanolamine to the first mannose of the glycosylphosphatidylinositol. *J. Biol. Chem. 274*, 35099-35106.

81. Gaynor, E. C., Mondesert, G., Grimme, S. J., Reed, S. I., Orlean, P., and Emr, S. D. (**1999**) Mcd4 encodes a conserved endoplasmic reticulum membrane protein essential for glycosylphosphatidylinositol anchor synthesis in yeast. *Mol. Biol. Cell 10*, 627-648.

82. Sutterlin, C., Horvath, A., Gerold, P., Schwarz, R. T., Wang, Y., Dreyfuss, M., and Riezman, H. (**1997**) Identification of a species-specific inhibitor of glycosylphosphatidylinositol synthesis. *EMBO. J. 16*, 6374-6383.

83. Flury, I., Benachour, A., and Conzelmann, A. (**2000**) Yll031c belongs to a novel family of membrane proteins involved in the transfer of

ethanolaminephosphate onto the core structure of glycosylphosphatidylinositol anchors in yeast. *J. Biol. Chem. 275*, 24458-24465.

84. Hong, Y., Maeda, Y., Watanabe, R., Inoue, N., Ohishi, K., and Kinoshita, T. (**2000**) Requirement of pig-f and pig-o for transferring phosphoethanolamine to the third mannose in glycosylphosphatidylinositol. *J. Biol. Chem. 275*, 20911-20919.

85. Hirose, S., Prince, G. M., Sevlever, D., Ravi, L., Rosenberry, T. L., Ueda, E., and Medof, M. E. (**1992**) Characterization of putative glycoinositol phospholipid anchor precursors in mammalian cells. Localization of phosphoethanolamine. *J. Biol. Chem. 267*, 16968-16974.

86. Imhof, I., Flury, I., Vionnet, C., Roubaty, C., Egger, D., and Conzelmann, A. (**2004**) Glycosylphosphatidylinositol (gpi) proteins of saccharomyces cerevisiae contain ethanolamine phosphate groups on the alpha1,4-linked mannose of the gpi anchor. *J. Biol. Chem. 279*, 19614-19627.

87. Shishioh, N., Hong, Y., Ohishi, K., Ashida, H., Maeda, Y., and Kinoshita, T. (**2005**) Gpi7 is the second partner of pig-f and involved in modification of glycosylphosphatidylinositol. *J. Biol. Chem. 280*, 9728-9734.

88. Benachour, A., Sipos, G., Flury, I., Reggiori, F., Canivenc-Gansel, E., Vionnet, C., Conzelmann, A., and Benghezal, M. (**1999**) Deletion of gpi7, a yeast gene required for addition of a side chain to the glycosylphosphatidylinositol (gpi) core structure, affects gpi protein transport, remodeling, and cell wall integrity. *J. Biol. Chem. 274*, 15251-15261.

89. Baumann, N. A., Vidugiriene, J., Machamer, C. E., and Menon, A. K. (**2000**) Cell surface display and intracellular trafficking of free glycosylphosphatidylinositols in mammalian cells. *J. Biol. Chem. 275*, 7378-7389.

90. Wu, X., and Guo, Z. (**2007**) Convergent synthesis of a fully phosphorylated gpi anchor of the cd52 antigen. *Org. Lett. 9*, 4311-4313.

91. Wu, X., Shen, Z., Zeng, X., Lang, S., Palmer, M., and Guo, Z. (**2008**) Synthesis and biological evaluation of sperm cd52 gpi anchor and related derivatives as binding receptors of pore-forming camp factor. *Carbohydr. Res. 343*, 1718-1729.

92. Schofield, L., Hewitt, M. C., Evans, K., Siomos, M. A., and Seeberger, P. H. (**2002**) Synthetic gpi as a candidate anti-toxic vaccine in a model of malaria. *Nature 418*, 785-789.

93. Seeberger, P. H., Soucy, R. L., Kwon, Y. U., Snyder, D. A., and Kanemitsu, T. (**2004**) A convergent, versatile route to two synthetic conjugate anti-toxin malaria vaccines. *Chem. Commun. (Camb)*, 1706-1707.

94. Xue, J., and Guo, Z. (**2003**) Convergent synthesis of a gpi containing an acylated inositol. *J. Am. Chem. Soc. 125*, 16334-16339.

95. Xue, J., Shao, N., and Guo, Z. (**2003**) First total synthesis of a gpi-anchored peptide. *J. Org. Chem. 68*, 4020-4029.

96. Xue, J., and Guo, Z. (**2003**) Efficient synthesis of complex glycopeptides based on unprotected oligosaccharides. *J. Org. Chem. 68*, 2713-2719.

97. John, F., and Hendrickson, T. L. (**2010**) Synthesis of truncated analogues for studying the process of glycosyl phosphatidylinositol modification. *Org. Lett. 12*, 2080-2083.

98. Shao, N., Xue, J., and Guo, Z. (**2003**) Chemical synthesis of cd52 glycopeptides containing the acid-labile fucosyl linkage. *J. Org. Chem. 68*, 9003-9011.

99. Olschewski, D., Seidel, R., Miesbauer, M., Rambold, A. S., Oesterhelt, D., Winklhofer, K. F., Tatzelt, J., Engelhard, M., and Becker, C. F. (**2007**) Semisynthetic murine prion protein equipped with a gpi anchor mimic incorporates into cellular membranes. *Chem. Biol. 14*, 994-1006.

100. Paulick, M. G., Wise, A. R., Forstner, M. B., Groves, J. T., and Bertozzi, C. R. (**2007**) Synthetic analogues of glycosylphosphatidylinositol-anchored proteins and their behavior in supported lipid bilayers. *J. Am. Chem. Soc. 129*, 11543-11550.

101. Guo, X., Wang, Q., Swarts, B. M., and Guo, Z. (**2009**) Sortase-catalyzed peptide-glycosylphosphatidylinositol analogue ligation. *J. Am. Chem. Soc. 131*, 9878-9879.

102. Tate, S. S., and Meister, A. (**1974**) Stimulation of the hydrolytic activity and decrease of the transpeptidase activity of gamma-glutamyl transpeptidase by maleate; identity of a rat kidney maleate-stimulated glutaminase and gamma-glutamyl transpeptidase. *Proc Natl Acad Sci U S A 71*, 3329-3333.

103. Maxwell, S. E., Ramalingam, S., Gerber, L. D., Brink, L., and Udenfriend, S. (**1995**) An active carbonyl formed during glycosylphosphatidylinositol addition

to a protein is evidence of catalysis by a transamidase. *J. Biol. Chem. 270*, 19576-19582.

104. Maxwell, S. E., Ramalingam, S., Gerber, L. D., and Udenfriend, S. (**1995**) Cleavage without anchor addition accompanies the processing of a nascent protein to its glycosylphosphatidylinositol-anchored form. *Proc. Natl. Acad. Sci. U. S. A. 92*, 1550-1554.

105. Ramalingam, S., Maxwell, S. E., Medof, M. E., Chen, R., Gerber, L. D., and Udenfriend, S. (**1996**) Cooh-terminal processing of nascent polypeptides by the glycosylphosphatidylinositol transamidase in the presence of hydrazine is governed by the same parameters as glycosylphosphatidylinositol addition. *Proc. Natl. Acad. Sci. U. S. A 93*, 7528-7533.

106. Nakahara, Y., Nonaka, T., and Hojo, H. (**2003**) Synthesis of an unnatural n-glycan-linked dolichyl pyrophosphate precursor. *Biosci. Biotechnol. Biochem. 67*, 1761-1766.

107. Ikezawa, H. (**2002**) Glycosylphosphatidylinositol (gpi)-anchored proteins. *Biol. Pharm. Bull. 25*, 409-417.

108. Ng, D. T., Brown, J. D., and Walter, P. (**1996**) Signal sequences specify the targeting route to the endoplasmic reticulum membrane. *J. Cell. Biol. 134*, 269-278.

109. Wang, J., Maziarz, K., and Ratnam, M. (**1999**) Recognition of the carboxyl-terminal signal for gpi modification requires translocation of its hydrophobic domain across the er membrane. *J. Mol. Biol. 286*, 1303-1310.

110. Howell, S., Lanctot, C., Boileau, G., and Crine, P. (**1994**) A cleavable n-terminal signal peptide is not a prerequisite for the biosynthesis of glycosylphosphatidylinositol-anchored proteins. *J. Biol. Chem. 269*, 16993-16996.

111. Micanovic, R., Kodukula, K., Gerber, L. D., and Udenfriend, S. (**1990**) Selectivity at the cleavage/attachment site of phosphatidylinositol-glycan anchored membrane proteins is enzymatically determined. *Proc. Natl. Acad. Sci. U. S. A. 87*, 7939-7943.

112. Micanovic, R., Gerber, L. D., Berger, J., Kodukula, K., and Udenfriend, S. (**1990**) Selectivity of the cleavage/attachment site of phosphatidylinositol-glycan-anchored membrane proteins determined by site-specific mutagenesis at asp-484 of placental alkaline phosphatase. *Proc. Natl. Acad. Sci. U. S. A. 87*, 157-161.

113. Udenfriend, S., Micanovic, R., and Kodukula, K. (**1991**) Structural requirements of a nascent protein for processing to a pi-g anchored form: Studies in intact cells and cell-free systems. *Cell Biol. Int. Rep. 15*, 739-759.

114. Kodukula, K., Micanovic, R., Gerber, L., Tamburrini, M., Brink, L., and Udenfriend, S. (**1991**) Biosynthesis of phosphatidylinositol glycan-anchored membrane proteins. Design of a simple protein substrate to characterize the enzyme that cleaves the cooh-terminal signal peptide. *J. Biol. Chem. 266*, 4464-4470.

115. Moran, P., Raab, H., Kohr, W. J., and Caras, I. W. (**1991**) Glycophospholipid membrane anchor attachment. Molecular analysis of the cleavage/attachment site. *J. Biol. Chem. 266*, 1250-1257.

116. Moran, P., and Caras, I. W. (**1991**) A nonfunctional sequence converted to a signal for glycophosphatidylinositol membrane anchor attachment. *J. Cell. Biol. 115*, 329-336.

117. Coyne, K. E., Crisci, A., and Lublin, D. M. (**1993**) Construction of synthetic signals for glycosyl-phosphatidylinositol anchor attachment. Analysis of amino acid sequence requirements for anchoring. *J. Biol. Chem. 268*, 6689-6693.

118. Nuoffer, C., Horvath, A., and Riezman, H. (**1993**) Analysis of the sequence requirements for glycosylphosphatidylinositol anchoring of saccharomyces cerevisiae gas1 protein. *J. Biol. Chem. 268*, 10558-10563.

119. Kodukula, K., Gerber, L. D., Amthauer, R., Brink, L., and Udenfriend, S. (**1993**) Biosynthesis of glycosylphosphatidylinositol (gpi)-anchored membrane proteins in intact cells: Specific amino acid requirements adjacent to the site of cleavage and gpi attachment. *J. Cell. Biol. 120*, 657-664.

120. Gerber, L. D., Kodukula, K., and Udenfriend, S. (**1992**) Phosphatidylinositol glycan (pi-g) anchored membrane proteins. Amino acid requirements adjacent to the site of cleavage and pi-g attachment in the cooh-terminal signal peptide. *J. Biol. Chem. 267*, 12168-12173.

121. Caras, I. W. (**1991**) Probing the signal for glycophosphatidylinositol anchor attachment using decay accelerating factor as a model system. *Cell Biol. Int. Rep. 15*, 815-826.

122. Furukawa, Y., Tsukamoto, K., and Ikezawa, H. (**1997**) Mutational analysis of the c-terminal signal peptide of bovine liver 5'-nucleotidase for gpi anchoring: A study on the significance of the hydrophilic spacer region. *Biochim. Biophys. Acta 1328*, 185-196.

123. Caras, I. W., and Weddell, G. N. (**1989**) Signal peptide for protein secretion directing glycophospholipid membrane anchor attachment. *Science 243*, 1196-1198.

124. Caras, I. W., Weddell, G. N., and Williams, S. R. (**1989**) Analysis of the signal for attachment of a glycophospholipid membrane anchor. *J. Cell Biol. 108*, 1387-1396.

125. Berger, J., Howard, A. D., Brink, L., Gerber, L., Hauber, J., Cullen, B. R., and Udenfriend, S. (**1988**) Cooh-terminal requirements for the correct processing of a phosphatidylinositol-glycan anchored membrane protein. *J. Biol. Chem. 263*, 10016-10021.

126. Su, B., and Bothwell, A. L. (**1989**) Biosynthesis of a phosphatidylinositol-glycan-linked membrane protein: Signals for posttranslational processing of the ly-6e antigen. *Mol. Cell Biol. 9*, 3369-3376.

127. Yan, W., Shen, F., Dillon, B., and Ratnam, M. (**1998**) The hydrophobic domains in the carboxyl-terminal signal for gpi modification and in the amino-terminal leader peptide have similar structural requirements. *J. Mol. Biol. 275*, 25-33.

128. Moran, P., and Caras, I. W. (**1994**) Requirements for glycosylphosphatidylinositol attachment are similar but not identical in mammalian cells and parasitic protozoa. *J. Cell Biol. 125*, 333-343.

129. Chen, R., Knez, J. J., Merrick, W. C., and Medof, M. E. (**2001**) Comparative efficiencies of c-terminal signals of native glycophosphatidylinositol (gpi)-anchored proproteins in conferring gpi-anchoring. *J. Cell. Biochem. 84*, 68-83.

130. Takos, A. M., Dry, I. B., and Soole, K. L. (**2000**) Glycosyl-phosphatidylinositol-anchor addition signals are processed in nicotiana tabacum. *Plant. J. 21*, 43-52.

131. Morissette, R., Varma, Y., and Hendrickson, T. L. (**2012**) Defining the boundaries of species specificity for the saccharomyces cerevisiae glycosylphosphatidylinositol transamidase using a quantitative in vivo assay. *Biosci. Rep. 32*, 577-586.

132. Ahmad, M. F., Yadav, B., Kumar, P., Puri, A., Mazumder, M., Ali, A., Gourinath, S., Muthuswami, R., and Komath, S. S. (**2012**) The gpi anchor signal sequence dictates the folding and functionality of the als5 adhesin from candida albicans. *PLoS. One 7*, e35305.

133. Bangs, J. D., Hereld, D., Krakow, J. L., Hart, G. W., and Englund, P. T. (**1985**) Rapid processing of the carboxyl terminus of a trypanosome variant surface glycoprotein. *Proc. Natl. Acad. Sci. U. S. A. 82*, 3207-3211.

134. Ferguson, M. A., Duszenko, M., Lamont, G. S., Overath, P., and Cross, G. A. (**1986**) Biosynthesis of trypanosoma brucei variant surface glycoproteins. N-

glycosylation and addition of a phosphatidylinositol membrane anchor. *J. Biol. Chem. 261*, 356-362.

135. Mayor, S., Menon, A. K., and Cross, G. A. (**1991**) Transfer of glycosyl-phosphatidylinositol membrane anchors to polypeptide acceptors in a cell-free system. *J. Cell. Biol. 114*, 61-71.

136. Amthauer, R., Kodukula, K., Brink, L., and Udenfriend, S. (**1992**) Phosphatidylinositol-glycan (pi-g)-anchored membrane proteins: Requirement of atp and gtp for translation-independent cooh-terminal processing. *Proc. Natl. Acad. Sci. U. S. A. 89*, 6124-6128.

137. Amthauer, R., Kodukula, K., Gerber, L., and Udenfriend, S. (**1993**) Evidence that the putative cooh-terminal signal transamidase involved in glycosylphosphatidylinositol protein synthesis is present in the endoplasmic reticulum. *Proc. Natl. Acad. Sci. U. S. A. 90*, 3973-3977.

138. Fraering, P., Imhof, I., Meyer, U., Strub, J. M., van Dorsselaer, A., Vionnet, C., and Conzelmann, A. (**2001**) The gpi transamidase complex of saccharomyces cerevisiae contains gaa1p, gpi8p, and gpi16p. *Mol. Biol. Cell 12*, 3295-3306.

139. Nagamune, K., Ohishi, K., Ashida, H., Hong, Y., Hino, J., Kangawa, K., Inoue, N., Maeda, Y., and Kinoshita, T. (**2003**) Gpi transamidase of trypanosoma brucei has two previously uncharacterized (trypanosomatid transamidase 1 and 2) and three common subunits. *Proc. Natl. Acad. Sci. U. S. A. 100*, 10682-10687.

140. Zhu, Y., Fraering, P., Vionnet, C., and Conzelmann, A. (**2005**) Gpi17p does not stably interact with other subunits of glycosylphosphatidylinositol transamidase in saccharomyces cerevisiae. *Biochim. Biophys. Acta 1735*, 79-88.

141. Ohishi, K., Inoue, N., and Kinoshita, T. (**2001**) Pig-s and pig-t, essential for gpi anchor attachment to proteins, form a complex with gaa1 and gpi8. *EMBO. J. 20*, 4088-4098.

142. Benghezal, M., Lipke, P. N., and Conzelmann, A. (**1995**) Identification of six complementation classes involved in the biosynthesis of glycosylphosphatidylinositol anchors in saccharomyces cerevisiae. *J. Cell Biol. 130*, 1333-1344.

143. Benghezal, M., Benachour, A., Rusconi, S., Aebi, M., and Conzelmann, A. (**1996**) Yeast gpi8p is essential for gpi anchor attachment onto proteins. *EMBO. J. 15*, 6575-6583.

144. Chen, R., Udenfriend, S., Prince, G. M., Maxwell, S. E., Ramalingam, S., Gerber, L. D., Knez, J., and Medof, M. E. (**1996**) A defect in glycosylphosphatidylinositol (gpi) transamidase activity in mutant k cells is responsible for their inability to display gpi surface proteins. *Proc. Natl. Acad. Sci. U. S. A. 93*, 2280-2284.

145. Yu, J., Nagarajan, S., Knez, J. J., Udenfriend, S., Chen, R., and Medof, M. E. (**1997**) The affected gene underlying the class k glycosylphosphatidylinositol (gpi) surface protein defect codes for the gpi transamidase. *Proc. Natl. Acad. Sci. U. S. A. 94*, 12580-12585.

146. Lillico, S., Field, M. C., Blundell, P., Coombs, G. H., and Mottram, J. C. (**2003**) Essential roles for gpi-anchored proteins in african trypanosomes revealed using mutants deficient in gpi8. *Mol. Biol. Cell 14*, 1182-1194.

147. Ruepp, S., Furger, A., Kurath, U., Renggli, C. K., Hemphill, A., Brun, R., and Roditi, I. (**1997**) Survival of trypanosoma brucei in the tsetse fly is enhanced by the expression of specific forms of procyclin. *J. Cell. Biol. 137*, 1369-1379.

148. Ellis, M., Sharma, D. K., Hilley, J. D., Coombs, G. H., and Mottram, J. C. (**2002**) Processing and trafficking of leishmania mexicana gp63. Analysis using gp18 mutants deficient in glycosylphosphatidylinositol protein anchoring. *J. Biol. Chem. 277*, 27968-27974.

149. Zacks, M. A., and Garg, N. (**2006**) Recent developments in the molecular, biochemical and functional characterization of gpi8 and the gpi-anchoring mechanism [review]. *Mol. Membr. Biol. 23*, 209-225.

150. Sharma, D. K., Hilley, J. D., Bangs, J. D., Coombs, G. H., Mottram, J. C., and Menon, A. K. (**2000**) Soluble gpi8 restores glycosylphosphatidylinositol anchoring in a trypanosome cell-free system depleted of lumenal endoplasmic reticulum proteins. *Biochem. J. 351 Pt 3*, 717-722.

151. Meyer, U., Benghezal, M., Imhof, I., and Conzelmann, A. (**2000**) Active site determination of gpi8p, a caspase-related enzyme required for glycosylphosphatidylinositol anchor addition to proteins. *Biochemistry 39*, 3461-3471.

152. Meitzler, J. L., Gray, J. J., and Hendrickson, T. L. (**2007**) Truncation of the caspase-related subunit (gpi8p) of saccharomyces cerevisiae gpi transamidase: Dimerization revealed. *Arch. Biochem. Biophys. 462*, 83-93.

153. Kang, X., Szallies, A., Rawer, M., Echner, H., and Duszenko, M. (**2002**) Gpi anchor transamidase of trypanosoma brucei: In vitro assay of the recombinant protein and vsg anchor exchange. *J. Cell. Sci. 115*, 2529-2539.

154. Vidugiriene, J., Vainauskas, S., Johnson, A. E., and Menon, A. K. (**2001**) Endoplasmic reticulum proteins involved in glycosylphosphatidylinositol-anchor attachment: Photocrosslinking studies in a cell-free system. *Eur. J. Biochem. 268*, 2290-2300.

155. Spurway, T. D., Dalley, J. A., High, S., and Bulleid, N. J. (**2001**) Early events in glycosylphosphatidylinositol anchor addition. Substrate proteins associate with the transamidase subunit gpi8p. *J. Biol. Chem. 276*, 15975-15982.

156. Rawlings, N. D., and Barrett, A. J. (**1994**) Families of cysteine peptidases. *Methods. Enzymol. 244*, 461-486.

157. Abe, Y., Shirane, K., Yokosawa, H., Matsushita, H., Mitta, M., Kato, I., and Ishii, S. (**1993**) Asparaginyl endopeptidase of jack bean seeds. Purification, characterization, and high utility in protein sequence analysis. *J. Biol. Chem. 268*, 3525-3529.

158. Ohishi, K., Inoue, N., Maeda, Y., Takeda, J., Riezman, H., and Kinoshita, T. (**2000**) Gaa1p and gpi8p are components of a glycosylphosphatidylinositol (gpi) transamidase that mediates attachment of gpi to proteins. *Mol. Biol. Cell 11*, 1523-1533.

159. Hamburger, D., Egerton, M., and Riezman, H. (**1995**) Yeast gaa1p is required for attachment of a completed gpi anchor onto proteins. *J. Cell. Biol. 129*, 629-639.

160. Hiroi, Y., Chen, R., Sawa, H., Hosoda, T., Kudoh, S., Kobayashi, Y., Aburatani, H., Nagashima, K., Nagai, R., Yazaki, Y., Medof, M. E., and Komuro, I. (**2000**) Cloning of murine glycosyl phosphatidylinositol anchor attachment protein, gpaa1. *Am. J. Physiol. Cell. Physiol. 279*, C205-212.

161. Hiroi, Y., Komuro, I., Chen, R., Hosoda, T., Mizuno, T., Kudoh, S., Georgescu, S. P., Medof, M. E., and Yazaki, Y. (**1998**) Molecular cloning of human homolog of yeast gaa1 which is required for attachment of glycosylphosphatidylinositols to proteins. *FEBS. Lett. 421*, 252-258.

162. Vainauskas, S., Maeda, Y., Kurniawan, H., Kinoshita, T., and Menon, A. K. (**2002**) Structural requirements for the recruitment of gaa1 into a functional glycosylphosphatidylinositol transamidase complex. *J. Biol. Chem. 277*, 30535-30542.

163. Vainauskas, S., and Menon, A. K. (**2004**) A conserved proline in the last transmembrane segment of gaa1 is required for glycosylphosphatidylinositol (gpi) recognition by gpi transamidase. *J. Biol. Chem. 279*, 6540-6545.

164. Ohishi, K., Nagamune, K., Maeda, Y., and Kinoshita, T. (**2003**) Two subunits of glycosylphosphatidylinositol transamidase, gpi8 and pig-t, form a functionally important intermolecular disulfide bridge. *J. Biol. Chem. 278*, 13959-13967.

165. Hong, Y., Ohishi, K., Kang, J. Y., Tanaka, S., Inoue, N., Nishimura, J., Maeda, Y., and Kinoshita, T. (**2003**) Human pig-u and yeast cdc91p are the fifth subunit of gpi transamidase that attaches gpi-anchors to proteins. *Mol. Biol. Cell. 14*, 1780-1789.

166. Grimme, S. J., Gao, X. D., Martin, P. S., Tu, K., Tcheperegine, S. E., Corrado, K., Farewell, A. E., Orlean, P., and Bi, E. (**2004**) Deficiencies in the endoplasmic reticulum (er)-membrane protein gab1p perturb transfer of glycosylphosphatidylinositol to proteins and cause perinuclear er-associated actin bar formation. *Mol. Biol. Cell 15*, 2758-2770.

167. Doering, T. L., and Schekman, R. (**1996**) Gpi anchor attachment is required for gas1p transport from the endoplasmic reticulum in cop ii vesicles. *EMBO. J. 15*, 182-191.

168. McDowell, M. A., Ransom, D. M., and Bangs, J. D. (**1998**) Glycosylphosphatidylinositol-dependent secretory transport in trypanosoma brucei. *Biochem. J. 335 (Pt 3)*, 681-689.

169. Mayor, S., and Riezman, H. (**2004**) Sorting gpi-anchored proteins. *Nat. Rev. Mol. Cell Biol. 5*, 110-120.

170. Fujita, M., Watanabe, R., Jaensch, N., Romanova-Michaelides, M., Satoh, T., Kato, M., Riezman, H., Yamaguchi, Y., Maeda, Y., and Kinoshita, T. (**2011**) Sorting of gpi-anchored proteins into er exit sites by p24 proteins is dependent on remodeled gpi. *J. Cell Biol. 194*, 61-75.

171. Tanaka, S., Maeda, Y., Tashima, Y., and Kinoshita, T. (**2004**) Inositol deacylation of glycosylphosphatidylinositol-anchored proteins is mediated by mammalian pgap1 and yeast bst1p. *J. Biol. Chem. 279*, 14256-14263.

172. Fujita, M., Maeda, Y., Ra, M., Yamaguchi, Y., Taguchi, R., and Kinoshita, T. (**2009**) Gpi glycan remodeling by pgap5 regulates transport of gpi-anchored proteins from the er to the golgi. *Cell 139*, 352-365.

173. Jensen, D., and Schekman, R. (**2011**) Copii-mediated vesicle formation at a glance. *J. Cell Sci. 124*, 1-4.

174. Takida, S., Maeda, Y., and Kinoshita, T. (**2008**) Mammalian gpi-anchored proteins require p24 proteins for their efficient transport from the er to the plasma membrane. *Biochem. J. 409*, 555-562.

175. Lisanti, M. P., Caras, I. W., Davitz, M. A., and Rodriguez-Boulan, E. (**1989**) A glycophospholipid membrane anchor acts as an apical targeting signal in polarized epithelial cells. *J. Cell Biol. 109*, 2145-2156.

176. Brown, D. A., Crise, B., and Rose, J. K. (**1989**) Mechanism of membrane anchoring affects polarized expression of two proteins in mdck cells. *Science 245*, 1499-1501.

177. Lisanti, M. P., Le Bivic, A., Saltiel, A. R., and Rodriguez-Boulan, E. (**1990**) Preferred apical distribution of glycosyl-phosphatidylinositol (gpi) anchored proteins: A highly conserved feature of the polarized epithelial cell phenotype. *J. Membr. Biol. 113*, 155-167.

178. Maeda, Y., Tashima, Y., Houjou, T., Fujita, M., Yoko-o, T., Jigami, Y., Taguchi, R., and Kinoshita, T. (**2007**) Fatty acid remodeling of gpi-anchored proteins is required for their raft association. *Mol. Biol. Cell 18*, 1497-1506.

179. Paladino, S., Sarnataro, D., Pillich, R., Tivodar, S., Nitsch, L., and Zurzolo, C. (**2004**) Protein oligomerization modulates raft partitioning and apical sorting of gpi-anchored proteins. *J. Cell Biol. 167*, 699-709.

180. Paladino, S., Sarnataro, D., Tivodar, S., and Zurzolo, C. (**2007**) Oligomerization is a specific requirement for apical sorting of glycosyl-phosphatidylinositol-anchored proteins but not for non-raft-associated apical proteins. *Traffic 8*, 251-258.

181. Benting, J. H., Rietveld, A. G., and Simons, K. (**1999**) N-glycans mediate the apical sorting of a gpi-anchored, raft-associated protein in madin-darby canine kidney cells. *J. Cell Biol. 146*, 313-320.

182. Delacour, D., Cramm-Behrens, C. I., Drobecq, H., Le Bivic, A., Naim, H. Y., and Jacob, R. (**2006**) Requirement for galectin-3 in apical protein sorting. *Curr. Biol. 16*, 408-414.

183. Catino, M. A., Paladino, S., Tivodar, S., Pocard, T., and Zurzolo, C. (**2008**) N- and o-glycans are not directly involved in the oligomerization and apical sorting of gpi proteins. *Traffic 9*, 2141-2150.

184. Kollar, R., Reinhold, B. B., Petrakova, E., Yeh, H. J., Ashwell, G., Drgonova, J., Kapteyn, J. C., Klis, F. M., and Cabib, E. (**1997**) Architecture of the yeast cell wall. Beta(1-->6)-glucan interconnects mannoprotein, beta(1-->)3-glucan, and chitin. *J. Biol. Chem. 272*, 17762-17775.

185. Caro, L. H., Tettelin, H., Vossen, J. H., Ram, A. F., van den Ende, H., and Klis, F. M. (**1997**) In silicio identification of glycosyl-phosphatidylinositol-anchored plasma-membrane and cell wall proteins of saccharomyces cerevisiae. *Yeast 13*, 1477-1489.

186. Hamada, K., Terashima, H., Arisawa, M., Yabuki, N., and Kitada, K. (**1999**) Amino acid residues in the omega-minus region participate in cellular localization of yeast glycosylphosphatidylinositol-attached proteins. *J. Bacteriol. 181*, 3886-3889.

187. Frieman, M. B., and Cormack, B. P. (**2004**) Multiple sequence signals determine the distribution of glycosylphosphatidylinositol proteins between the plasma membrane and cell wall in saccharomyces cerevisiae. *Microbiology 150*, 3105-3114.

188. Popolo, L., and Vai, M. (**1999**) The gas1 glycoprotein, a putative wall polymer cross-linker. *Biochim. Biophys. Acta 1426*, 385-400.

189. Teparic, R., Stuparevic, I., and Mrsa, V. (**2004**) Increased mortality of saccharomyces cerevisiae cell wall protein mutants. *Microbiology 150*, 3145-3150.

190. Solomon, K. R., Chan, M., and Finberg, R. W. (**1995**) Expression of gpi-anchored complement regulatory proteins cd55 and cd59 differentiates two subpopulations of human cd56+ cd3- lymphocytes (nk cells). *Cell Immunol. 165*, 294-301.

191. Ivanov, D., Philippova, M., Antropova, J., Gubaeva, F., Iljinskaya, O., Tararak, E., Bochkov, V., Erne, P., Resink, T., and Tkachuk, V. (**2001**) Expression of

cell adhesion molecule t-cadherin in the human vasculature. *Histochem. Cell Biol. 115*, 231-242.

192. Chan, S. Y., Empig, C. J., Welte, F. J., Speck, R. F., Schmaljohn, A., Kreisberg, J. F., and Goldsmith, M. A. (**2001**) Folate receptor-alpha is a cofactor for cellular entry by marburg and ebola viruses. *Cell 106*, 117-126.

193. Stefanova, I., Horejsi, V., Ansotegui, I. J., Knapp, W., and Stockinger, H. (**1991**) Gpi-anchored cell-surface molecules complexed to protein tyrosine kinases. *Science 254*, 1016-1019.

194. Stulnig, T. M., Berger, M., Sigmund, T., Stockinger, H., Horejsi, V., and Waldhausl, W. (**1997**) Signal transduction via glycosyl phosphatidylinositol-anchored proteins in t cells is inhibited by lowering cellular cholesterol. *J. Biol. Chem. 272*, 19242-19247.

195. Fleming, T. J., and Malek, T. R. (**1994**) Multiple glycosylphosphatidylinositol-anchored ly-6 molecules and transmembrane ly-6e mediate inhibition of il-2 production. *J. Immunol. 153*, 1955-1962.

196. Malek, T. R., Fleming, T. J., and Codias, E. K. (**1994**) Regulation of t lymphocyte function by glycosylphosphatidylinositol (gpi)-anchored proteins. *Semin. Immunol. 6*, 105-113.

197. Fang, C., Miwa, T., and Song, W. C. (**2011**) Decay-accelerating factor regulates t-cell immunity in the context of inflammation by influencing costimulatory molecule expression on antigen-presenting cells. *Blood 118*, 1008-1014.

198. Nagpal, J. K., Dasgupta, S., Jadallah, S., Chae, Y. K., Ratovitski, E. A., Toubaji, A., Netto, G. J., Eagle, T., Nissan, A., Sidransky, D., and Trink, B. (**2008**) Profiling the expression pattern of gpi transamidase complex subunits in human cancer. *Mod. Pathol. 21*, 979-991.

199. Ferguson, M. A. (**1999**) The structure, biosynthesis and functions of glycosylphosphatidylinositol anchors, and the contributions of trypanosome research. *J. Cell Sci. 112 (Pt 17)*, 2799-2809.

200. Chandra, S., Ruhela, D., Deb, A., and Vishwakarma, R. A. (**2010**) Glycobiology of the leishmania parasite and emerging targets for antileishmanial drug discovery. *Expert. Opin. Ther. Targets 14*, 739-757.

201. Prusiner, S. B. (**1991**) Molecular biology of prion diseases. *Science 252*, 1515-1522.

202. Kocisko, D. A., Come, J. H., Priola, S. A., Chesebro, B., Raymond, G. J., Lansbury, P. T., and Caughey, B. (**1994**) Cell-free formation of protease-resistant prion protein. *Nature 370*, 471-474.

203. Deleault, N. R., Harris, B. T., Rees, J. R., and Supattapone, S. (**2007**) Formation of native prions from minimal components in vitro. *Proc. Natl. Acad. Sci. U. S. A. 104*, 9741-9746.

204. Chesebro, B., Trifilo, M., Race, R., Meade-White, K., Teng, C., LaCasse, R., Raymond, L., Favara, C., Baron, G., Priola, S., Caughey, B., Masliah, E., and Oldstone, M. (**2005**) Anchorless prion protein results in infectious amyloid disease without clinical scrapie. *Science 308*, 1435-1439.

205. Chen, R., Udenfriend, S., Prince, G. M., Maxwell, S. E., Ramalingam, S., Gerber, L. D., Knez, J., and Medof, M. E. (**1996**) A defect in glycosylphosphatidylinositol (gpi) transamidase activity in mutant k cells is responsible for their inability to display gpi surface proteins. *Proc. Natl. Acad. Sci. U. S. A. 93*, 2280-2284.

206. Berger, J., Howard, A. D., Brink, L., Gerber, L., Hauber, J., Cullen, B. R., and Udenfriend, S. (**1988**) Cooh-terminal requirements for the correct processing of a phosphatidylinositol-glycan anchored membrane protein. *J. Biol. Chem. 263*, 10016-10021.

207. Caras, I. W., Weddell, G. N., and Williams, S. R. (**1989**) Analysis of the signal for attachment of a glycophospholipid membrane anchor. *J. Cell Biol. 108*, 1387-1396.

208. Berger, J., Micanovic, R., Greenspan, R. J., and Udenfriend, S. (**1989**) Conversion of placental alkaline phosphatase from a phosphatidylinositol-glycan-anchored protein to an integral transmembrane protein. *Proc. Natl. Acad. Sci. U. S. A. 86*, 1457-1460.

209. Fasel, N., Rousseaux, M., Schaerer, E., Medof, M. E., Tykocinski, M. L., and Bron, C. (**1989**) In vitro attachment of glycosyl-inositolphospholipid anchor structures to mouse thy-1 antigen and human decay-accelerating factor. *Proc. Natl. Acad. Sci. U. S. A. 86*, 6858-6862.

210. Bailey, C. A., Howard, A., Micanovic, R., Berger, J., Heimer, E., Felix, A., Gerber, L., Brink, L., and Udenfriend, S. (**1988**) Site-directed antibodies for probing the structure and biogenesis of phosphatidylinositol glycan-linked

membrane proteins: Application to placental alkaline phosphatase. *Anal. Biochem. 170*, 532-541.

211. Kodukula, K., Cines, D., Amthauer, R., Gerber, L., and Udenfriend, S. (**1992**) Biosynthesis of phosphatidylinositol-glycan (pi-g)-anchored membrane proteins in cell-free systems: Cleavage of the nascent protein and addition of the pi-g moiety depend on the size of the cooh-terminal signal peptide. *Proc. Natl. Acad. Sci. U. S. A. 89*, 1350-1353.

212. Chen, R., Anderson, V., Hiroi, Y., and Medof, M. E. (**2003**) Proprotein interaction with the gpi transamidase. *J. Cell Biochem. 88*, 1025-1037.

213. Chen, R., Walter, E. I., Parker, G., Lapurga, J. P., Millan, J. L., Ikehara, Y., Udenfriend, S., and Medof, M. E. (**1998**) Mammalian glycophosphatidylinositol anchor transfer to proteins and posttransfer deacylation. *Proc. Natl. Acad. Sci. U. S. A. 95*, 9512-9517.

214. Sharma, D. K., Smith, T. K., Weller, C. T., Crossman, A., Brimacombe, J. S., and Ferguson, M. A. (**1999**) Differences between the trypanosomal and human glcnac-pi de-n-acetylases of glycosylphosphatidylinositol membrane anchor biosynthesis. *Glycobiology 9*, 415-422.

215. Bailey, C. A., Gerber, L., Howard, A. D., and Udenfriend, S. (**1989**) Processing at the carboxyl terminus of nascent placental alkaline phosphatase in a cell-free system: Evidence for specific cleavage of a signal peptide. *Proc. Natl. Acad. Sci. U. S. A. 86*, 22-26.

216. Varma, Y., and Hendrickson, T. (**2010**) Methods to study gpi anchoring of proteins. *Chembiochem 11*, 623-636.

217. Hale, G. (**1995**) Synthetic peptide mimotope of the campath-1 (cd52) antigen, a small glycosylphosphatidylinositol-anchored glycoprotein. *Immunotechnology 1*, 175-187.

218. Xia, M. Q., Tone, M., Packman, L., Hale, G., and Waldmann, H. (**1991**) Characterization of the campath-1 (cdw52) antigen: Biochemical analysis and cdna cloning reveal an unusually small peptide backbone. *Eur. J. Immunol. 21*, 1677-1684.

219. Xia, M. Q., Hale, G., Lifely, M. R., Ferguson, M. A., Campbell, D., Packman, L., and Waldmann, H. (**1993**) Structure of the campath-1 antigen, a glycosylphosphatidylinositol-anchored glycoprotein which is an exceptionally good target for complement lysis. *Biochem. J. 293 (Pt 3)*, 633-640.

220. Dalley, J. A., and Bulleid, N. J. (**2003**) The endoplasmic reticulum (er) translocon can differentiate between hydrophobic sequences allowing signals for glycosylphosphatidylinositol anchor addition to be fully translocated into the er lumen. *J. Biol. Chem. 278*, 51749-51757.

221. Morissette, R. (**2007**) Methods to characterize and assay the s. Cerevisiae gpi transamidase - a membrane bound, multi subunit enzyme that post-translationally modifies proteins In *Chemistry* Johns Hopkins University, Baltimore.

222. Rigaut, G., Shevchenko, A., Rutz, B., Wilm, M., Mann, M., and Seraphin, B. (**1999**) A generic protein purification method for protein complex characterization and proteome exploration. *Nat. Biotechnol. 17*, 1030-1032.

223. Puig, O., Caspary, F., Rigaut, G., Rutz, B., Bouveret, E., Bragado-Nilsson, E., Wilm, M., and Seraphin, B. (**2001**) The tandem affinity purification (tap) method: A general procedure of protein complex purification. *Methods 24*, 218-229.

224. Edwards, O. J., and Pearson, G. R. (**1962**) The factors determining nucleophilic reactivities. *J. Am. Chem. Soc. 84*, 16-24.

225. Holmberg, A., Blomstergren, A., Nord, O., Lukacs, M., Lundeberg, J., and Uhlen, M. (**2005**) The biotin-streptavidin interaction can be reversibly broken using water at elevated temperatures. *Electrophoresis 26*, 501-510.

226. Eisenhaber, B., Bork, P., and Eisenhaber, F. (**1998**) Sequence properties of gpi-anchored proteins near the omega-site: Constraints for the polypeptide binding site of the putative transamidase. *Protein. Eng. 11*, 1155-1161.

227. Ferguson, M. A., and Williams, A. F. (**1988**) Cell-surface anchoring of proteins via glycosyl-phosphatidylinositol structures. *Annu. Rev. Biochem. 57*, 285-320.

228. Vidugiriene, J., and Menon, A. K. (**1995**) Soluble constituents of the er lumen are required for gpi anchoring of a model protein. *EMBO. J. 14*, 4686-4694.

229. http://mendel.imp.ac.at/gpi/fungi/pred/fungi.scerevisiae.html.

230. Eisenhaber, B., Eisenhaber, F., Maurer-Stroh, S., and Neuberger, G. (**2004**) Prediction of sequence signals for lipid post-translational modifications: Insights from case studies. *Proteomics 4*, 1614-1625.

231. McNally, K. L., Ward, A. E., and Priola, S. A. (**2009**) Cells expressing anchorless prion protein are resistant to scrapie infection. *J. Virol. 83*, 4469-4475.

232. Thornberry, N. A., and Lazebnik, Y. (**1998**) Caspases: Enemies within. *Science 281*, 1312-1316.

233. Schrantz, N., Blanchard, D. A., Mitenne, F., Auffredou, M. T., Vazquez, A., and Leca, G. (**1999**) Manganese induces apoptosis of human b cells: Caspase-dependent cell death blocked by bcl-2. *Cell Death Differ. 6*, 445-453.

234. Chun, H. S., Lee, H., and Son, J. H. (**2001**) Manganese induces endoplasmic reticulum (er) stress and activates multiple caspases in nigral dopaminergic neuronal cells, sn4741. *Neurosci. Lett. 316*, 5-8.

235. Ito, Y., Oh-Hashi, K., Kiuchi, K., and Hirata, Y. (**2006**) P44/42 map kinase and c-jun n-terminal kinase contribute to the up-regulation of caspase-3 in manganese-induced apoptosis in pc12 cells. *Brain. Res. 1099*, 1-7.

236. Velazquez-Delgado, E. M., and Hardy, J. A. (**2012**) Zinc-mediated allosteric inhibition of caspase-6. *J. Biol. Chem. 287*, 36000-36011.

237. Huber, K. L., and Hardy, J. A. (**2012**) Mechanism of zinc-mediated inhibition of caspase-9. *Protein. Sci. 21*, 1056-1065.

238. Truong-Tran, A. Q., Carter, J., Ruffin, R. E., and Zalewski, P. D. (**2001**) The role of zinc in caspase activation and apoptotic cell death. *Biometals. 14*, 315-330.

239. Tardito, S., Bassanetti, I., Bignardi, C., Elviri, L., Tegoni, M., Mucchino, C., Bussolati, O., Franchi-Gazzola, R., and Marchio, L. (**2011**) Copper binding agents acting as copper ionophores lead to caspase inhibition and paraptotic cell death in human cancer cells. *J. Am. Chem. Soc. 133*, 6235-6242.

240. Sliskovic, I., and Mutus, B. (**2006**) Reversible inhibition of caspase-3 activity by iron(iii): Potential role in physiological control of apoptosis. *FEBS. Lett. 580*, 2233-2237.

241. Roth, J. A., Feng, L., Walowitz, J., and Browne, R. W. (**2000**) Manganese-induced rat pheochromocytoma (pc12) cell death is independent of caspase activation. *J. Neurosci. Res. 61*, 162-171.

242. Telford, W. G., and Fraker, P. J. (**1995**) Preferential induction of apoptosis in mouse cd4+cd8+ alpha beta tcrlocd3 epsilon lo thymocytes by zinc. *J. Cell. Physiol. 164*, 259-270.

243. Schrantz, N., Auffredou, M. T., Bourgeade, M. F., Besnault, L., Leca, G., and Vazquez, A. (**2001**) Zinc-mediated regulation of caspases activity: Dose-dependent inhibition or activation of caspase-3 in the human burkitt lymphoma b cells (ramos). *Cell Death Differ. 8*, 152-161.

244. Kondoh, M., Tasaki, E., Araragi, S., Takiguchi, M., Higashimoto, M., Watanabe, Y., and Sato, M. (**2002**) Requirement of caspase and p38mapk activation in zinc-induced apoptosis in human leukemia hl-60 cells. *Eur. J. Biochem. 269*, 6204-6211.

ABSTRACT

DEVELOPMENT AND OPTIMIZATION OF THE FIRST HIGH THROUGHPUT *IN VITRO* FRET ASSAY TO CHARACTERIZE THE *SACCHAROMYCES CEREVISIAE* GPI TRANSAMIDASE

by

SANDAMALI AMARASINGHA EKANAYAKA

December 2013

Advisor: Dr. Tamara L. Hendrickson

Major: Biochemistry

Degree: Doctor of Philosophy

The enzyme glycosylphosphatidylinositol transamidase (GPI-T) mediates the attachment of a glycosylphosphatidylinositol (GPI) anchor to the C-terminus of specific proteins to produce GPI anchored proteins. This post-translational modification is essential for viability of eukaryotic organisms. However, very little is known about GPI-T and its catalytic activity. Thus, the research described in this abstract was conducted to develop an *in vitro* assay to monitor GPI-T. A high-throughput assay for GPI-T will facilitate innumerable new experiments to study this complicated enzyme. The three core subunits of GPI-T (Gpi8, Gpi16, and Gaa1) were co-purified from a *GPI8* knockout *Saccharomyces cerevisiae* strain containing a plasmid that expresses Gpi8 with an appended glutathione-*S*-transferase (GST) domain. Peptide substrates for GPI-T were synthesized and modified to contain a pair of chromophores suitable for the development of a fluorescence resonance

energy transfer (FRET) assay. GPI-T activity was observed as a time-dependent increase in fluorescence by incubating peptides with pure, solubilized GPI-T in the presence of hydroxylamine, a small GPI anchor mimic. A FRET assay was developed and optimized to monitor GPI anchoring activity *in vitro*. The assay was used to investigate various aspects of GPI-T, including the importance of the C-terminal hydrophobic region in peptide substrates, the identity of the residue at the site of modification, substrate selectivity, and the effect of cofactors, co-substrates and inhibitors for GPI-T .To date no one has demonstrated robust GPI-T activity with *pure solubilized GPI-T*. Thus, this new FRET assay represents the first high-throughput method to quantitatively analyze GPI-T activity *in vitro.*

AUTOBIOGRAPHICAL STATEMENT

SANDAMALI AMARASINGHA EKANAYAKA

Education

Ph.D. in Chemistry (Major: Biological chemistry), August 2013
Department of Chemistry, Wayne State University, Detroit, Michigan, USA.

Bachelor of Science (B.Sc.), Chemistry, May 2005
University of Peradeniya, Peradeniya, Sri Lanka

Bachelor of Science (B.Sc.), Information Technology, May 2005
British Computer Society, The Chartered Institute for IT, United Kingdom

Research Experience

Wayne State University 2008–2013 Advisor: Dr. T. L. Hendrickson

Wayne State University 2006–2008 Advisor: Dr. W. Guo

University of Peradeniya 2001–2005 Advisor: Dr. N. Karunaratne

Publications

Wang, Q., **Ekanayaka, S.A.**, Wu, J., Zhang, J., and Guo, Z. **(2008)** Synthetic and Immunological Studies of 5′-N-Phenylacetyl sTn to Develop Carbohydrate-Based Cancer Vaccines and to Explore the Impacts of Linkage between Carbohydrate Antigens and Carrier Proteins. *Bioconjugate Chem*. *19*, 2060–2067.

.

Presentations (presenter is underlined)

Ekanayaka, S. A; Hendrickson, T. L. "Development and Optimization of a FRET Based In Vitro Assay to Characterize the Saccharomyces cerevisiae GPI-T." Graduate Exhibition, Wayne State University, March 6, 2012; Poster

Ekanayaka, S. A; Hendrickson, T. L. "The First High-Throughput In Vitro Assay to Characterize the Saccharomyces cerevisiae GPI-T" Sixteenth Graduate Student Research Day, Wayne State University, September 27, 2012; Poster

Ekanayaka, S. A; Hendrickson, T. L. " The First High-Throughput In Vitro Assay to Characterize the Saccharomyces cerevisiae GPI-T" The Eighth Midwest Carbohydrate Research Symposium, Wayne State University, October 5,6 ,2012; Poster

Gamage, G. D; **Ekanayaka, S. A;** Varma, Y; Seetharaman S; Hendrickson, T. L. " Breaking the Boundaries of the GPI Transamidase Complex" The Eighth Midwest Carbohydrate Research Symposium, Wayne State University, October 5,6 ,2012; Poster